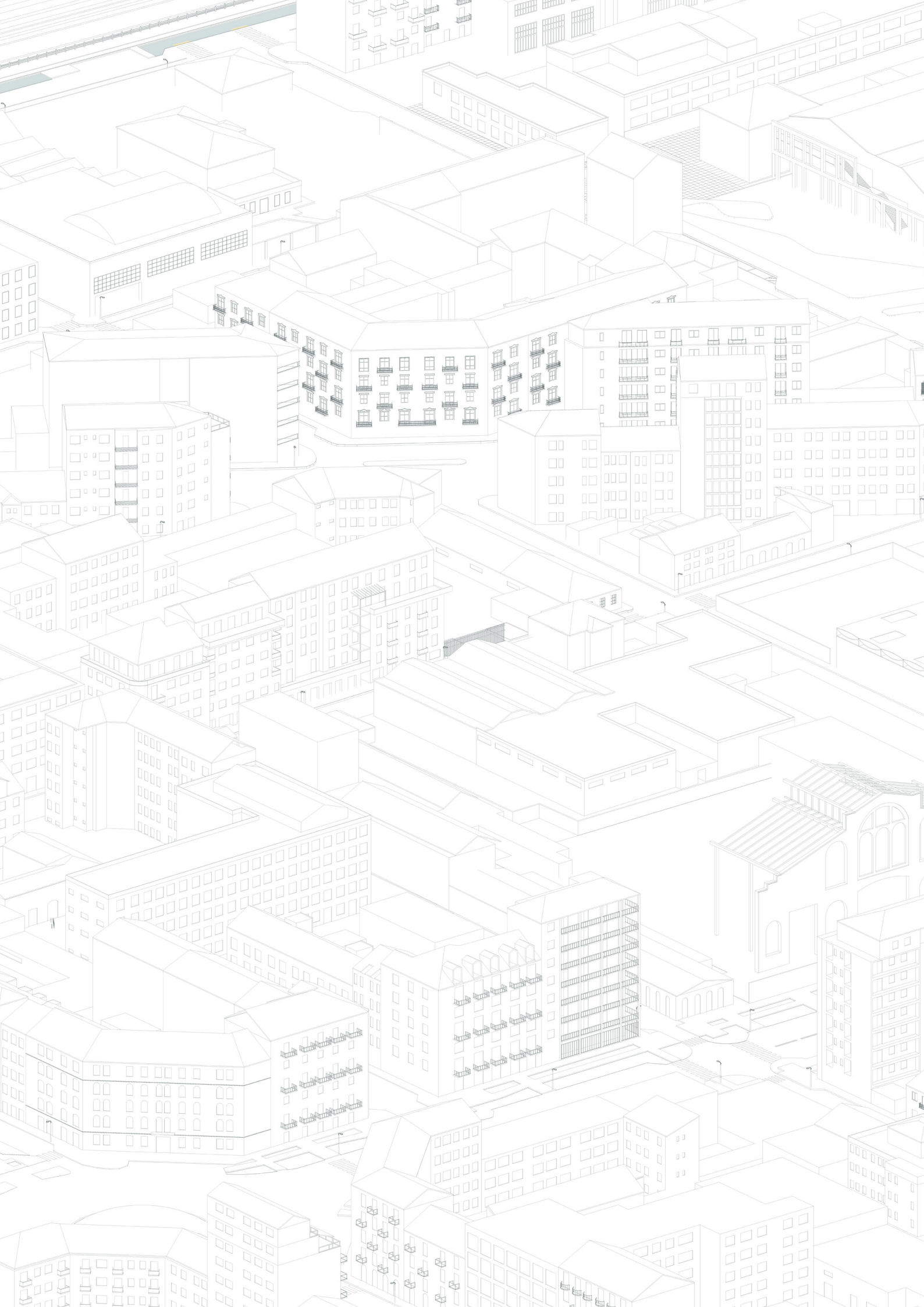

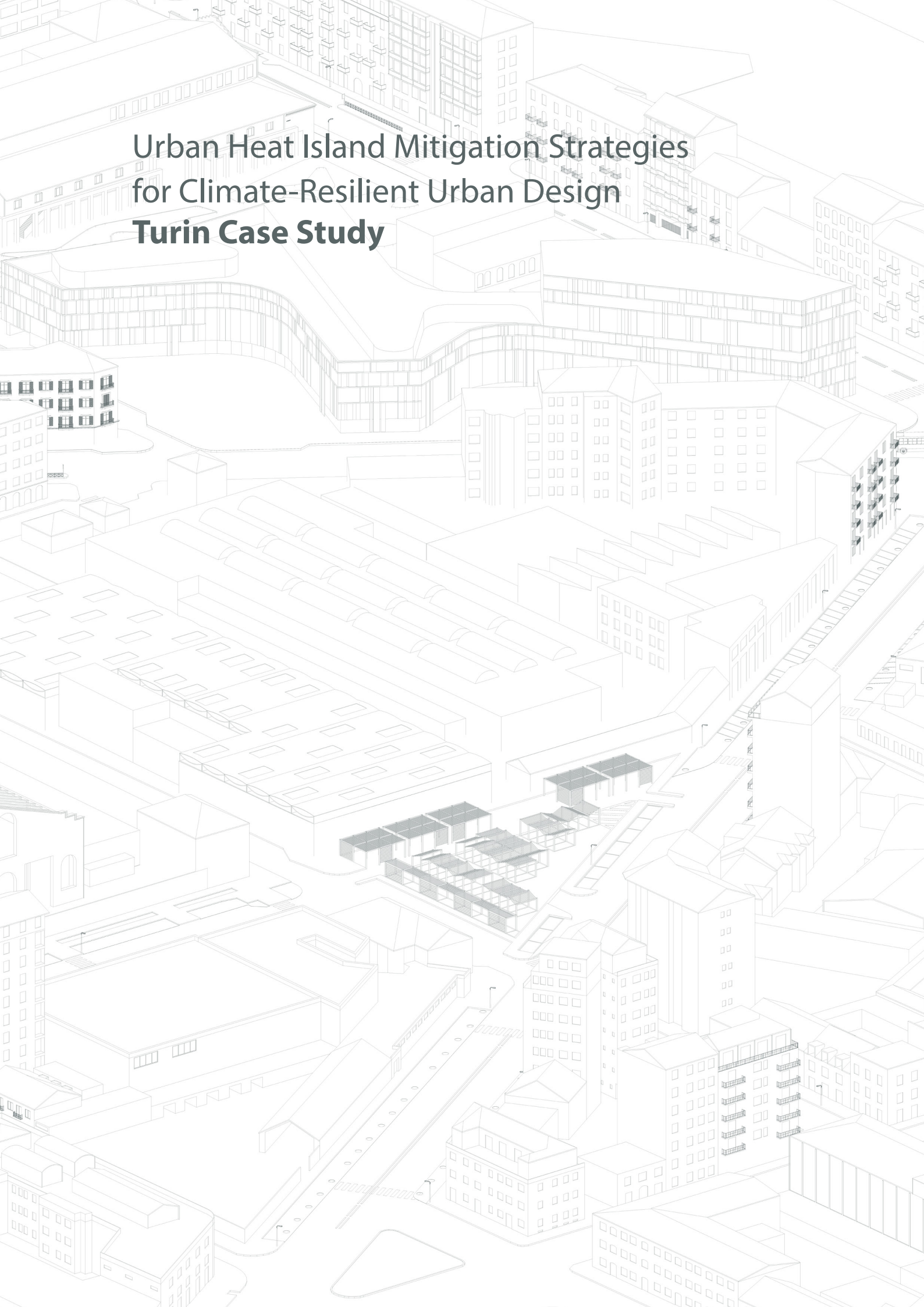

Urban Heat Island Mitigation Strategies for Climate-Resilient Urban Design

Turin Case Study

Politecnico di Torino

Urban Heat Island Mitigation Strategies for Climate-Resilient Urban Design

Case study of Turin

Politecnico di Torino

Master of science program in Architecture for Sustainability

year 2024-2025

Master's Thesis

Supervisor Riccardo Pollo

Co-Supervisor Anja Pejović

Student Ala Nouri

First and foremost, I would like to express my sincere gratitude to my thesis supervisor, Professor Riccardo Pollo, and my co-supervisor, Anja Pjević, for their valuable guidance, support, and encouragement throughout the development of this thesis.

I am deeply thankful to my family and friends for their continuous love, patience, and support.

03 Turin Case Study

3.1 Turin's Urban Condition

3.2 Mapping the Zone

3.3 Microclimate Analysis

3.4 Strategies

04 Conclusion

05 Bibliography and Sitography

Chapter 00

0.1 Glossary

Albedo
The ability of a surface that allows it to reflect solar radiation, measured between 0 and 1, 0 being full absorption and 1 being full reflectivity) (Lopez-Cabeza et al, 2022)

Adaptation
Adjustments in natural or built environments in response to the expected or actual outcomes of climate change (Intergovernmental Panel on Climate Change, 2001).

Aspect Ratio *(Urban Canyon)*
The ratio between the height of buildings and the width of the street. It affects solar exposure, shading, and ventilation (Emmanuel, 2021).

Emissivity
The ability of a surface to emit absorbed heat. Materials with low emissivity retain heat, while high-emissivity materials release it more quickly (Musikant, 2003).

Local Climate Zones (LCZ)
A classification system used to standardize the description of urban and rural landscapes based on surface cover, structure, and function. Useful in UHI studies (Stewart, 2012; Oke, 2012).

Microclimate
The set of atmospheric conditions (e.g., temperature, humidity, wind, solar radiation) in a small, specific area that can differ significantly from the surrounding regional climate, often influenced by urban form, vegetation, and surface materials. (Oke, 1987).

Mitigation
Interventions that deal with the causes of climate change, such as to reduce the emission sources (Locatelli, 2011).

Nature based Solutions (NbS)
Actions to protect, sustainably manage, and restore natural or modified ecosystems, that address societal challenges effectively and adaptively, simultaneously providing human well-being and biodiversity benefits (IUCN, 2016).

Psychological Equivalent Temperature (PET)
The air temperature at which, in a typical indoor setting (without wind and solar radiation), the heat budget of the human body is balanced with the same core and skin temperature as under the complex outdoor conditions to be assessed (Erell et al., 2011).

Thermal Comfort
The condition of mind that expresses satisfaction with the thermal environment, influenced by factors such as air temperature, humidity, radiant temperature, clothing, and activity level (ISO 7730:2005).

Urban Morphology
The study of urban form that examines the formation and transformation of cities, towns and villages (Chen, 2014).

Urban Heat Island (UHI)
An urban or metropolitan area where the temperature is significantly higher compared to that of its surroundings, commonly associated with intense human activities (Taha, 2004).

0.2 Abstract

The impact of urban design on the microclimate of cities and its relation to global warming is becoming more and more important. It directly affects the surrounding environment and the health of the people. This thesis focuses on the mitigation of the microclimate in a mixed-use area in Turin. This area has a mix of industrial, residential, and commercial uses and is considered one of the most important and busiest areas of the city. The aim of this thesis is to mitigate the UHI through effective, neighbourhood-scale strategies that have already been tested in urban projects or studies in cities with climatic conditions similar to Turin. The research looks at how the shape and layout of the urban environment affect thermal stress, studying where the design of the area makes heat conditions worse or helps reduce them. To do this, it analyzes factors like surface temperature, air temperature, and the PET, which gives a clearer picture to improve thermal comfort toward more sustainable and resilient cities. The thesis combines theoretical research and environmental analyses and simulations to understand the drivers of UHI and to identify the most critical zones. The thesis is divided into four sections: The first part describes a framework that reviews the principles of urban microclimate and UHI dynamics, defining the relationship between urban morphology and LCZs with the intensification of the UHI effect. This section also reviews the tools that are used for environmental analysis. The second part represents academic research and design practices, and compares the different strategies in each project to understand the most effective mitigation strategies. The final phase focuses on the site-specific analysis. First, the city of Turin and its weather conditions were studied, and afterwards, analyses were conducted at the neighborhood scale and then at the street level. Furthermore, simulations using ENVI-met software are done to analyse the results of four key parameters: air temperature, surface temperature, wind speed, and PET. These simulations are done once, considering the existing condition of the area, and another time, including the strategies and comparing the results. support the identification of spatial vulnerabilities and allow for the proposition of climate-responsive design strategies.

Keywords: Microclimate - Climate Adaptation - Urban Morphology - Local Climate Zone - Climate-Responsive Design - Thermal Comfort - Sustainable Cities - Urban Heat Island

0.3 Introduction

Cities generate 70 percent of global emissions, houses half of humanity, and faces catastrophic warming impacts. "Cities will be the defining battlefields in the fight against climate change," according to UN Secretary-General António Guterres in 2023. Urban outdoor spaces contribute to the livability and vitality of cities by providing a variety of benefits for citizens: physical, environmental, economic, and social (Woolley, 2003). As it will be discussed, urban environments, both outdoors and indoors, relate directly to human health and wellbeing. Since the strategic planning action has the capability to anticipate and adapt to such change, the role of urban microclimate design is very important. This is so because its dynamics have an influence on buildings, and outside areas at an individual level. Effective planning action must address microclimatic elements at the city, neighborhood, and site level to safeguard human health and environmental quality (Smith, 2024). We have to actively work on this subject because "the durability and longevity of the built environment means that design decisions made today will lock in climate vulnerabilities for decades," as Jones & Taylor noted in 2019. The equitability factor for making this change is also very relevant in ensuring that climate change does not lead to further disequilibrium among societies, but strives to conduct a just distribution of the climate change burden, as argued by Emmanuel in 2021. "Climate justice demands that urban adaptation strategies prioritize the most vulnerable communities to avoid deepening socio-economic disparities." - Patel, 2022

The functioning nexus of cities includes the interaction of land use, energy, water systems, waste services, and transport infrastructure, along with biodiversity and public health. Consequently, actions that address climate change mitigation may positively or negatively contribute to adaptation and other societal objectives. Similarly, for actions that enhance adaptation to climate impacts, 'adaptation' is the main benefit while the co-benefit may be emission reductions or enhanced equity. The "Integrated approaches recognize that reducing greenhouse gas emissions (mitigation) can simultaneously lower climate-related risks (adaptation) and enhance societal well-being (cobenefits)" (IPCC, 2018).

The research into the urban thermohygrometric climate in architecture forms a consolidated field of studies that has elaborated theories, methodologies, and software for the definition and simulation both of the microclimate and of well-being in urban open spaces. The variables of the local climate of a specific geographical location have been related to the behaviour of buildings, urban forms and materials. The urban and building project can intervene on all these elements (Pollo et al., 2020). For proposing and designing those strategies, the conditions of the climate must be analyzed.

Environmental simulation models and field measurements provide the necessary quantitative data to assess the thermal performance of urban design alternatives, which are essential health determinants" (Brown & Lee, 2023). However, these actions must be verified and measured in the specific and complex situations of the places, considering the interaction between microclimate, anthropogenic emissions (e.g., from traffic, industry, and building energy use), and inhabitants, assessing the conditions prior to the intervention and subsequent to it. Then, on-site validation and verification of the use of simulation can be performed (pollo et al., 2020). This thesis explores how urban design can effectively respond to climatic challenges by integrating microclimate analysis into the architectural process to contribute to healthier, more equitable, and climate-resilient urban environments..

0.4 Research questions

I. What specific microclimatic characteristics does the selected zone, in the Aurora district of Turin, have within its LCZ, and which of the zones are most critically vulnerable to thermal stress?

II. How can microclimate modeling tools, such as ENVI-met, be used to evaluate the effectiveness of site-specific urban interventions on air temperature, wind speed, and thermal comfort?

III. How can climate-responsive urban design strategies improve local microclimatic conditions in the case study area, and what is their measurable impact on reducing potential air temprature, surface temprature and, PET in the identified critical zones compared to the baseline scenario?

0.5 Methodology

01 Litrature Review

This section introduces the scientific background of the thesis by defining key concepts. It includes a review of the most relevant academic papers, reports, and guidelines to create a theoretical framework for climate-responsive urban design. The aim is to understand the drivers of UHI, as well as the effectiveness of mitigation strategies at different scales

Data

Academic papers, Precedent thesis, Urban Climate, Building and Environment journals, EU reports, UN reports, Guidelines for urban heat mitigation and thermal comfort

Outputs

A theoretical framework highlighting causes of UHI and potential mitigation strategies

02 Analysis of Best Practices

This phase involves Both academic and practical case studies, to identify successful design strategies and evaluate their performance. The goal is to understand applicable and most effective approaches for urban heat mitigation, focusing on solutions that are replicable in the chosen study area.

Data

Academic papers, Precedent thesis,
Envi-Met Website

Outputs

Comparative analysis of effective urban design solutions,

03 Urban Morphology and Contextual Analysis

The selected area in Turin is analyzed in terms of urban morphology, building density, land use, street patterns, and surface characteristics. A local climate zone (LCZ) classification is performed to identify the physical and functional characteristics of the zone that contribute to local microclimatic conditions, serving as a foundation for understanding the spatial and surface factors influencing UHI in the district.

Data Sources

Geoportale di Torino, Arpa Piemonte, Google Earth, Google Maps

Tools

Q-GIS, Adobe Illustrator

Outputs

Spatial analysis maps showing urban density, land use, street geometry, and material characteristics

Microclimate Modelling and Simulation

Based on the contextual analysis, a 3D model of the area with the existing urban condition is created and simulated using ENVI-met software to evaluate key microclimatic indicators such as air temperature, mean radiant temperature, and PET in the existing situation. The results are illustrated through heatmaps and data visualizations to identify critical hot areas most affected by thermal discomfort.

Data Sources

Geoportale Torino, ARPA Piemonte, Google Earth and Google Maps

Tools

ENVI-met, Adobe Photoshop, Adobe Illustrator

Outputs

Microclimate analysis maps and charts, including thermal comfort, Potential air temperature, Wind flow, surface temprature and comparison maps of based scenario and the one including strategies

Design Strategies and Climate Adaptation Proposals

Based on the simulation outputs, targeted design strategies are proposed for the most critical areas with the strategies included. Each proposal aims at improving thermal comfort and UHI mitigation. a 3D model of the area including strategies is created and simulated to show the difference of thermal stress in both conditions.

Data

The outputs of ENVI-met analysis, microclimate maps and charts

Tools

Revit, Adobe Photoshop, Adobe Illustrator

Outputs

Images and drawings illustrating the zone after the proposed strategies

04 Conclusion

The final section summarizes the key findings of the research and design process. It reflects on the effectiveness of proposed strategies, the simulation tools, and the potential for implementing these interventions in real urban contexts. It also outlines possible directions for sustainable urban climate adaptation

Chapter 01

Scientific Background

1.1 Sustainable Development Goals
1.1.1 Goal 3: Good health and well-being
1.1.2 Goal 11: Sustainable cities and communities
1.1.3 Goal 13: Climate Action
1.1.4 SDGs and climate challenges

1.2 Microclimate
1.2.1 Urban Heat Island
1.2.2 Local Climate Zones
1.2.3 Urban Morphology
1.2.4 Thermal Comfort

1.3 Microclimate Adaptation and Mitigation Strategies
1.3.1 Mitigation and adaptation
1.3.2 Surface and Material based Strategies
1.3.3 Green Infrastructure
1.3.4 Building-Integrated Strategies
1.3.5 Naturebased Solutions (NbS)

1.4 Analytical Tools and Climate Modeling
1.4.1 The importance of utilizing climate modeling tools
1.4.2 ENVI-met

1.1 Sustainable Development Goals

In the year 2015, the United Nations introduced the Sustainable Development Goals as a plan to improve the condition of the planet and ensure that the current generations are able to meet their needs without compromising future generation's ability to meet their own. The SDGs present a 15-year plan (2015–2030) within the 2030 Agenda for Sustainable Development (United Nations, 2015). These goals are summarized in Figure 1.

Since most of the goals are connected, action in one area can affect outcomes in other areas. True sustainable development needs a balance between social, environmental, and economical aspects to be achieved. This is according to the "United Nations Development Programme, 2015". They create a broad set of mechanics by which governments, institutions, and society can move toward long-term sustainability by focusing on growth, care for the environment, and social equity. The ambition of the SDGs lies both in the solution of immediate problems and, the shaping of a resilient, and livable future for current and future generations.

Fig. 1 Sustainable Development Goals source: https://www.un.org/sustainabledevelopment/news/communications-material/

This thesis aligns with SDGs 3, 11, and 13 respectively being: Good Health and Well-Being , Sustainable Cities and Communities, and Climate Action which emphasizes the importance of making cities inclusive, safe, resilient, and sustainable.

Fig. 2 Sustainable Development Goal 3 source: https://sdgs.un.org/goals

Fig. 3 Sustainable Development Goal 11 source: https://sdgs.un.org/goals

Fig. 4 Sustainable Development Goal 13 source: https://sdgs.un.org/goals

1.1.1 SDG 3: Ensure healthy lives and promote well-being for all at all ages

Goal 3 seeks to ensure health and well-being for all, at every stage of life. The Goal addresses all major health priorities, including reproductive, maternal and child health; communicable, non-communicable and environmental diseases; universal health coverage; and access for all to safe, effective, quality and affordable medicines and vaccines. It also calls for more research and development, increased health financing, and strengthened capacity of all countries in health risk reduction and management (UN, Global Sustainable Development Report 2016). The United Nations is advancing universal health coverage and promoting equitable, people-centred health systems, focusing on fragile, conflict-affected regions and areas with significant health inequalities (UN, Global Sustainable Development Report 2025).

The World Health Organization (WHO) expresses how the environment, and especially the urban environment, can influence people's health quality. Modern urban life style is associated with chronic stress, insufficient physical activity and exposure to anthropogenic environmental hazards. Urban green spaces, such as parks, playgrounds, and residential greenery, can promote mental and physical health, and reduce morbidity and mortality in urban residents by providing psychological relaxation and stress alleviation, stimulating social cohesion, supporting physical activity, and reducing exposure to air pollutants, noise and excessive heat (WHO, Urban green spaces and health, 2016). Researchers have proposed a model that emphasizes respiratory health and resilience to heat-related illness, social capital and cohesion, and physical activity (Villanueva et al., 2015). Heat related morbidity in cities is a major public health concern (WHO and WMO, 2015). The Urban Heat Island effect can be a serious health hazard during heat waves and extreme heat events. It arises due to replacement of vegetation with impervious heat-absorbing surfaces in urban areas. Exposure to excessive heat is linked to increased morbidity and mortality, especially in vulnerable subpopulations, such as the elderly (Smargiassi et al., 2009; Basagaña et al., 2011). Urban warming driven by global climate change and the urban heat island effect threatens the thermal safety and comfort of urban residents, as moderate and extreme heat exposure are well-documented contributors to morbidity and mortality (Sarofim, et al 2016) Given the strong connection between both mental and physical health and the urban environment, it is essential to take actions to improve our cities, and in consequence, people's physical and mental health.

1.1.2 SDG 11: Make cities and human settlements inclusive, safe, resilient and sustainable

With over half of the world's population living in cities today-the number is forecast to be nearly 70 percent by 2050-cities are experiencing mounting challenges, from increasing urban poverty and growing slum populations to inadequate public transport and threats to infrastructure from disasters. The progress of Goal 11 requires integrated strategies for cities that must be focused on affordable and inclusive housing, participatory urban planning, heritage preservation, and stronger local governance-all supported by robust disaggregated data. Initiatives for accelerating progress on Goal 11 also include the Local2030 Coalition, which galvanizes action on the Goals at the level of the locality by convening United Nations entities, local governments, and other partners (UN, Global Sustainable Development Report 2025). Informality shapes people's vulnerability, and as metropolitan areas continue their expansion, the gap between availability and needs will increase. Driven by demographic change, rapid urbanization, social and economic pressures as well as policy failures, vulnerability to climate change is growing in urban areas (UNH report, The Critical Role of Nature-Based Solutions for Enhancing Climate Resilience, 2023). In light of the rapid pace of urbanization and the increasing vulnerability of city populations, achieving the goals of SDG 11 requires urgent and coordinated action. Pressures include increased exposure to climate risks as urban areas grow. Inclusive sustainable strategies include affordable planning, local governance, and equitable access to services. Strengthening these, supported by reliable, disaggregated data and collaborative efforts such as the Local2030 Coalition, is important for closing the widening gap between urban development and human needs.

1.1.3 SDG 13: Take urgent action to combat climate change and its impacts

Climate change is, in fact, the single biggest threat to development, and its far-reaching, unprecedented impacts disproportionally affect the world's poorest and most vulnerable. Urgent action to combat climate change and minimize its disruptions is integral to the successful implementation of the Sustainable Development Goals.

Because climate change is a global phenomenon, extensive international cooperation is urgently needed to build resilience and adaptive capacity to its adverse effects, develop sustainable low-carbon paths up to the future, and accelerate the reduction of global greenhouse gas emissions. On 22 April 2016, 175 Member States signed the Paris Agreement under the United Nations Framework Convention on Climate Change. The new agreement will lessen the pace of climate change while fast-tracking and intensifying the actions and investments needed for a sustainable low-carbon future. Parallel to this, cities, towns, and regions need to adapt to climate change and enhance climate resilience across all sectors in all systems and processes. For that, local and regional governments have to set a clear goal and advance rapidly following a holistic and integrated approach (ICLEI's Climate Neutrality Framework, 2020).

Addressing the Urban Heat Island effect becomes one of the most fundamental parts of local climate action and urban resilience. With the increasing temperature and frequency of heatwaves in cities, UHI mitigation should be incorporated into urban design as a matter of urgency to protect public health, reduce energy consumption, and enhance climate adaptability in general. This research aims to help address these with urgency and innovation.

Sustainable development goals as urban challenges antidote

There are several links between CC, urban heat-related challenges, and the SDGs. To support these ambitious goals, the research presented in this contribution examined a variety of urban heat-related challenges, including (but not limited to) urban overheating, health impacts related to heat, inadequate monitoring and prediction systems, the need for effective adaptation and mitigation strategies, differential energy consumption patterns, reduced air quality, infrastructure deterioration, social vulnerability, and economic challenges (He et al., 2021; Kamel et al., 2024; Shahmohamadi et al., 2011). This was done alongside suggested solutions and their linkages to relevant SDGs (Ahmed et al., 2024).

Fig. 5 illustrates how the SDGs could support the mitigation of these urban challenges. For instance, strategies for "Urban Overheating" involve green infrastructure; the creation of public awareness of the problem; and early warning systems consistent with SDG 11 (Sustainable Cities and Communities) and SDG 3 (Good Health and Well-being). The problems brought forth by "Urban Heat Islands" may be mitigated through green roofs, reflective pavements, and various forms of urban design that incorporate open spaces, all corresponding to SDG 11 and SDG 7 (Affordable and Clean Energy). Thirdly, "Air Pollution" can be minimized by the addition of renewable energies, more energy-efficient means of transportation, and enhanced waste collection methods linked to SDG 7, SDG 9 (Industry, Innovation, and Infrastructure), and SDG 11. The integration of these SDGs into urban policies would therefore allow a comprehensive and at the same time effective approach to dealing with the multi-dimensional impacts of urban heating, and thus assure the building of more sustainable, resilient, and healthier cities.

Urban Microclimate Challenges

Urban Overheating	Air Conditioning Facilities Outdoor Activity Patterns Sheltering Area	Air Conditioning Facilities Outdoor Activity Patterns Sheltering Area	SDG 7 SDG11
Health related Impacts	Knowledge and awareness of Impact	Increse public awareness and education about heat related health risks Develope early warning systems	SDG 3 SDG13
Climate Monitoring and Predictive Tools	Measures, Strategies and Services Monitoring, Forecasting and Warnings	Implement comprehensive monitoring and forecasting systems Provide timely and actionable heat-related allerts	SDG 9 SDG13
Mitigation Strategies	Green Infrastructures Cool and Permeable materials Blue Infrastructure Urban Planning and Design	Increase urban green spaces and water supplies Integrate heat mitigation design principles	SDG 3 SDG11 SDG15
Energy Consumption and Energy	Differential Impacts on energy Consumption in commercial and residential sectors	Implement energy efficient building codes Promote distributed energy generation	SDG 7 SDG15
Poor Air Quality	Exacerbation of ground-level ozone and other pollutants due to higher tempratures	Enhance air quality monitoring Implement pollution control measures	SDG 3 SDG11 SDG13
Infrastructure Challenges	Diterioration of roads, bridges and buildings Increased risk of power outage	Use heat resistant construction materials Invest in resiliant infrastructure systems	SDG 9 SDG11

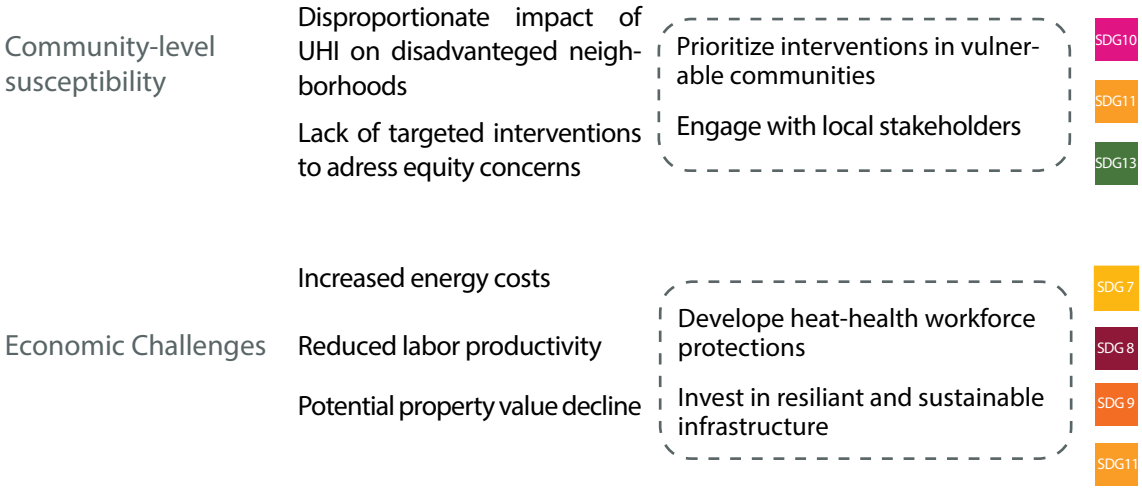

Fig. 5 Relation between SDGs and Urban Heat Challenges, Source: Nour M. Ahmed, et al., 2024

1.2 Microclimate

A microclimate defines the climate conditions in a relatively small and well-localized area, which differs from the larger climate surrounding the area(Oke, 2012). Several microclimatic factors create a variation in the general climate of specific areas, such as topography, vegetation, water bodies, and human activities. These factors create a variation in temperature, humidity, wind patterns, and other climatic elements within a specific region Oke, 2012) .According to Figure 6, microclimates are defined as climate conditions at a "microscale" on the earth's underlying surface as opposed to macroscales and mesoscales (Orlanski, 1975). Based on an article by (Williams, 1991), climate studies were classified by the region of investigation. In urban microclimate, climatic phenomena are considered at a variety of scales, from the neighborhood and small community scales of several kilometers (Antoniou, et al., 2019) to street canyons of a few meters (Chen, et al., 2020; Senwen Yang, 2024). Urban Microclimate is profoundly influenced by various parameters, each playing a critical role in shaping the microenvironment within urban areas. Temperature variations, particularly the formation of Urban Heat Islands (UHI), result from factors such as building materials, urban disturbances, and anthropogenic heat generation (Hadavi, et al,. 2021).

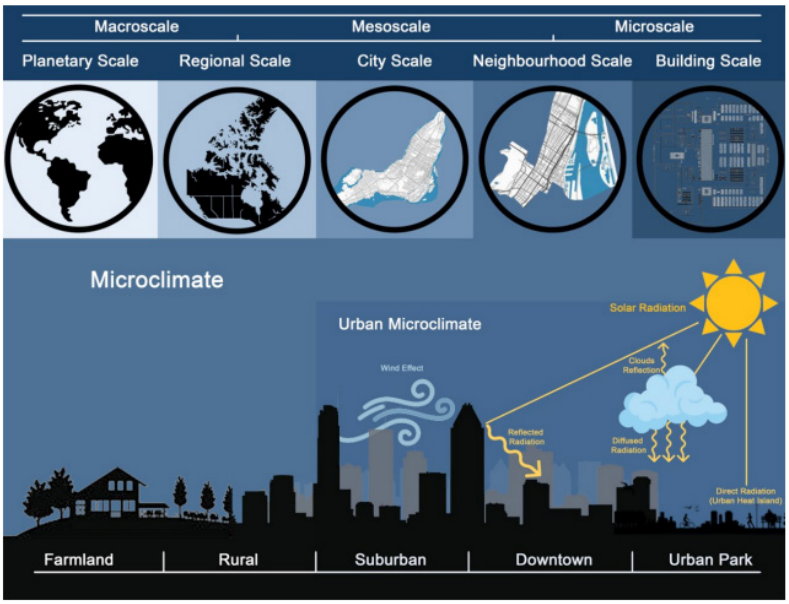

Fig. 6 Climatological scales classified by horizontal extension and climatic condition type by region scale, Source: Orlanski, (1975)

1.2.1 Urban Heat Island (UHI)

UHI is one of the most discussed topics in urban microclimates.
Urban areas can retain and generate more heat than rural regions, leading to higher ground surface and air temperatures near the ground. The UHI is the result of inadequate urban development control (Santamouris, et al,. 2001). Besides UHI, urban surface morphing also modifies the urban wind environment and urban pollution dispersion due to the thermal buoyancy from heated surfaces. The underlying urban surfaces can also affect building energy consumption. For example, urban thermal aerodynamics affects pollution dispersion in street canyons, especially in stratified conditions (Yang, 1972), and indoor air quality, especially for naturally ventilated buildings (Cui, et al., 2015). In the last few decades, the phenomenon of UHI has been a critical area of study in terms of urban planning and environmental science. The prime cause of UHI can be related to the alteration of natural landscapes into built environments where urbanization replaces vegetation, with asphalt, concrete, and buildings. These surfaces absorb and retain solar radiation more than the natural landscape. This absorption of heat is then strongly enhanced by anthropogenic heat releases from vehicles, industrial processes, and air conditioning units, adding to the rises in temperature (Zhou et al., 2014).

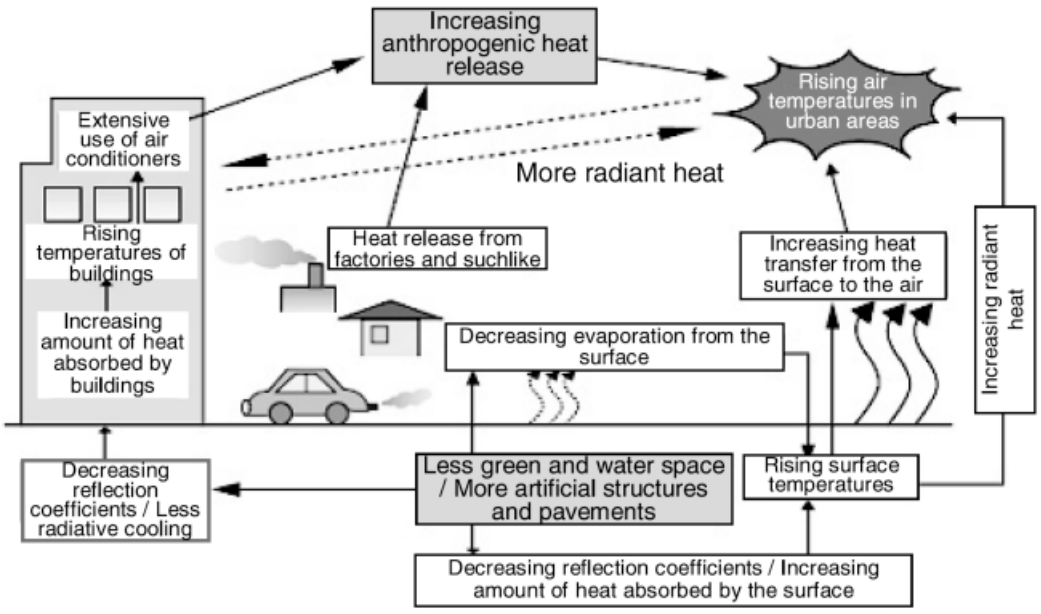

Fig. 7 Causes of UHI, Source: Yamamoto (2006)

The UHI can be illustrated by drawing a curve from one side of a city to the other, mapping graphically thetemperature change from the rural to the urban environment and back to the rural environment. The 'island' would be represented by the large spike in the centre of the graph, shown in figures 8 and 9, which generally mimics the outline of the structures within the urban area, and is bound by the cliffs either side that mark the urban and ruralboundary (Oke, 1982).

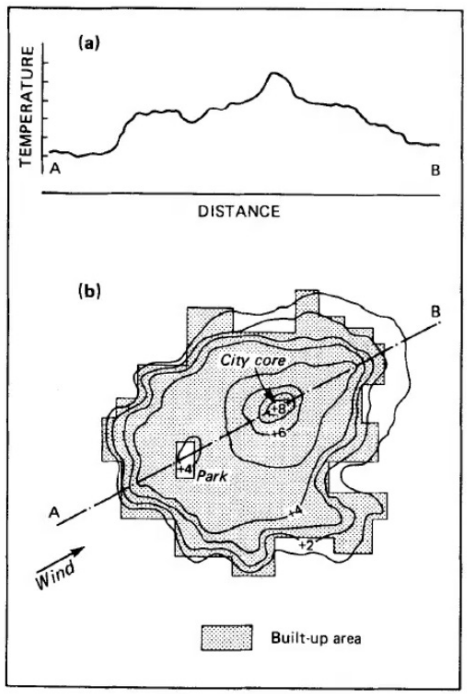

Fig. 8 Hypothetical representation of the spatial and temporal features of UHI. Source: Oke, 1982

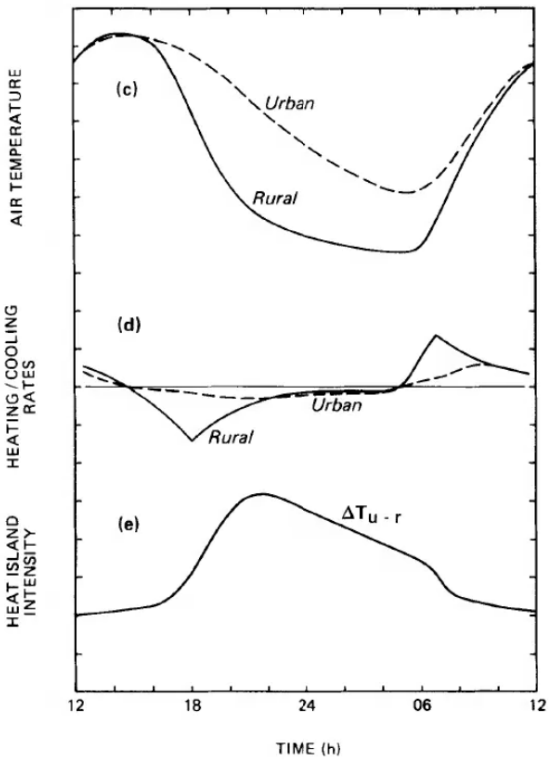

Fig. 9 The energetic basis of the UHI. Source: Oke, 1982

UHI effects and consequences

UHI does not only create uncomfortably warm environments, but also causes problems, such as the need for cooling solutions that results to energy consumption and costs for construction and infrastructure maintenance (Coffel, 2018).

Under the influence of local urbanization and global climate change, many cities over the world have experienced significant temperature increase in past decades. (Masson et al., 2018) Urban heat island effect which caused by the process of urbanization with changes in land surface structure and human behaviours, tends to be reinforced by high temperature periods. It results in additional hot days at local scale, associated with elevated energy consumption for cooling and increased heat-related health risks(Goggins et al., 2012).

The UHI effect strengthen the impacts of global warming on urban populations, making it a concern for sustainable urban development(Ward et al., 2016).Some of the main drivers for the UHI effect include climate, anthropogenic heat, sky view factor, heat absorbing surface materials, and building morphology. The implications of the UHI effect are increased energy demands for cooling, increased emissions of air pollutants and greenhouse gasses, a rise in heat-related illnesses, and degradation of thermal comfort (Oke, 2015). These consequences imply that there is a pressing need to determine effective strategies to mitigate the UHI effect and measure it with accuracy with a view to improving urban living and resilience to climate change. Among the set of factors that influence the UHI phenomenon, the material composition of urban facades and pavements stands out because of its direct interaction with solar radiation (Baldinelli et al., 2024).Properties such as albedo (the measure of reflectivity), thermal emissivity, and specific heat capacity determine the extent to which urban surfaces absorb, retain, and emit heat (Doulos et al., 2004). The urban heat island has a very important impact on the energy consumption of buildings during the summer period, increases the concentration of pollutants and cause discomfort and health problems(Erell et al., 2011).

1.2.2 Local Climate Zones (LCZ)

The Local Climate Zones Classification system was proposed in 2012 by Stewart and Oke to depict the complexity of urban morphology. However, until the present, a long-time series product of LCZ was rarely available or reliably consistent due to its mapping difficulty. Jiao Zhao et al. (2023) proposed a framework to map annual LCZ time series with spatiotemporal consistency in the three major urban agglomerations of China, and it also revealed that the high-rise and open urban LCZ types tended to occupy a higher proportion in the urban area in the past two decades, and urban morphology varied distinctly in the urban expansion areas and urban renewal areas.

The concept of Local Climate Zone was developed to quantify the relationship between urban morphology and urban heat island phenomenon. Each LCZ is supposed to represent homogeneous air temperature. However, there is inadequate data for verifying the air temperature differences between LCZ classes. Therefore, it is necessary to utilize alternative temperature data which allow more comprehensive assessment of the effect of LCZ on local climatic conditions. Land surface temperature (LST) acquired from satellite images can be used to establish the relationship between LST and LCZ by providing continuous data on surface temperature. (Cai et al, 2018).

Local Climate Zones serve as a comprehensive climate-based classification of urban and rural sites for temperature studies.(Figure 10) The cultural and geographic appeal of the classification has been demonstrated, as has the potential to improve consistency and accuracy in urban climate reporting. The system functions easily and inexpensively in any city or region. The original authors, Stewart and Oke, therefore anticipate that it can meet a basic requirement in urban climate studies through standardized description of surface structure and cover (Stewart et al., 2012).

Several studies have been performed based on the classification system by Stewart and Oke (2012). One of these has been carried out by Taubenböck et al. (2020), with the aim of classifying 110 cities into 7 types, depending on the spatial urban configuration differences. In conclusion, the findings raise two main discussions: The first result demonstrates that similar cultural, demographical and socio-economic conditions result in similar configurations in sense of physical layout, density, and structural characteristics whereas the second proves that different geographies and climates can share significantly common characteristics when it comes to urban spatial configuration (Taubenböck et al., 2020).

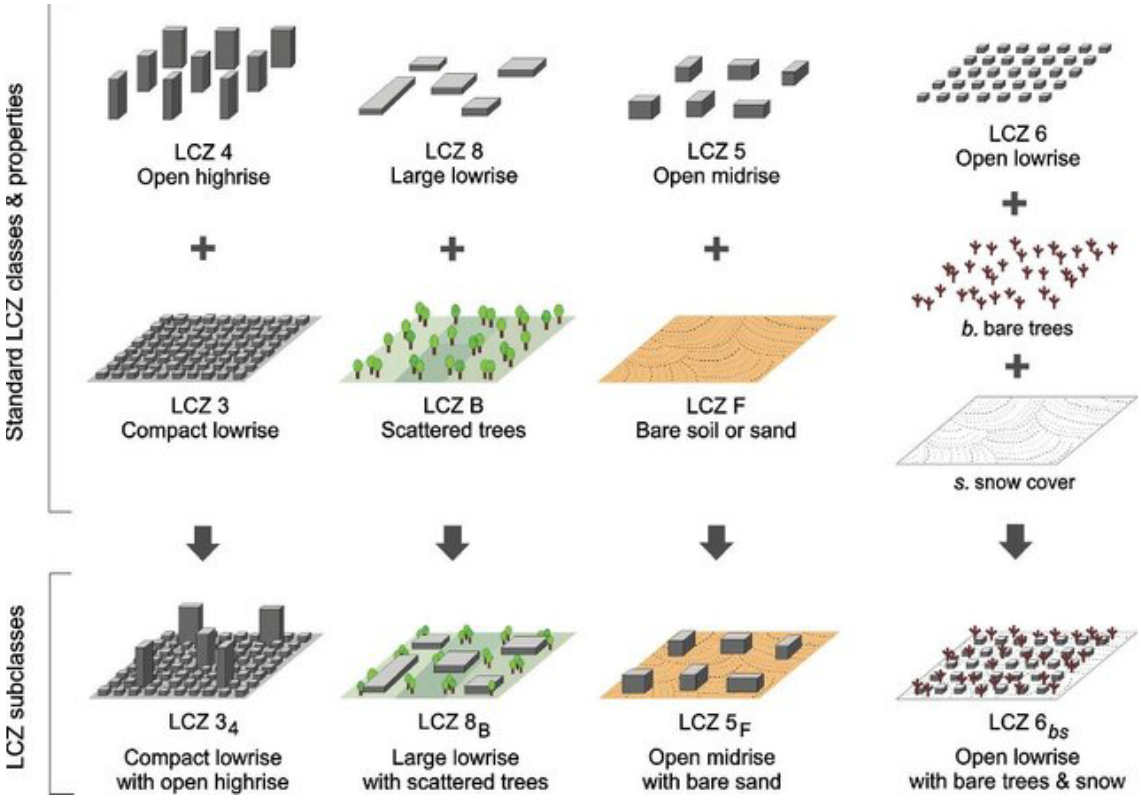

Fig. 10 LCZ subclasses to represent combinations of "built" and "land cover" types.
Source: Stewart & Oke, (2012)

1.2.3 Urban Morphology

Urban morphology defines and represents the main character of the city. The main components that shape urban morphology are the three primary elements of the urban form: street network and block structure, building forms and functions, and land use patterns (Oke, 2012). These physical components could be considered as variables that evolve over time as cities grow, and this growing process results in different states of balance between these urban components.

The process might cause additional variables to emerge, such as the Urban Heat Island effect, while simultaneously influencing outcomes like microclimate, thermal comfort, vegetation, density, and urban quality. The geometric and material properties of the urban fabric determine the amount of incoming solar radiation that is stored and re-released as sensible heat (Grimmond, 2007). Changes in the albedo, heat storage capacity, and evaporation of land covers are the side effects of changing urban morphology, which consequently alter the thermal characteristics of the land surface (Dihkan, et al., 2015; Hu et al., 2010).

These thermal changes lead to temperature differences between cities and their surrounding rural areas (Sheng, Tang, You, Gu, & Hu, 2017). The magnitude of the UHI effect is primarily regulated by the arrangement and composition of the city's surface, notably through the canyon aspect ratio and the fraction of impervious surface (Oke, 1988; Emmanuel et al., 2007).

However, due to the weakness of mutual dialogue between climatology and planning (Oke, 1984), the results of climatology researches have been far from applicable planning practices (Alcoforado, et al., 2009; Xu et al., 2017). Thus, urban climatology or urban meteorology have experienced a paradigm shift to analyze climatic effects of urbanization (Mills, 2014) by using planning parameters (Petralli et al., 2014).

Impact of morphology on microclimate

Urban Morphology Characteristics significantly affect the Urban Climate.
According to the wind and temperature simulations performed by Rafail-Kouklis et al. (2021), it was realized that in cases where urban canyons are perpendicular to the wind flow, the air temperature is lowered compared to the parallel orientation of these two variables (for the summer season). Rafail-Kouklis et al. (2021) also mention that in cases where airflows were perpendicular to the urban canyon, the high H/W ratio and the lack of through openings were responsible for the urban environment's lack of ventilation. At the same time, the tall buildings at the corners of the building blocks appeared to create strong local gusts of wind.
Figure 11, which summarizes all the controlled factors related to urban morphology impacting the formation of the microclimate.

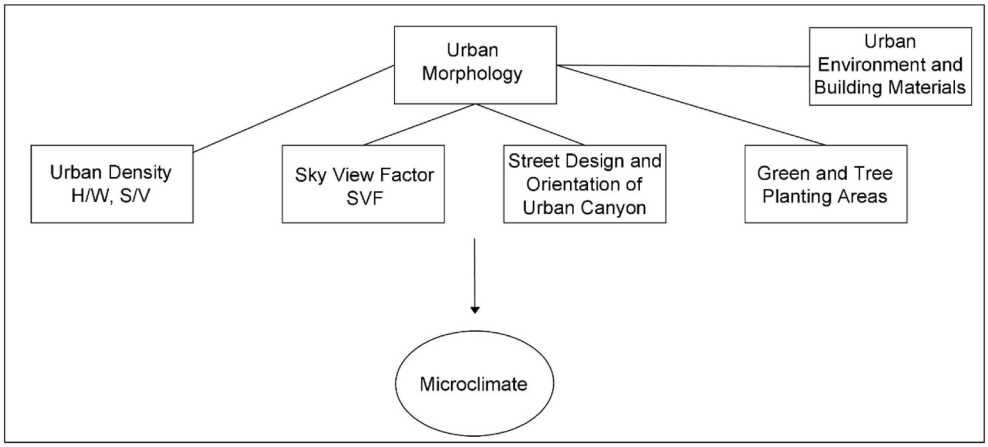

Fig. 11 Controlled factors related to urban morphology and influencing the formation of the microclimate, Source: Rafail-Kouklis and Yiannakou (2021)

Urban Canyon (UC)

At street level, the height of buildings with respect to the width of streets (also known as the aspect ratio) and the direction of the wind with respect to the street layout determine the nature of air flow within resultant canyons.(Emmanuel, 2005)
The urban canyon is a descriptive term for roads and pathways surrounded by the buildings, walls and roofs of an urban environment. This combination of roads and buildings essentially creates canyon-like structures that are subjected to many reflections. The geometry of an urban canyonwill affect the magnitude of radiation reaching street level and escaping back into the atmosphere(Santamouris, 2015).

The urban canyon of tall buildings and narrow streets trap heat, and prevent aircirculation (Rajgopalan, Jamei et al., 2014). The urban geometry is also the greatest man madeinfluence on wind flow characteristics through an urban zone (Memon, Leung and Liu 2010). Therefore,understanding the holistic effect of UHI mitigation measures on the entire urban street environment is animportant point of the current research. (Jamei et al. 2016).

Figure 12, summarises street geometry, built form, vegetation and the thermal properties of materials are the key levers to control urban climate at local scales.

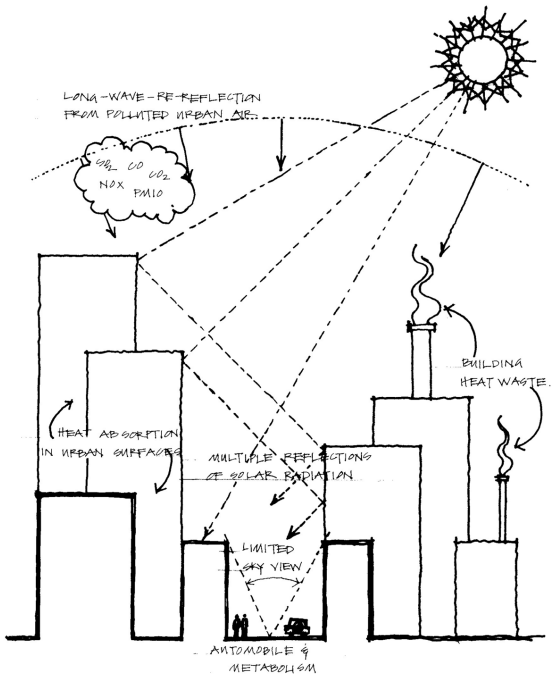

Fig. 12 Summary view of the factors affecting the urban climate. Source: Emmanuel (2005)

Morphology and Ventilation

Wind plays an important role in city climatology due to its relevance for urbanventilation and transport processes, such as heat and pollutant transport (Fernando et al,. 2010). Thus, understanding how to design urban ventilation patterns in order to improve wind flow is one of the key strategies for achieving good air quality , Urban Heat Island mitigation, and Outdoor Thermal Comfort (OTC) especially in densely-builturban areas (Buccolieri, R et al,. 2010)

The tall buildings of modern cities prevent air circulation and disrupt the convection of heat away from the city, which also prevents the dissipation of pollutants. In addition, many UHI mitigation techniques would be improved by circulating the cooler temperatures throughout the urban zone. Wind moves along paths of low surface roughness and it is therefore possible to model and predict wind paths. Computational fluid dynamics (CFD) provide a valuable tool for evaluating urban wind paths and the effect of water bodies on the urban environment (Memon, Leung and Liu 2010; Tominaga, Sato and Sadohara 2015).

Figure 13 illustrates the atmospheric processes acting across the meso-local-, and micro-scales within urban environments. As shown, urban morphology influences wind flow, heat distribution, and boundary-layer structure, from regional heat-island circulation down to street-canyon dynamics. These multi-scale interactions help explain how urban form affects microclimate and ventilation patterns. (Oke, 1987)

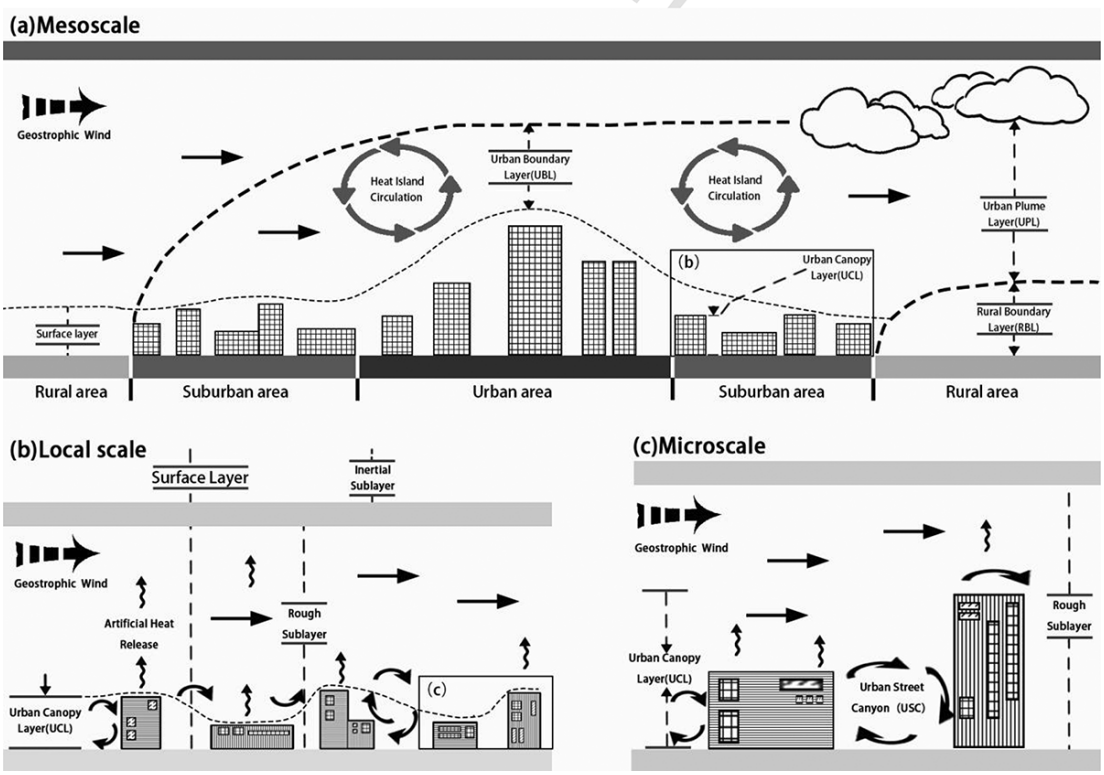

Fig. 13 Multi-scale atmospheric processes in urban environments, showing the interaction between wind flow, heat distribution, Source: Oke, Urban Environments, (1987)

1.2.4 Thermal Comfort

Generally, humans are comfortable within a relatively small range of temperature and humidity conditions, roughly between 20–26.7 °C and 20–80% relative humidity (RH), referred to on psychrometric charts as the "comfort zone." These provide a partial description of conditions required for comfort. Other variables include environmental indices – radiant temperature and rate of airflow as well as clothing and activity (metabolic rate). (watson,1983; Givoni, 1979)

The public space plays a key role in improving the quality of today's cities, especially in terms of providing places for citizens to meet and socialize in adequate thermal conditions. Thermal comfort affects perception of the environment, so microclimate conditions can be decisive for the success or failure of outdoor urban spaces and the activities held in them. (Tumini I. et al., 2016) Among many factors that determine the qualityof outdoor spaces, the urban microclimate is an important one. Pedestrians aredirectly exposed to their immediate environment in terms of variations of air temperature, relative humidity, wind speed, and solar radiation. Therefore, people's sensation of thermal comfort is greatly affected by the local microclimate (Chen, L., et al., 2011). There are different indices to measure the thermal comfort of pedestrians.

PET: The Physiological Equivalent Temperature (PET) is a notable example of a steady-state model. It is defined as the air temperature at which, in a typical indoor setting (air temperature = mean radiant temperature, relative humidity = 50%, wind speed = 0.1 m/s), the heat budget of the human body is balanced with the same core and skin temperature as those under complex outdoor conditions (Höppe, P., 1999). PET enables to compare the integral effects of complex thermal conditions outside with a person's own experience in indoors (Lin, 2009; Nikolopoulou, 2001).

UTCI: The Universal Thermal Climate Index is a state-of-the-art indicator that estimates the thermal stress the human body undergoes when exposed to outdoor conditions. The UTCI is an international index developed by the European Cooperation in Science and Technology (COST) Action 730. It is defined as the air temperature of a reference outdoor environment that would elicit in the human body the same physiological response (sweat production, shivering, skin wettedness, skin blood flow and rectal, mean skin and face temperatures) as the actual environment (Jen dritzky G, et al., 2012)

MRT: Mean Radiant Temperature is the uniform temperature of a fictive black-body radiation enclosure which would result in the same net radiation energy exchange with a human subject as the actual, more complex radiation environment. The MRT is a key required parameter for thermal environment ergonomics, as specified by the International Organization for Standardization (ISO 7726, 1998).

SET: Standard Effective Temperature is defined as the dry-bulb temperature of a hypothetical isothermal environment at 50% relative humidity (RH) in which a human subject, while wearing clothing standardized for the activity concerned, would have the same skin wettedness and heat exchange at the skin surface as they would have in the actual test environment (Gagge et al., 1986).

WBGT: The Wet-Bulb Globe Temperature is a heat stress index that combines the effects of air temperature, humidity, radiant heat, and air movement on human thermal comfort. It is calculated based on three factors: the natural wet-bulb temperature, globe temperature, and the air temperature. It is one of the most widely used heat stress indices globally, particularly for assessing heat exposure in occupational or sports settings (Mahgoub et al., 2020).

Microclimate Adaptation and Mitigation Strategies 1.3

1.3.1 Mitigation and Adaptation

Adaptation refers to the process of adjusting systems and practices in response to actual or expected climatic changes, with the aim of minimizing harm or capitalizing on beneficial outcomes (IPCC, 2022). According to the IPCC AR6, it is characterized as "the process of adjustment to actual or expected climate and its effects".
In urban environments, adaptation involves deploying a variety of measures ranging from natural solutions such as shade-bearing trees and water features to behavioral changes such as heat action plans and redesigning public spaces (Le et al., 2020 ; MDPI Climate Risk, 2022). These interventions primarily address the vulnerability of communities to heat stress and extreme weather events.

Mitigation in contrast, involves reducing the sources or enhancing the sinks of greenhouse gases in order to slow the pace and magnitude of global warming, as defined by the IPCC AR6 Working Group III ("a human intervention to reduce emissions or enhance the sinks of greenhouse gases") (IPCC AR6 WGIII, 2022). In the context of Urban Heat Island research, mitigation strategies take the form of cool roofs, high-albedo pavements, green infrastructure, and energy-efficient urban design, which collectively reduce heat retention, improve surface reflectivity, and lower building energy demands. (Jong et al., 2013) review finds that reflective surfaces and green roofs can decrease ambient temperatures by several degrees, both by reducing daytime heat storage and minimizing radiative heat flux at night.

While often treated separately, adaptation and mitigation are interconnected strategies that, when combined, foster stronger urban resilience. (Lee et al., 2020) demonstrate this synergy: cities with robust mitigation programs are significantly more likely to adopt complementary adaptation measures, as their institutional frameworks and financing channels are often shared. With the term 'adaptation', we mean the regulation in human or natural systems to the stimuli or their effects coming from the climate change in progress, aiming to moderate its damage or exploit its benefits (IPCC, 2007). On the other hand, through 'mitigation' policies, the action is taken directly on the causes of climate change; efforts in this regard aim to reduce the release of climate-changing gases into the atmosphere. (Pollo and Trane, 2021)

The analyses by (Lee et al., 2020; Biesbroek et al., 2008), examining the relationship between adaptation and mitigation, shows that these two climate responses operate through fundamentally different logics.

Adaptation is characterized by short-term, place-specific actions that address immediate climatic impacts and are largely managed at the local or regional level. In contrast, mitigation requires long-term planning, global coordination, and sustained policy commitments, with benefits that emerge only after decades due to the long atmospheric lifetime of greenhouse gases (IPCC, 2007; Klein et al., 2007).

Dimension	Mitigation	Adaptation
Temporal	Long-term (future decades/ centuries)	Immediate
Spatial	From the national to global one	Almost local (micro-urban, urban, regional)
Economic	Short and long-term investments,deferred over time	Mostly short-term investments
Politic and collaborative	Involvement of the major GHG emitters (global level) and policymakers (national level) Conscious participation/collaboration of the populations is necessary Fields involved: energy production, transport, industry	Involvement of policymakers at local (urban, regional) and national level Fields involved: city project and territorial governance, coastal zone protection, risk and emergency management
Psychological and social	Barriers related to: Limited cognition; Ideological beliefs; Comparison with others; Sunk costs; 'Discredence', radical scepticism; Perceived risks. Limited behaviours	

This asymmetry means that even strong mitigation efforts cannot remove the necessity for local adaptation, particularly within the micro-urban scale where heat stress and climate risks manifest most directly (McEvoy et al., 2006)

Adaptation and mitigation differ not only in purpose but also in temporal reach, spatial relevance, and institutional responsibility. The comparative table 1, adapted from Pollo and Trane (2021), synthesizes these distinctions and provides a clear framework for understanding how the two approaches function within urban climate strategies.

Adaptation feat Mitigation Approach
Immediate and Long-term
Local (micro-urban, urban, regional), national, global
Short and long-term investments, deferred over time
Involvement of policymakers at local (urban) and national level Conscious
participation/collaboration of the populations is necessary
Fields involved: city planning and territorial governance, coastal zone protection, risk and emergency management
Need to adopt an intergenerational approach
Possibility to overcome some of the barriers thanks to: Perception of the immanence of risk and the effectiveness of actions undertaken to contrast it Perception of the need to cure the territory
Awareness of the mitigation influence policies on future scenarios; Involvement of the inhabitants in solidarity actions beyond the emergency

Table 1- Adaptation and mitigation approaches for Microclimate, Source: Pollo and Trane (2021), Smart Urban Metabolism towards the Ecological Transition

The figure 14, illustrates some of the common mitigation measures. Many measures have been developed over time,and some of the key measures are outlined in this review. These include designing cool pavements by increasing the albedo of surfaces and making them more reflective, permeable, porous and waterretentive; the increased utilisation of green spaces within our urban landscape (Gorsevski et al., 1998; Santamouris 2013), and harnessing the cooling effects of wind and water.

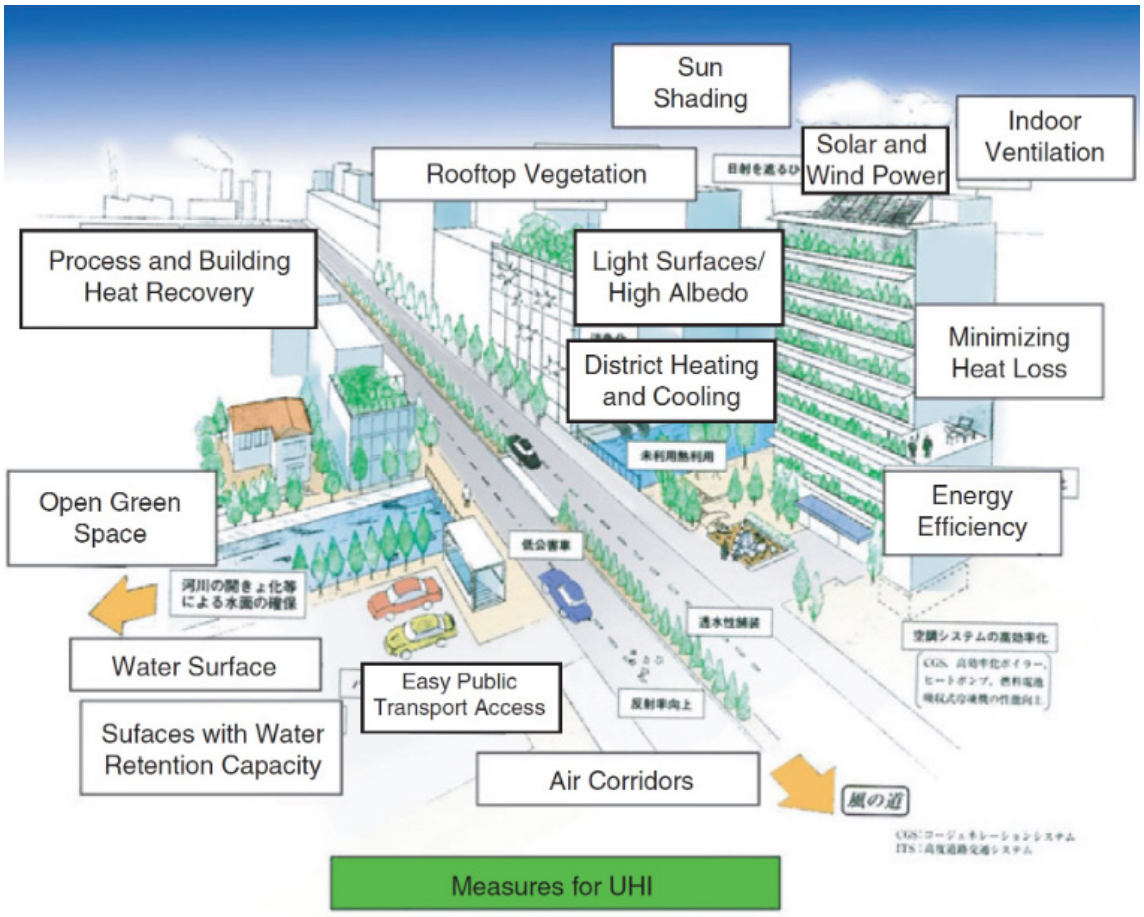

Fig. 14 Mitigation Measures for the Urban Heat Island – Source: Ichinose, Matsumoto and Kataoka (2008).

1.3.2 Surface and material based solutions

Materials with high albedo values, capable of reflecting a substantial portion of incoming solar radiation, present a promising avenue for UHI mitigation (Nazarian, N et al., 2019). However, the heterogeneity of urban environments, composed of a vast array of materials, presents a significant challenge for systematically identifying and analyzing these surfaces on a large scale. Although most building materials exhibit high long-wave emissivity, it's the variability in albedo that notably affects mean radiant temprature.

However, several studies caution that while high-albedo materials effectively reduce surface temperatures, the increased reflection of shortwave radiation can elevate pedestrian-level radiant loads and, in some configurations, contribute to indoor heat gains—highlighting that high reflectance does not always translate into improved outdoor thermal comfort (Santamouris, 2013; Levinson & Akbari, 2010; Taleghani, 2018).

Pavements

Reflective or "cool" pavements materials and coatings with elevated solar reflectance are among the most widely studied and cost-effective interventions for lowering pavement surface temperatures and reducing sensible heat release to the urban environment (Synnefa et al., 2006/2011; Qin, 2015; Rossi et al., 2014). By increasing surface albedo, cool pavements reduce surface temperatures and can lower local radiant loads, which may also translate into reduced building cooling demand in favorable configurations (Santamouris, 2013; LBNL, 2019). Reflective pavements can be implemented as new high-albedo aggregates or as surface coatings, allowing retrofit of existing pavements in some locations (Qin, 2015; Kappou et al., 2022).

However, field studies and reviews emphasize several important caveats. First, the effect of cool pavements on air temperature at neighborhood scale is often small or inconsistent and depends on coverage area, urban geometry, and atmospheric conditions (LBNL, 2019; Santamouris, 2013). Second, increased reflection can cause glare and redirect shortwave radiation onto adjacent façades or through windows, with potential negative impacts on pedestrian comfort and building heat gains in specific settings (LBNL, 2019; Rossi et al., 2014).

Third, the effective albedo of pavement surfaces degrades with soiling and wear; solar reflectance may decline substantially over time, requiring maintenance or re-application (LBNL, 2019; Qin, 2015). Finally, some reflective coatings have higher embodied energy or lifecycle GHGs than conventional surfaces, so net climate benefits depend on material choice, durability, and maintenance regimes (LBNL, 2019; Giorio et al., 2023).

Quantitative estimates of global mitigation potential should be treated with caution but are useful for scale illustration. For example, Sanjuán et al. (2021) calculate that hypothetically covering a 4.72 km^2 central zone of Madrid with very high-albedo surfaces (albedo > 0.5) would correspond to a large equivalent CO_2 reduction figure (reported as ~0.43 $GtCO_2$/yr in that paper), a value that stems from a simplified radiative-forcing CO_2 equivalence and should therefore be read as illustrative rather than directly realizable without further system-level life-cycle accounting. In practice, cities should prioritize cool pavement deployment in high-exposure pedestrian areas and large impervious surfaces (e.g., parking lots, plazas), pair coatings with shading and permeable designs, and account for maintenance, glare, and life-cycle impacts when selecting products (LBNL, 2019; Santamouris, 2013).

Façades

The mitigation potential of cool facades has attracted important consideration in recent years. This might be due to the fact that in the process of urbanization, many cities in the world show a three-dimensional development trend of intensive and tall buildings. Building facades occupy an increasing proportion of the surface area. For example, in Xi'an City, the proportion of middle/high rise buildings has reached more than 30% (He et al., 2019). The thermal impact of building facades might be more significant compared to that of roofs. After facades retrofit measures, a reduction of building energy consumption by 20%–30% was believed to be possible (Xu , 2019). Therefore, studies on building facades are of great importance to improve the thermal performance of buildings, decreasing the energy consumption and alleviate UHI effects.(Hong et al., 2022) During the daytime, solar reflectance is the dominant factor while emissivity has little effect on the surface temperature. During the nighttime, emissivity influences the thermal performance of the building facades more significantly than the reflectance (Santamouris et al., 2011).

Although a reduction in building energy consumption can be achieved by changing the surface emissivity, modifying the solar reflectance is still believed to be a more effective retrofit measure (Alonso et al., 2016).
(Bishara et al., 2017), have found that low total solar reflectance coatings result in high facades surface temperatures, and high-reflectance pigments could lower the surface temperature by more than 10°C. (Taleghani el al., 2021) found that high-reflectance facades could lead to a decrease in the PET value by about 1°C in the neighbourhood which improves the pedestrian thermal perception during the summertime.

1.3.3 Green Infrastructure

The microclimate-friendly effects of trees are most effective when vegetation is arranged in clusters rather than isolated individuals, as grouped canopies create larger shaded zones, enhance evapotranspiration, and enable greater reductions in surface and air temperatures (Shashua-Bar & Hoffman, 2000). Tree groupings also influence wind behavior: studies show that clustered vegetation can act as a porous barrier that disrupts hot airflow and reduces local wind-driven heat transport, thereby improving pedestrian-level thermal comfort (Bowler et al., 2010). The lack of dense tree clusters and shading within open areas prevents the formation of this protective barrier against hot wind flow, resulting in higher thermal loads and uncomfortable microclimatic conditions (Ozalp, 2022).
Beyond cooling, increased vegetation contributes to broader environmental-impact mitigation. A higher amount of greenery reduces urban heat, limits smog formation (Gorsevski et al., 1998), lowers reflections and glare, and improves subjective thermal comfort for residents (Mullaney et al., 2015; Lau et al., 2016). The heat-related health impacts are also minimized when vegetation is prevalent, reducing heat-stress mortality and vulnerability during extreme heat events (Frumkin et al, 2010; Tan et al., 2015).
Green infrastructure also promotes energy savings: shading from trees can lower cooling energy demand in adjacent buildings by 10–30%, depending on species and canopy density (Akbari et al., 2001). There are many ways to increase the prevalence of vegetation in an urban zone, including expanding parks, introducing private gardens, planting street trees, and implementing green roofs and rooftop gardens.

1.3.4 Building-Integrated Strategies

Although buildings are major contributors to urban heat, they also present substantial opportunities for mitigation through the decarbonisation of the built environment. The concept of Green Buildings has emerged as a key strategy in this transition, integrating design and technological measures that improve energy performance and reduce environmental impact. Numerous studies including (Santamouris, 2014; Akbari et al. 2001; Salvati et al. 2019) demonstrate that Green Buildings mitigate urban heat through several mechanisms: reducing operational carbon emissions, increasing surface reflectivity and vegetative cover, decreasing the thermal storage of artificial materials, and enhancing building energy efficiency. Collectively, these approaches contribute to both lower indoor cooling demand and reduced outdoor heat accumulation. Recent evidence further indicates that Green Buildings can play a significant role in alleviating UHI intensity by minimizing waste heat, incorporating green roofs and façades, and promoting low-carbon material choices (Rastinifard et al., 2024).

1.3.5 Nature Based Solutions

Nature-based Solutions are defined as actions to protect, sustainably manage, and restore natural or modified ecosystems, that address societal challenges effectively and adaptively, simultaneously providing human well-being and biodiversity benefits (IUCN, 2016), They are increasingly recognized as strategic tools to tackle urban environmental challenges by leveraging ecological processes and natural infrastructure. Defined broadly as interventions that utilize ecosystems to address pressing societal needs while delivering biodiversity and human well-being benefits (UNEP, 2022), NBS play a key role in mitigating the Urban Heat Island (UHI) effect. Urban areas that integrate green and blue infrastructures such as urban forests, vegetated roofs, wetlands, and water-sensitive design—can significantly reduce surface and air temperatures through evapotranspiration, shading, and increased reflectivity (EEA, 2021).

These solutions also enhance resilience to climate extremes, support carbon sequestration, and contribute to healthier urban living environments (Kabisch et al., 2016). The effectiveness of NBS depends on their contextual integration; landscape structure, urban morphology, and climatic conditions all influence outcomes (Demuzere et al., 2014).

When embedded in urban planning frameworks and supported by inclusive governance, NBS can promote long-term sustainability by combining environmental, social, and economic co-benefits (Frantzeskaki, 2019).

Examples of NbS interventions include the conversion of underutilized land into pocket parks, planting tree corridors along major avenues, and restoring degraded riparian zones in dense city cores. By providing nature-driven thermal regulation and creating climate-adaptive urban spaces, NBS offer a viable pathway for cities aiming to reduce heat stress and improve quality of life.

A hypothetical scenario of an NbS is shown in Figure 15, This case illustrates two important points about NbS interventions: (i) they can complement other measures, and (ii) they can involve the use of natural areas or conservation measures that were originally established for a purpose other than that of the NbS (IUCN, 2016).

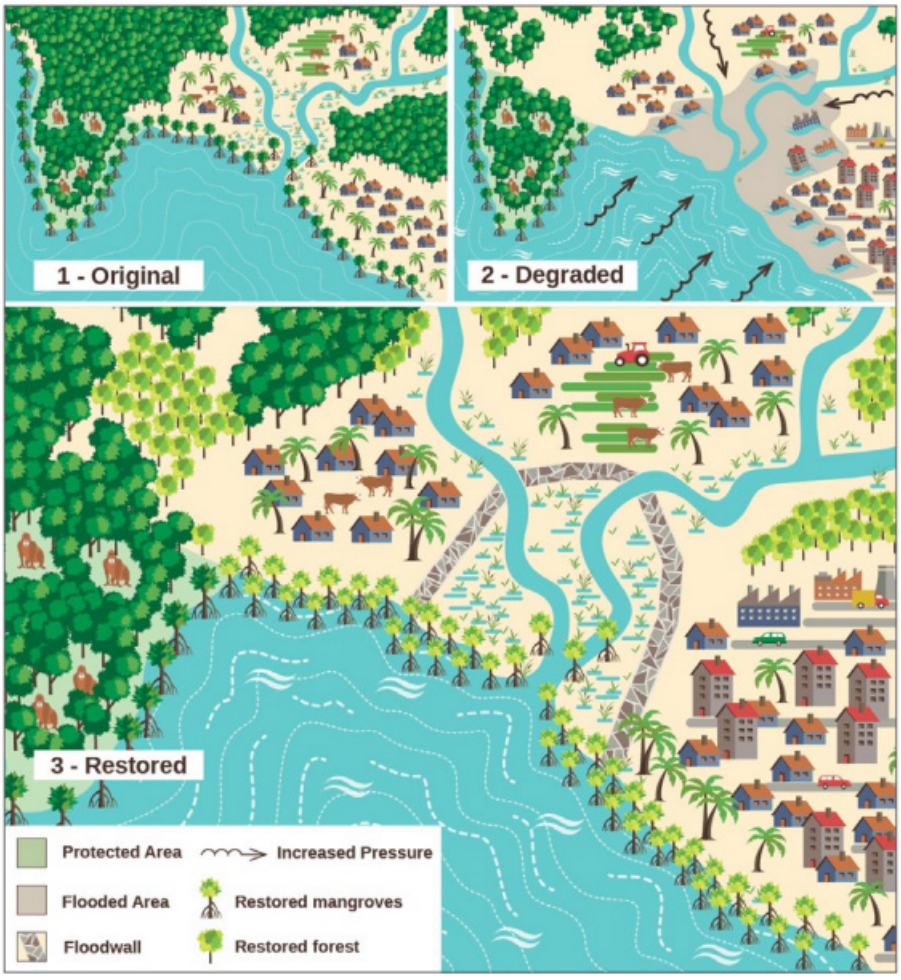

Fig. 15 Hypothetical scenario of Nature-based Solutions being used in conjunction with infrastructure development and protected area conservation, Source: IUCN, 2016

The UN's Sustainable Development Goals, the New Urban Agenda, and the Paris Agreement all underscore the need for cities to integrate nature-based solutions that enhance thermal comfort, reduce climate risks, and improve overall urban livability. However, while these frameworks offer broad strategic direction, cities often struggle to translate such high-level aspirations into concrete, measurable planning standards. One widely adopted principle that operationalizes these goals at the local scale is the 3–30–300 rule, proposed by urban forestry expert Cecil Konijnendijk (2021). This rule recommends that every person should be able to see at least three trees from their home; every neighborhood should achieve at least 30% tree canopy cover; and every resident should live within 300 meters of a high-quality green space. (Figure 16)

By providing clear quantitative thresholds, the 3–30–300 rule bridges the gap between international climate resilience objectives and practical, implementable urban greening strategies.

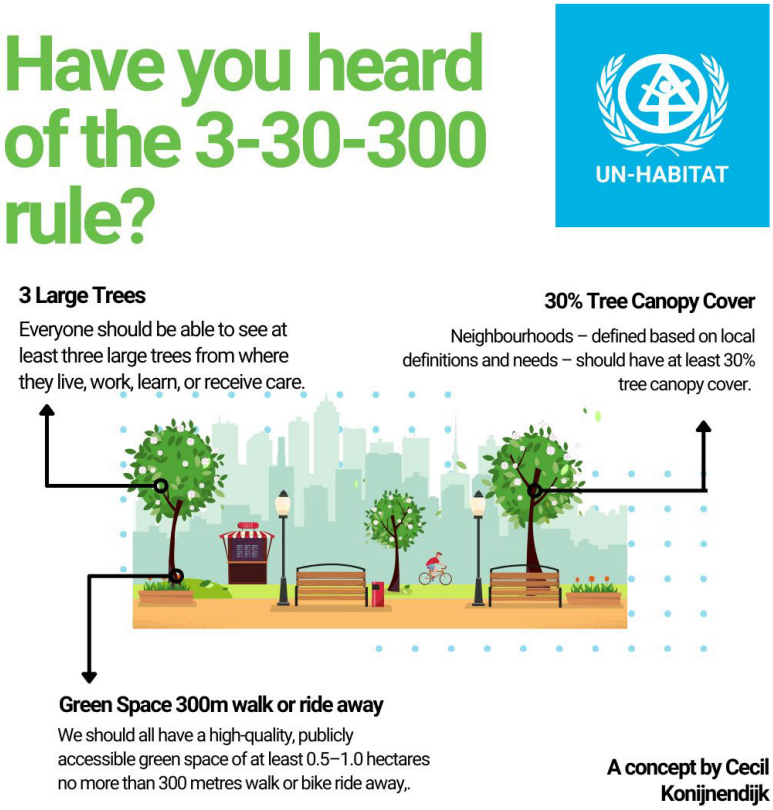

Fig. 16 3-30-300 Regulation By Dr. Konijnendjik, Suorce: 2024 World Cities Report on strategies to build nature and resilience into our cities

Analactycal Tools and Climate Modeling

1.4

1.4.1 The importance of utilizing climate modeling tools

Numerical models are essential tools for analyzing urban climate for engineers, architects, urban planners, and policymakers. This is because climate-sensitive urban planning needs to be predictive to account for different urban forms and climates (Erell, 2008). Numerical models enable built environment professionals to compare different urban design alternatives (Toparlar et al, 2017) Also, numerical models have the potential to simulate the study areas under varying meteorological conditions.

The development of simulation models can thus provide suitable urban planning measures based on the knowledge of urban human biometeorology (Lee et al., 2016). Recent years have witnessed an increased research interest in urban climate at varied spatial scales (Lauzet, et al., 2019). Numerical models can be broadly categorized into three categories on the basis of spatial scale (Mirzaei, 2015).

Building-scale models focus on isolated buildings, thermal comfort, indoor air quality, etc. These Building Energy Models (Prataviera, et al., 2021) are based on energy balance applied to the building volume.

Micro-scale models focus on the neighborhood scale and are mostly used in thermal comfort studies. The interaction between the building and its surroundings is the basis of the development of microclimate models. Different model types ranging from simple geometrical models to complex Computational Fluid Dynamic and Large Eddy Simulation models can be categorized to micro-scale models. These models are mostly utilized by scientists and architects.

City-scale models are much coarser in resolution and are used to evaluate urban scale policies to mitigate heat island effects. For parameterization of various urban features, such as vegetation and building density at the meso-scale, single- and multi-layer urban canopy models are often applied (Kwok, et al., 2021).

With regards to urban micro-climate and heat island considerations, several commercial tools/models are available, namely: RayMan (Wang et al., 2024), ENVI-met and CitySim (Miller et al., 2018). RayMan is mainly used for radiation calculation and human thermal comfort assessment, with more attention on thermal comfort in specific locations rather than the micro-climatic system in an urban space. According to (Lin et al., 2024), ENVI-met shows high accuracy in local climate simulation, but incurs high computation cost in handling large-scale urban blocks. CitySim is more oriented to building energy consumption simulation and does not fully assess the overall impact of climate change (Wang et al., 2024).

Among available tools, the ENVI-met model is widely regarded as one of the most effective for simulating the spatial distribution of thermal parameters across diverse climatic contexts and urban morphologies, including variations in building configurations and vegetation types (Zhang et al 2022; Kotharkar et al., 2024).

ENVI-met has demonstrated strong performance in numerous studies assessing the thermal exchange processes between vegetation, buildings, and the ground surface under different scenarios. For instance, it has been employed to simulate the thermal benefits of trees (Morakinyo et al.,2018). evaluate the cooling effects of different green roofs16, and analyze the thermal environment in specific urban spaces such as parks17 and school courtyards18. Moreover, its application in community-scale thermal comfort studies (Crank et al., 2023) highlights its value in shaping public space design and renewal.

1.4.2 ENVI-met

ENVI-met. ENVI-met is a Computational Fluid Dynamics 3D microclimate modeling software based on the fundamental laws of fluid dynamics and thermodynamics (Sharmin et al. 2017). It was designed by Professor M. Bruse in 1994 and has been under constant development and scientific expansion ever since. The software uses an urban weather generator to predict the meteorological parameters based on which the most probable weather conditions are recreated (Bande et al. 2019).

It reconstructs the microclimate dynamics of the urban environment through the interaction between climate variables, vegetation, surfaces and built environment (Bruse and Fleer 1998). ENVI-met simulates the atmosphere processes such as air flow, air temperature, humidity, turbulence, radiation fluxes and calculates the indexes and factors of comfort in the urban area - such as Physiological Equivalent Temperature, Predicted Mean Vote, Universal Thermal Comfort Index, and many others (Trane et al. 2023).

The software is grid-based and has high temporal and spatial resolution, allowing accurate microclimate analysis up to a street level. Due to holistic approach and complexity of the calculations, ENVI-met has certain limitations, mostly regarding the computation time with high space resolution and wide simulation domains, and the high temporal resolution of meteorological data needed (30-minute timesteps for full forcing mode) (Trane et al., 2023).

Chapter 02

Best Practices

2.1 Design and Research Practices

2.1.1 Super Blocks (Sant Antoni area)
2.2.2 Viale Carlo Felice gardens
2.2.3 Mitigation Effects of UHI in a Historical Center in Teramo
2.2.4 Virgen del Carmen Neighborhood

2.2 Overview

2.1 Design and Research practices

2.1.1 Super Blocks (Sant Antoni area)

Location: Barcelona, Spain
Year: 2019
Architect: Leku Studio
Area: 16180 m^2

The Superblocks program is a city-wide strategy that reorganizes traffic to reclaim streets for people, greenery, and local micro-climate comfort. It's big in ambition, but for the purposes of this thesis the focus is on the Sant Antoni area, where before/after micro-climate simulations with ENVI-met have been conducted. In Figure 17, the program's map is represented in the city scale and the Sant Antoni area which is the focuse of this case study, is shown.

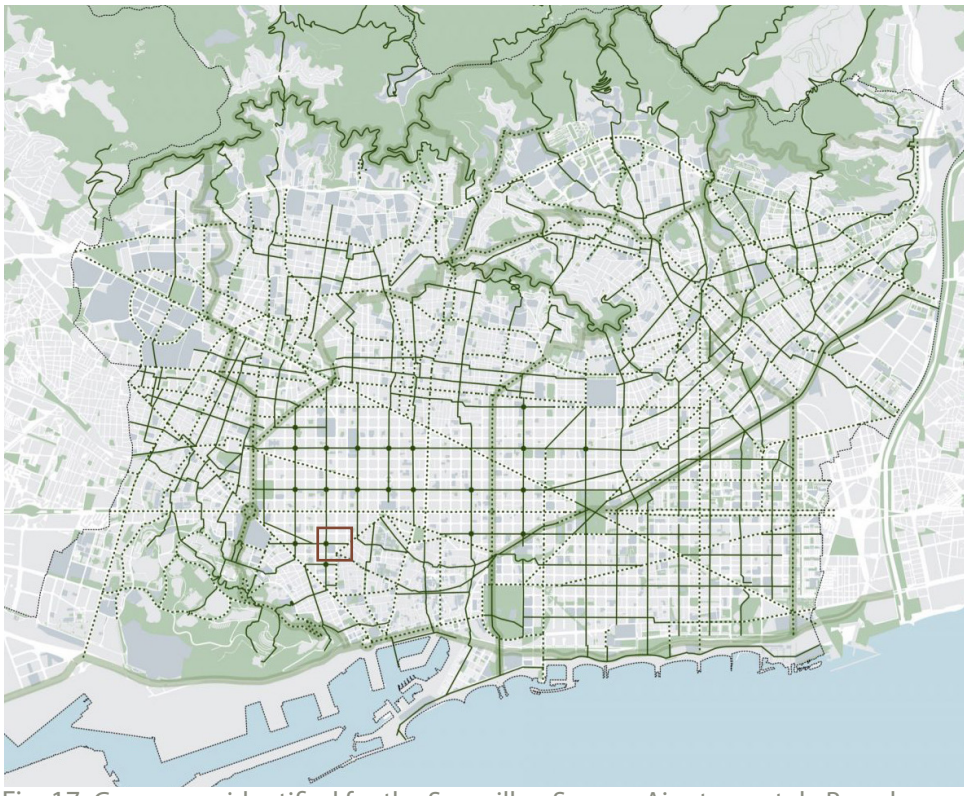

Fig. 17 Green axes identified for the Superilles, Source: Ajuntament de Barcelona

Eixample's regular grid and high density mean heavily paved surfaces, heat build-up, and limited shade. Before the intervention, carriageways and parking dominated the public realm; asphalt and darker finishes amplified radiant loads at street level. The municipality's broader Superblocks plan aims to reverse that by diverting through-traffic to the perimeter and converting inner streets into green, low-speed public spaces.
The figures 18 and 19 represent the Sant Antoni area, before and after the implementation of the strategies.

Fig. 18 Super Blocks (Sant Antoni area) Bfore and after implementatipon of strategies, Source: Archdaily

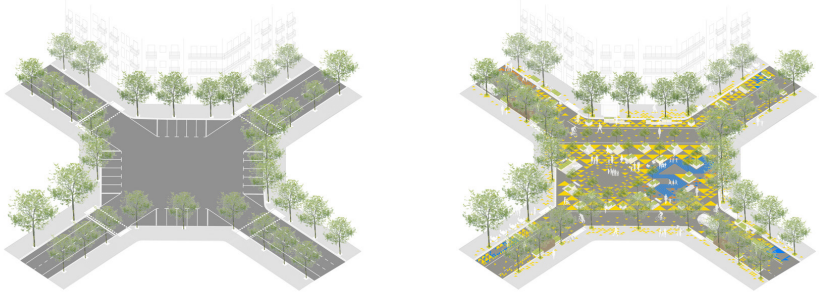

Fig. 19 Super Blocks (Sant Antoni area) Bfore and after implementatipon of strategies diagram, Source:Leku Studio project webpage

Design Strategies

Reprogramming the street section

Inner streets around the Sant Antoni Market were pedestrianized and leveled with sidewalks to create continuous ground planes for people, events, and markets. (Figure 20)

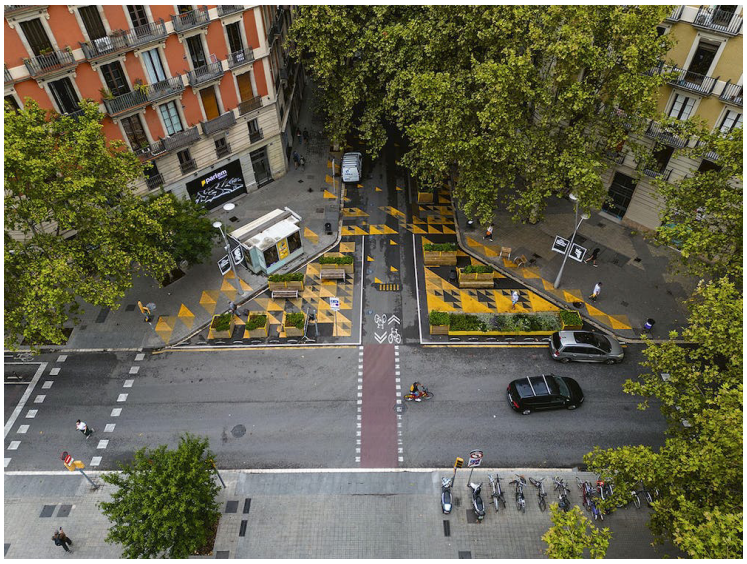

Fig. 20 Photos after interventions on the streets of Sant Antoni area, Source: leku studio webpage

High-albedo, light pavements

Dark surfaces and a peripheral dark roofed area around the market were removed; lighter, more reflective ground finishes were introduced to reduce surface heat. Figure 21, shows the area after the implementation of this strategy.

Fig. 21 Photos after interventions on the streets of Sant Antoni area, Source: leku studio webpage

Shading + vegetation

Trees, planters/flowerbeds, and light modular shading structures were added to create pockets of shade and evapotranspiration. The plan and section of the area after implementing this strategy are shown in Figure 22.

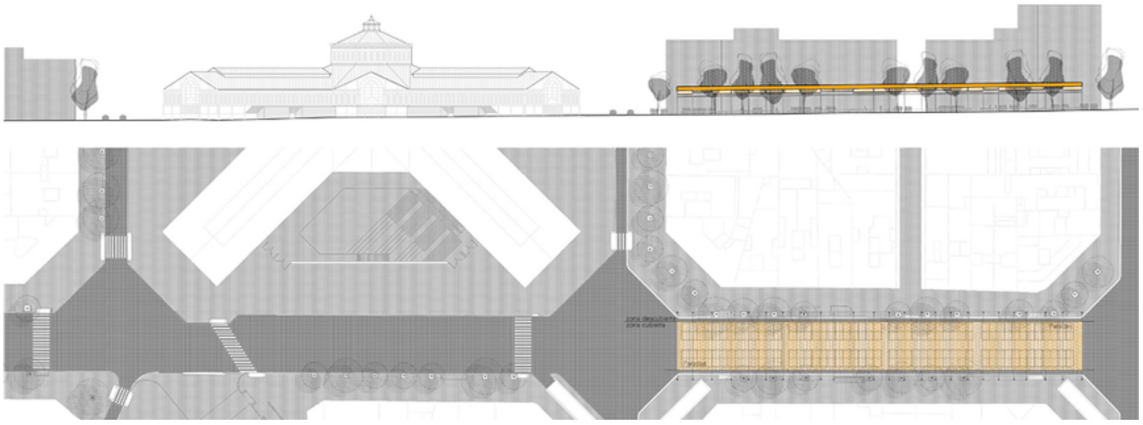

Fig. 22 Section and a plan view of Sant Antoni area showing the shading system, Source: leku studio webpage

Flexible, modular urban furniture

A reversible "kit" (patterns, signage, modular elements) supports phased rollout and easy adjustments, turning former traffic junctions into plazas and green healthy streets. (Figure 23)

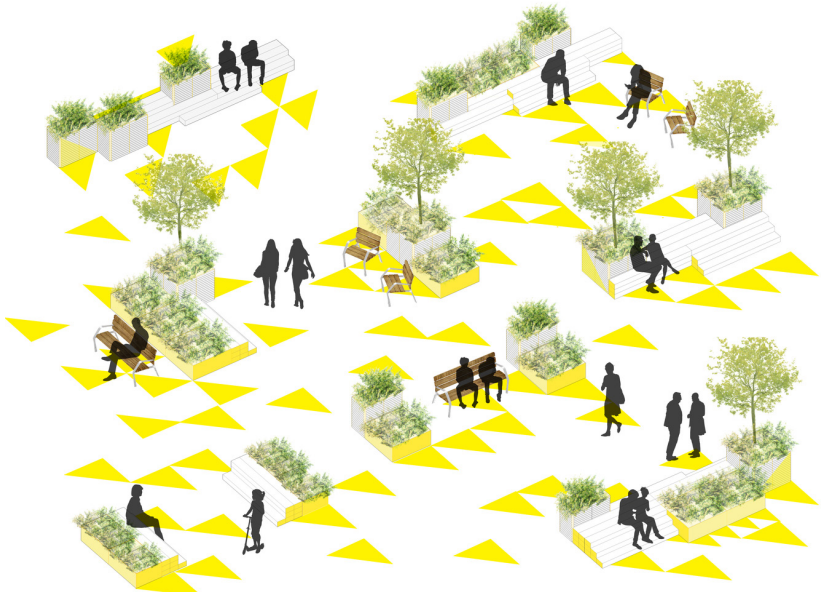

Fig. 23 Isometric view showing modular urban furniture designed for the Sant Antoni area, Source: leku studio webpage

Microclimatic Analysis

The microclimatic effects of the Superblock intervention in the Sant Antoni area have been assessed through ENVI-met simulations conducted by Kume et al. (2020). Using detailed three-dimensional models of the block around the Sant Antoni Market and measured weather forcing for hot, clear summer days (late July to early August), the study compared pre- and post-intervention scenarios. This approach made it possible to quantify how changes in pavement materials, vegetation, shading, and traffic circulation translated into differences in pedestrian-level climate conditions.

The main urban characteristics before and after the intervention are summarized in Table 2.

Urban characteristics of Sant Antoni area

	Before interventions	After interventions
Average pavement albedo	0.1710	0.1961
Tree coverage	11.43%	12.83%
Grass coverage	0.60%	1.05%
Asphalt Area	73,483m^2	57,453m^2
Average building height	19m	-
Building density	0.50	-
Vertical to horizontal	0.95	-

Table 2 Urban charascteristics of Sant Antoni area, table provided by the author, Data source: Eduardo Vidal-Kume, Edward Ng, and collaborators (2020)

Air temperature: The ENVI-met simulation of air temperature at 1.5 m height (pedestrian level), in Figure 24, illustrates the climatic improvement brought by the Sant Antoni Superblock.daytime average drop of about 0.6 K within the Superblock.
The comparison map (Figure 25), highlights that most of the pedestrian areas experienced lower daytime air temperatures.

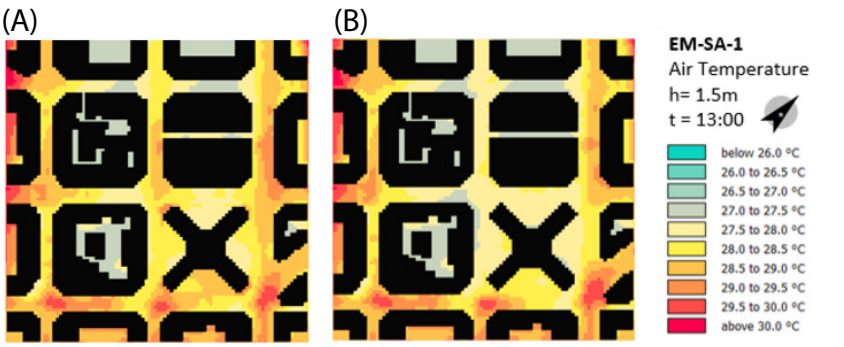

Fig. 24 ENVI-met 2D air temprature results, (A):before and (B):after interventions, Source: Vidal-Kume E, et al., (2020)

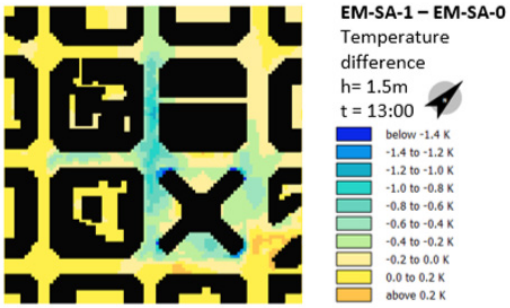

Fig. 25 ENVI-met 2D air temprature results, Comparison chart, Source: Vidal-Kume E, et al., (2020)

Ground surface temperature: local reductions up to ~20 K under new shade / lighter pavements; about 10 K average daytime decrease across the intervention area.(Figure 26-27)

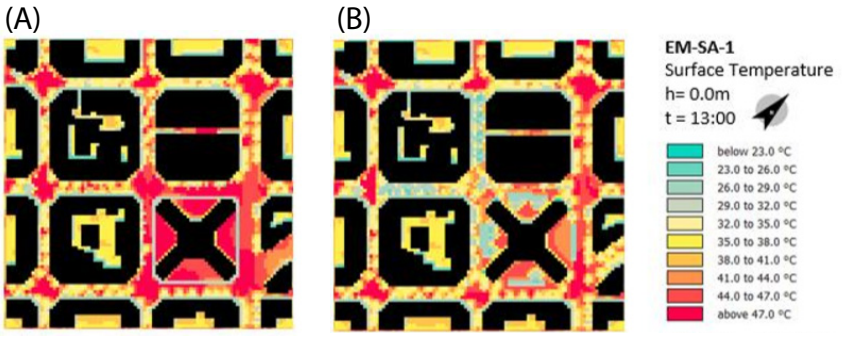

Fig. 26 ENVI-met 2D surface temprature results, (A):before and (B):after interventions, Source: Vidal-Kume E, et al., (2020)

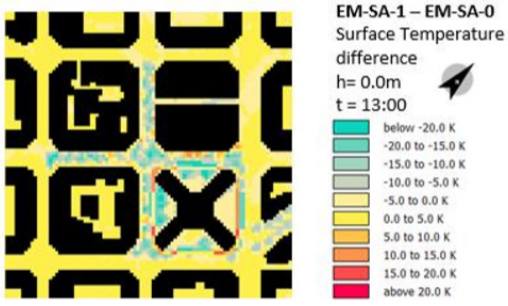

Fig. 27 ENVI-met 2D surface temprature results, Comparison chart, Source: Vidal-Kume E, et al., (2020)

Wind & humidity: slight decrease in air speed at 1.5 m where trees densified (peak ~0.9 m/s at 13:00 locally; ≈0.18 m/s on average) and a relative humidity increase up to ~3.8% at peak daytime.(Figure 28-29)

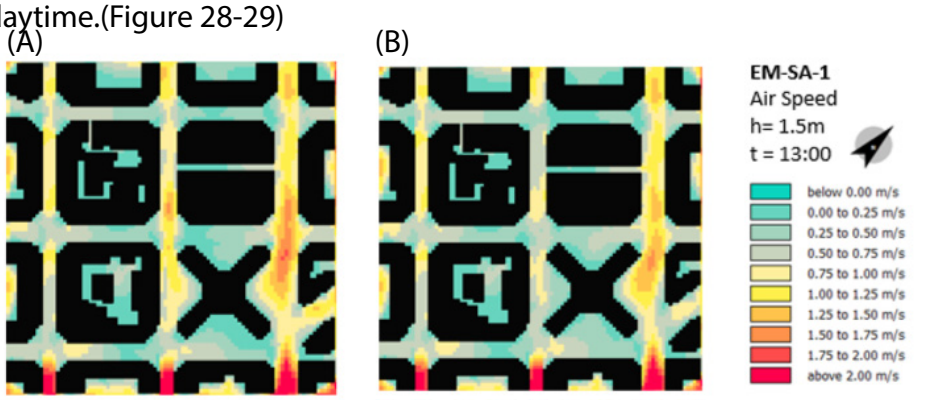

Fig. 28 ENVI-met 2D wind and humidity results, (A):before and (B):after interventions, Source: Vidal-Kume E, et al., (2020)

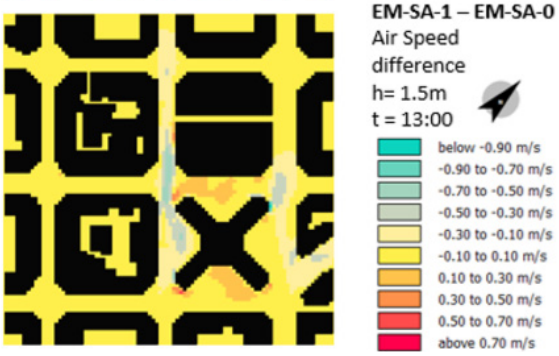

Fig. 29 ENVI-met 2D wind and humidity results, Comparison chart, Source: Vidal-Kume E, et al., (2020)

Thermal comfort (PET): up to ~12 K reduction at 13:00 in shaded zones; ~5 K average daytime drop across the area. A tiny ~0.2 K PET rise was observed at night (likely due to lower wind and slightly higher humidity despite small air-temperature gains). (Figure 30-31)

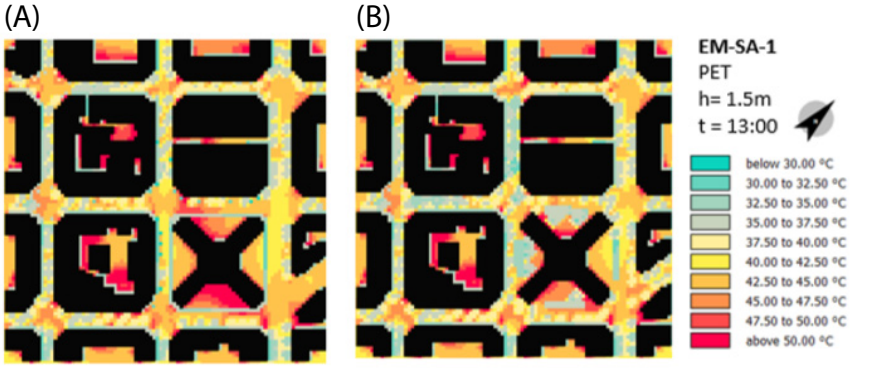

Fig. 30 ENVI-met 2D PET results, (A):before and (B):after interventions, Source: Vidal-Kume E, et al., (2020)

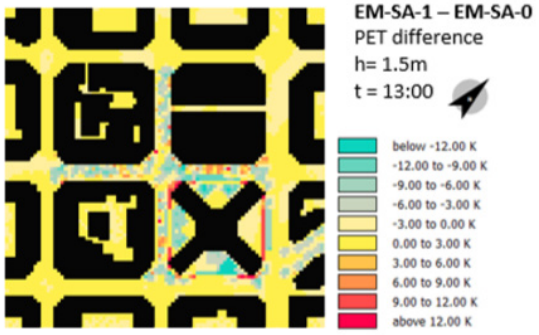

Fig. 31 ENVI-met 2 PET results, Comparison chart, Source: Vidal-Kume E, et al., (2020)

Results

More shade lowers mean radiant temperature for people in the sun.

Higher albedo pavements reflect more short-wave radiation, reducing ground surface temperatures.

Vegetation adds evapotranspiration (localized air-temperature and MRT relief) and wind tempering.

Traffic calming / removal reduces anthropogenic heat and allows the micro-climate benefits to dominate at pedestrian height.

The visual form of results can be seen in Figure 32, which shows the area before and after the strategies implementation.

Fig. 32 streets around the Sant Antoni Market before, and after interventions
Source: leku studio webpage

2.1.2 Viale Carlo Felice Gardens

Location: Rome, Italy
Year: 2024
Authors: Ahmed et al.
Area: 48800 m^2

This design case study demonstrates how the integration of vegetation, shading structures, and cool paving materials can reduce urban overheating in a dense historical area of Rome. The microclimatic simulations highlight how evidence-based design can guide climate-responsive urban renewal. The approach offers a transferable model for other Italian cities, including Turin, where similar climatic and morphological conditions exist. In Figure 33, the case study area is shown from an aerial view.

Fig. 33 Aerial view of Master plan map of the existing case of Viale Carlo Felice Gardens, Source: Google Maps," 41° 53' 12.1" N 12° 30' 38.5"

This project investigates a public open space in Rome the Viale Carlo Felice Gardens, as part of a broader effort to mitigate the urban heat island (UHI) effect and to enhance outdoor thermal comfort under extreme summer conditions.
The objective is to provide a design-informed, bioclimatic-sensitive masterplan for the gardens, showing how tactical interventions (greening, cool materials, shading structures) can be tested, quantified, and visually communicated.

The study sets up two major scenario types (baseline/existing and redesigned) to assess the effect of design interventions on microclimatic parameters.

Baseline (Existing Condition) Scenario

The current layout of the gardens and surrounding space, with existing tree canopy, paving materials, furnishings, and shade structures.(Figure 34) The model captures the dominance of impervious surfaces, limited vegetation, and exposure to solar radiation due to the open nature of paths and plazas.

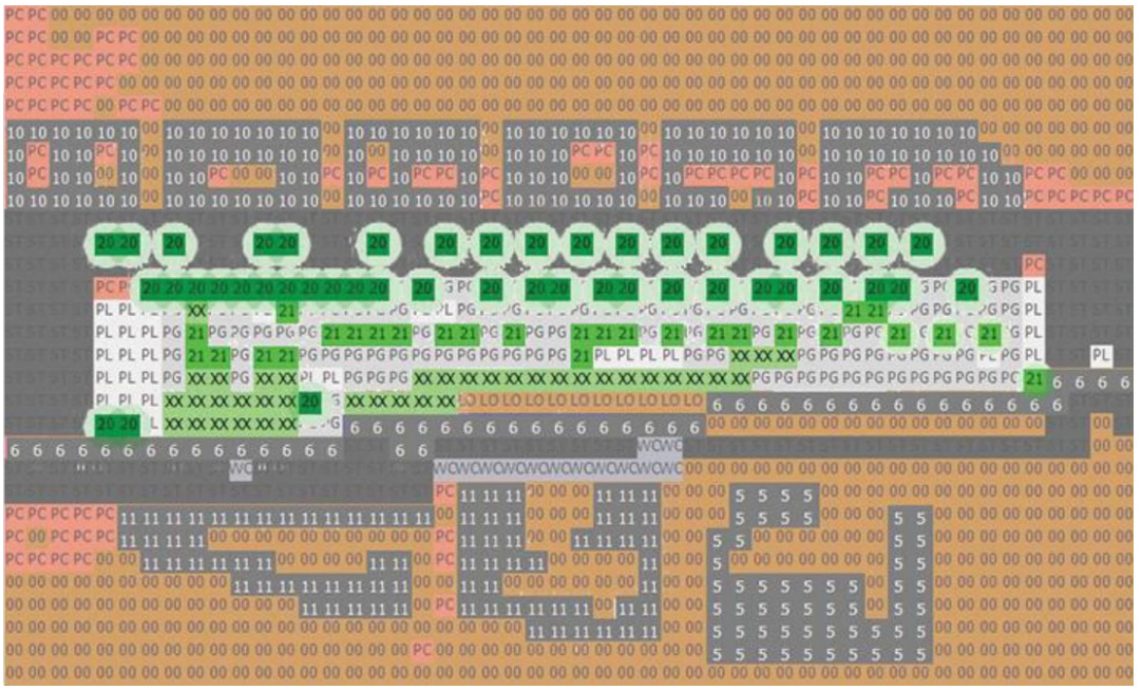

Fig. 34 Input environmental data and digitized model set for the base svenario simulation software ENVI-met v.5.1.5. Source: Ahmed, et al., 2024

Design / Intervention Scenario

The proposed redesign includes a combination of strategies: increased vegetation (native, low-water trees/shrubs), optimized tree placement to manage shade paths, replacement of standard paving with cooler, higher-albedo materials, addition of water features (fountains, splash zones) as localized evaporative cooling, and shading structures (pergolas, canopies) above gathering zones and pedestrian paths. (Figure 35)
These interventions are input into ENVI-met to create a "renovation" scenario. The model then compares thermal comfort metrics against the baseline to assess benefit.

Fig. 35 Master Plan of Viale Carlo Felice Gardens after the redesign with the adopted concept, Source: Ahmed, et al., 2024

In the baseline scenario, (figures 36,38) the thermal comfort indices indicate high stress levels: elevated air and mean radiant temperatures, limited shading, and strong solar exposure. The study reports significant potential for UHI effects within the modelled area.

In the intervention scenario, (figures 37,39) results show measurable improvements: reductions in air temperature and PET values, improvements in predicted mean vote/percentage dissatisfied (PMV/PPD), indicating greater thermal comfort for pedestrians. For example, the redesign scenario shows lower "hot-stress" zones and extended periods of acceptable comfort during the day.

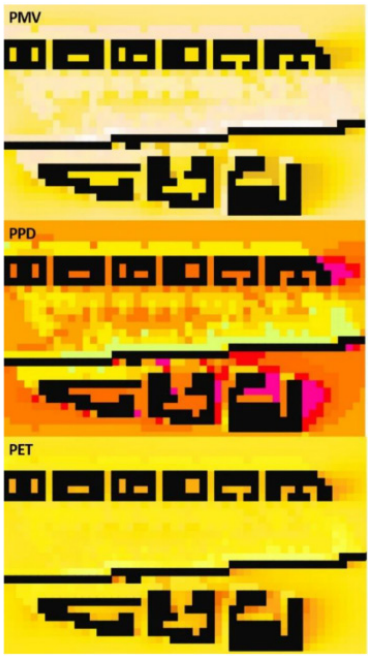

Fig. 36 Simulated PMV, PPD, and PET, existing results at 9 AM in summer. Source: Ahmed, et al., 2024

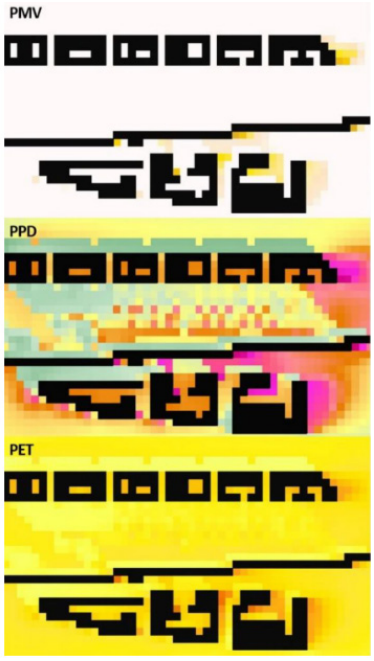

Fig. 37 Simulated PMV, PPD, and PET, renovated results at 9 AM in summer. Source: Ahmed, et al., 2024

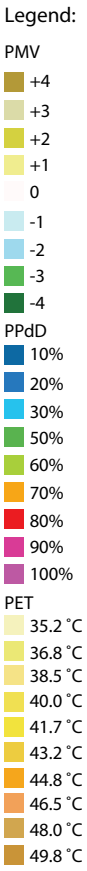

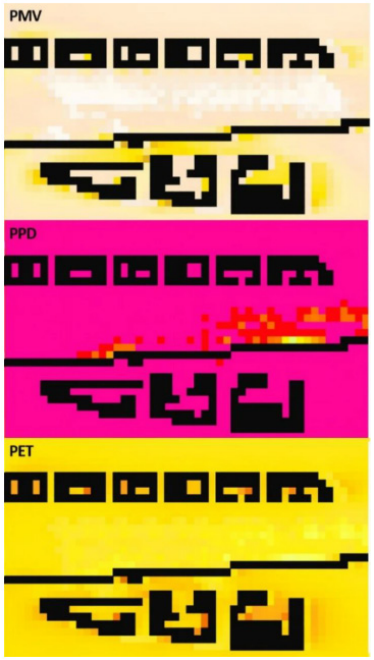

Fig. 38 Simulated PMV, PPD, and PET, existing results at 3 PM in summer. Source: Ahmed, et al., 2024

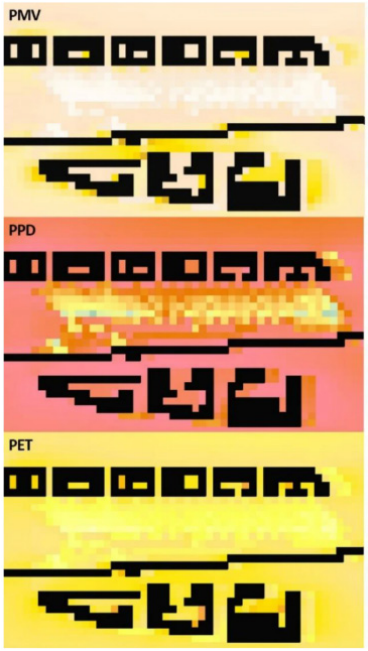

Fig. 39 Simulated PMV, PPD, and PET, renovated results at 3 PM in summer. Source: Ahmed, et al., 2024

Results

Existing at summer 03:00 PM

The 03:00 PM ENVI-met output maps shown in Fig. 18 reveal extreme heat stress conditions across the entire park area, with PET values ranging from 35.39 to 51.54 °C, PPD reaching up to 98.32%, and PMV between 1.83 and 3.97. These high thermal indices, quantifying "hot" to "very hot" thermal perceptions without any refuge zones, highlight the park's poor daytime thermal performance and the urgent need for heat mitigation strategies. Unlike the morning simulations, the results indicate a lack of spatial variations, with significant mid-afternoon overheating restricting occupancy and necessitating serious interventions to reduce thermal mass and improve microclimate conditions for public use.

Renovation at summer 03:00 PM

The post-redesign ENVI-met simulations at 9:00 AM shown in Figure 40, demonstrate the significant impact of mitigation strategies on thermal comfort indices. PET values ranged from 30.34 to 47 °C, PPD reached 54.3–65%, and PMV varied between +0.70 and + 1.5. Compared to pre-redesign conditions, the introduction of shading trees, increased vegetation, redirected walkways facilitating breezes, reflective pavers, misting features, and sheltered structures collectively lowered PET by up to 4 °C, reduced PPD by over 30 percentage points, and decreased PMV by over 2 points. These improvements verify the shift from uncomfortable to acceptable heat stress perceptions, providing accessible public space through passive yet effective techniques, despite some remaining hotspots requiring further intervention.

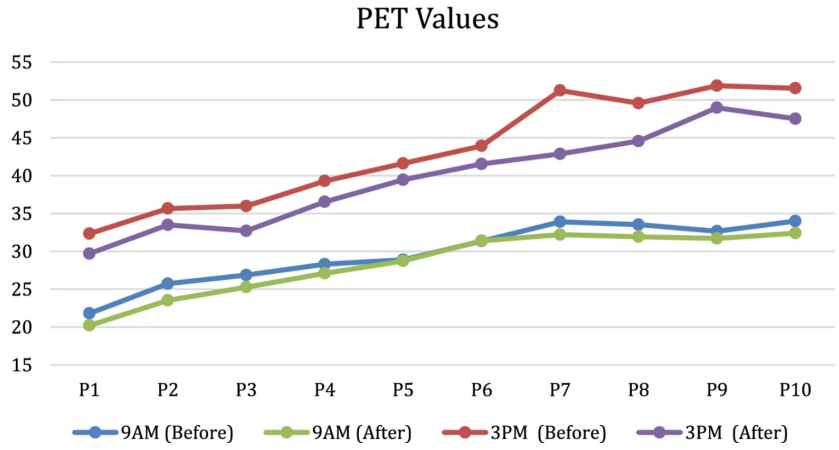

Fig. 40 Comparison of PET values after and before the redesign at 9 AM and 3 PM. Source: Nour M. Ahmed, et al., 2024

2.1.3 Mitigation Effects of UHI in a Historical Center in Teramo

Location: Teramo, Italy
Year: 2014
Authors: Amborsini et el.
Area: 110000 m^2

The case study focuses on the historical center of Teramo, a medium-sized city in the Abruzzo region of central Italy. Teramo is characterized by a compact medieval urban fabric, narrow streets, and limited vegetation conditions typical of many Italian towns that make them highly vulnerable to urban heat island (UHI) formation. The research aimed to evaluate how urban morphology and roof typology affect the local microclimate and to test potential mitigation strategies using the ENVI-met simulation model. The aerial view of the area is shown in Figure 41.

Fig. 41 Aerial view of the chosen area. The view is rotated of 32.50° to the North. Source: Dario Ambrosini, et al. 2014

The goal was to quantify the formation and intensity of the Urban Heat Island effect and to test two potential mitigation strategies:
the use of high-albedo reflective materials (Cool Case), and
the implementation of extensive green roofs (Green Case),
both compared to the existing configuration (Base Case).

Through the scenarios, the study analyzed changes in air temperature, mean radiant temperature, relative humidity, and wind flow, focusing particularly on pedestrian level conditions (1.2 m above ground). The results demonstrate how even small and historical cities are vulnerable to heat accumulation, and how targeted passive strategies can significantly improve microclimatic comfort.

Base Case (Existing Condition)

The base case represents the existing configuration of the historical center of Teramo, a small city in central Italy characterized by a semi-continental Mediterranean climate. The modeled area (≈ 385 × 285 m) includes narrow urban canyons, mid-rise masonry buildings (3–15 m), and limited vegetation concentrated near the main square.
Roofs and walls were modeled using standard radiative properties:
Roof albedo = 0.3 Wall albedo = 0.2

In the following figure, (Figure 42), thermal maps of the analyzed area in the base case are shown, considering the warmest moment of the day and for comparison 12 jours later.

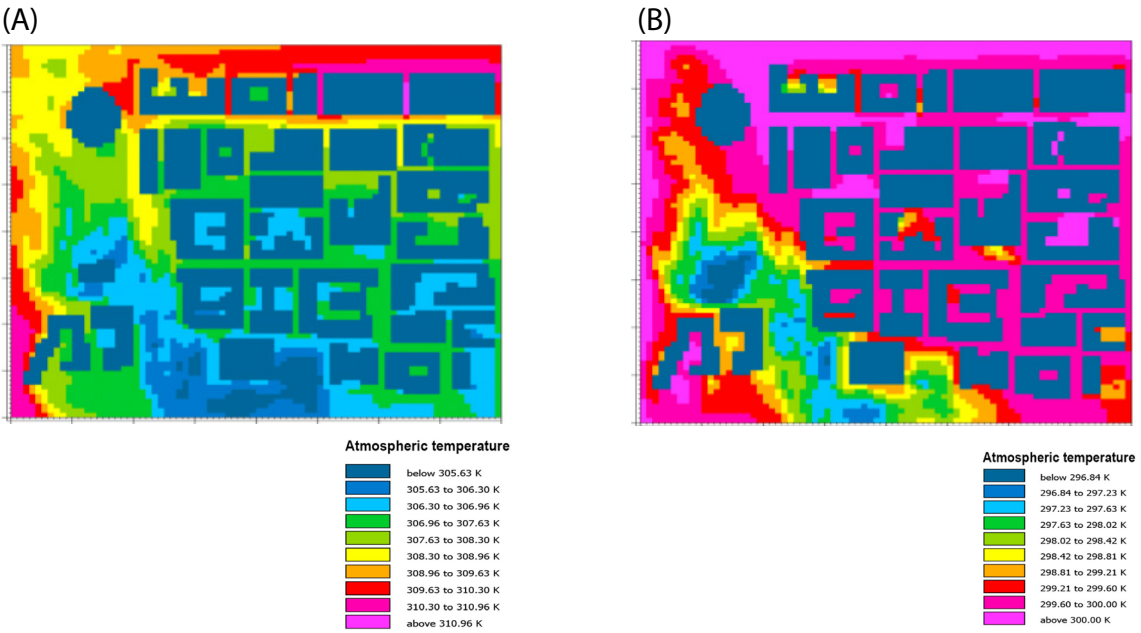

Fig. 42 Atmospheric temperature in "Base Case", x-y view at z = 1.20 m and x-z view at y = 220.5 m at (a) 2:00 p.m., 22 July 2013 (b) 2:00 a.m., 23 July 2013 Source: Ambrosini, et al., 2024

Cool Case

In the second configuration, all building roofs were replaced with high-reflectance materials, raising roof albedo from 0.3 to 0.9 while keeping walls' albedo unchanged (0.2). The simulation maintained identical geometry and boundary conditions to isolate the impact of albedo modification.

During the daytime (2 p.m.), results showed a general decrease of approximately 0.5 K in average air temperature across the built area, though spatial heterogeneity remained. Maximum temperature reached 40.2 °C (313.4 K) in the main street canyon, while the vegetated area recorded 31.7 °C (304.9 K).

Nighttime conditions (2 a.m.) were nearly identical to the base case (difference ≤ 0.25 K) because of the absence of solar radiation.

The authors noted that although the reflective roofs reduced surface heating, they might increase diffuse radiation and therefore local glare or radiant load for pedestrians an effect also observed in previous UHI studies.

Overall, the cool-roof scenario slightly lowered average air temperatures but had limited effect on nighttime cooling.

Figure 43, shows thermal maps of the analyzed area in the cool case, considering the warmest moment of the day and for comparison the half day after.

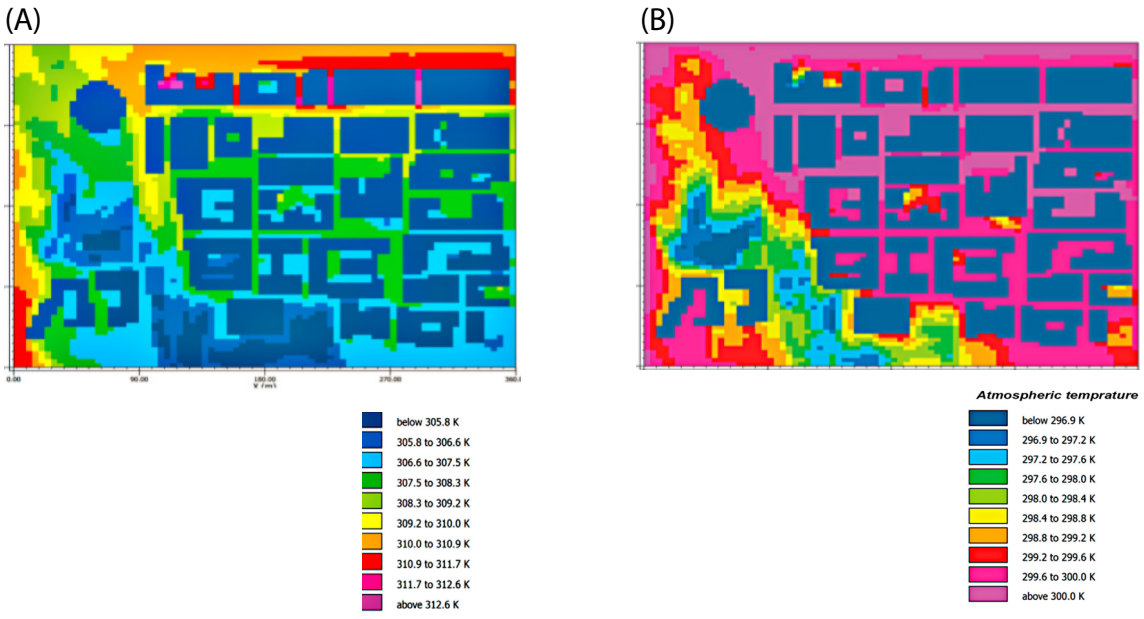

Fig. 43 Atmospheric temperature in "Cool Case", x-y view at z = 1.20 m and x-z view at y = 220.5 m at (a) 2:00 p.m., 22 July 2013 (b) 2:00 a.m., 23 July 2013 Source: Ambrosini, et al., 2024

Green case

In this case rows of trees and shrubs were introduced along streets and open courtyards to evaluate their shading and evapotranspirative cooling effect.

The configuration prioritized species with broad canopies to maximize shadow coverage on pedestrian areas and façades.

Figure 44, shows the model adopted for Green case on ENVI-met.

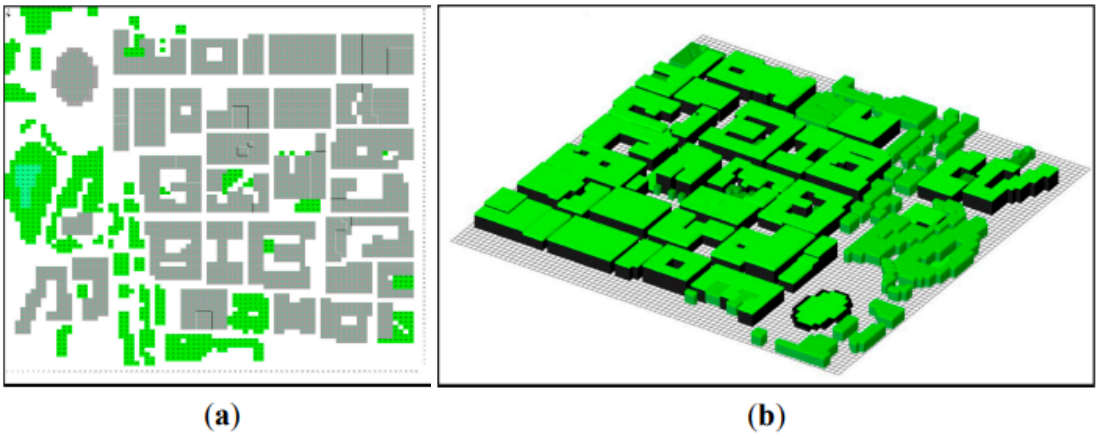

Fig. 44 The model adopted for the Green Case. It is similar to that employed in other cases but buildings have been covered with a 50 cm tall grass layer. (a) snapshot of the area input file; (b) 3D view taken from the output of the model. Source: Ambrosini, et al. 2014

This setup placed green roofs on all buildings, modeled as a 50 cm tall grass layer albedo ≈ 0.26 with the same wall properties as the base case.

Vegetation was introduced in the ENVI-met "Area Input File," creating a thin vegetative layer over each roof to model evapotranspiration and shading.

Daytime results at 2 p.m. highlighted an evident cooling benefit: the temperatures were as much as 1.2 K lower compared to the base case within the built-up area. The range was between 31.8 °C-39.1 °C (305 K-312.3 K).

At night, at 2 a.m., the UHI remained visible but with slightly lower intensities, temperature reductions of a few tenths of a degree compared to the base case, particularly near the southern part of the model.

The authors pointed out that the green-roof scenario provided the most stable improvement by lowering both air and surface temperatures through evapotranspiration and insulation effects and maintaining architectural compatibility with the historic context.

Figure 45, shows thermal maps of the analyzed area in the Green case, considering the warmest moment of the day and for comparison the half day after.

(A)

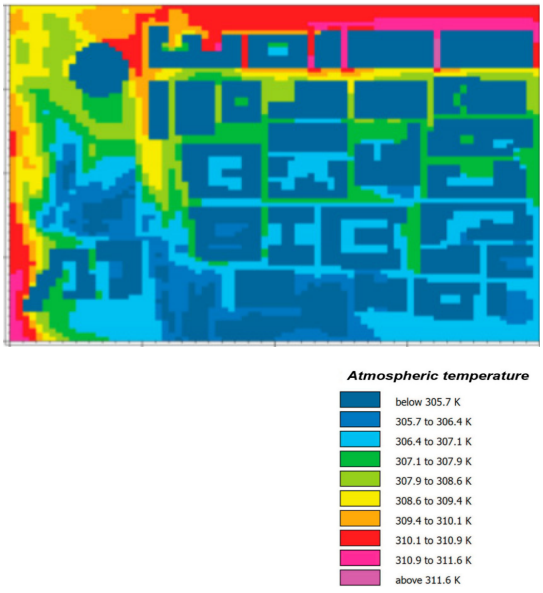

(B)

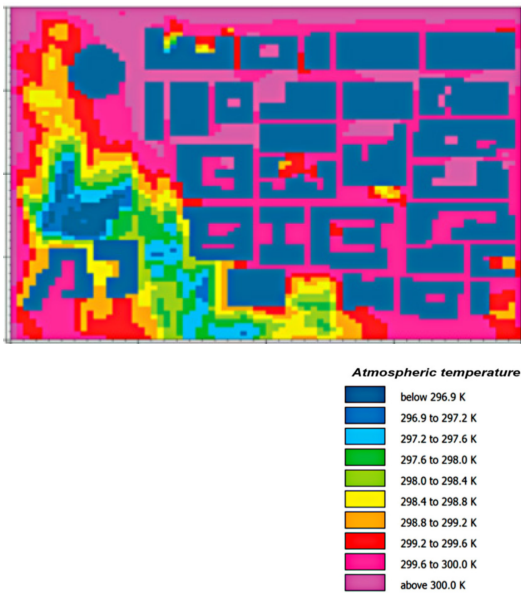

Fig. 45 Atmospheric temperature in "Green Case", x-y view at z = 1.20 m and x-z view at y = 220.5 m at (a) 2:00 p.m., 22 July 2013 (b) 2:00 a.m., 23 July 2013 Source: Ambrosini, et al., 2024

Results

The ENVI-met simulations demonstrated that even within the compact morphology of a small Italian town, distinct UHI patterns emerge, with temperature gradients up to 8 K during daytime and more than 3 K at night.

Both mitigation scenarios yielded improvements:

Cool roofs slightly reduced overall air temperature but offered minimal nighttime relief.

Green roofs achieved broader microclimatic benefits, with better daytime cooling and added ecological value.

2.1.4 Virgen del Carmen Neighborhood

Location: Valencia, Spain
Year: 2024
Authors: Caraballo et el.
Area: 215700 m^2

This case study will focus on the low-income residential area of Virgen del Carmen in Valencia, Spain. Originally designed and constructed in the 1960s, this neighborhood was exemplary of the Modern Movement when, in the post-war period, a new architectural and urbanistic tendency was needed to ensure healthy, efficient, and reasonably priced housing. Nowadays, MoMo neighborhoods-like that of Virgen del Carmen-are spread all over Europe and make up a large share of the existing residential fabric. However, these areas are progressively under strain from the growing climate crisis.
In poorer districts, such as Virgen del Carmen, residents are often more susceptible to changes due to their limited economic basis. Many of the dwellings in these neighborhoods are outdated and most often lack HVAC systems; their residents may well be unable to afford the running cost of these systems, a situation often described as energy or fuel poverty.
Figure 46, shows the photo taken in 1960 from this arrea which represents the urban configurations.

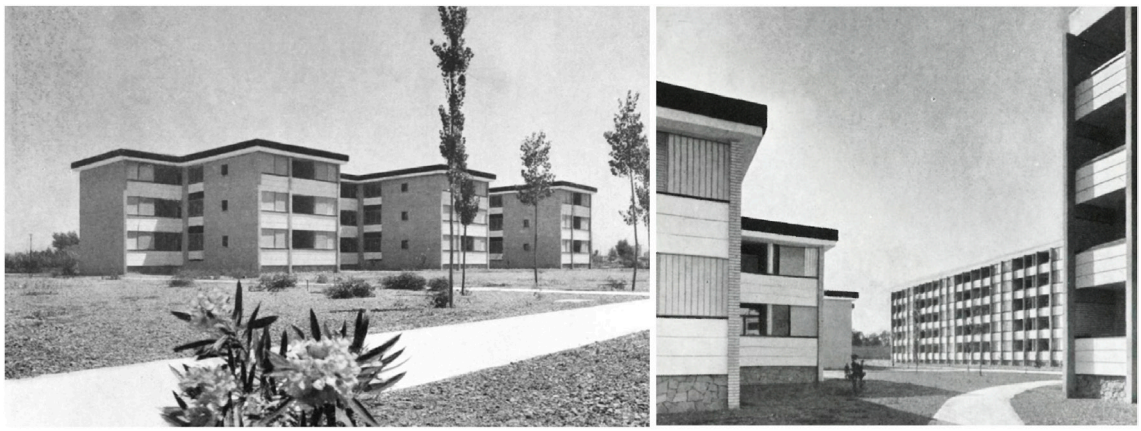

(a) (b)

Fig. 46 Virgen del Carmen area, (a) Public space aspect with the original MoMo urban configuration. Large open areas of sandy terrain, little vegetation, and isolated buildings. (b) Image of the space on between the buildings. Source: Grupo de viviendas Virgen del Carmen, Valencia

The public space of the case study has evolved in response to significant changes in the surrounding urban context. These transformations have led to major changes in the urban configuration and its microclimate performance. These different layouts are considered case study scenarios (SC) in this work.

Scenarios

SC-1 (1960s) This is the neighborhood as it was originally built, with the typical principles of the Modern Movement. Two large blocks of isolated buildings were placed amidst vast, open, sandy spaces with scarce vegetation and narrow transversal walkways. The public areas did not have any kind of shade or thermal protection and, consequently, presented bad microclimatic conditions on hot days.

SC-2 (2020s) represents the present urban structure in 2023, after many years of urban renovation. Large blocks have been divided into smaller ones, now separated by asphalt roads and new cobblestone sidewalks. Sharp rises in impervious surfaces, such as cement pavements, have altered the microclimate. A large-scale urban greening campaign brought many trees and shrubs, creating a considerable green canopy. Glazed balconies represent architectural changes that push the window plane outwards without substantially altering the glazed surface ratio.

SC-3 (2080s) is a study of the performance of the SC-2 configuration in the worst-case climate change scenario using IPCC RCP8.5, which projects an extreme temperature rise and then examines neighborhood resilience. This represents the possible weaknesses of the current configuration when exposed to intensified urban heat.

SC-4 and **SC-5** are the 2080s' improvement proposals that foresee future interventions aimed at improving thermal comfort and resilience to climate. Both scenarios consider identical boundary conditions for an extreme climate, as for SC-3.

SC-4 focuses on retrofitting pavements with affordable passive cooling materials that have proven their microclimatic performance. SC-5 extends this to include additional shading structures. Both proposals opted for low-maintenance, tested solutions to improve outdoor thermal comfort and reduce heat stress at the neighborhood scale.

This was a vast area with sandy soil with narrow transversal walkways that connected the buildings (Figure 47b). The public areas were large esplanades of terrain with almost no vegetation, apart from a few small trees and bushes dotted throughout (Figure 47a). As a result, these arid areas had no solar protection or spaces to shelter on warm days (Figure 47a). An SC-1 plan is shown in (Figure 47c).

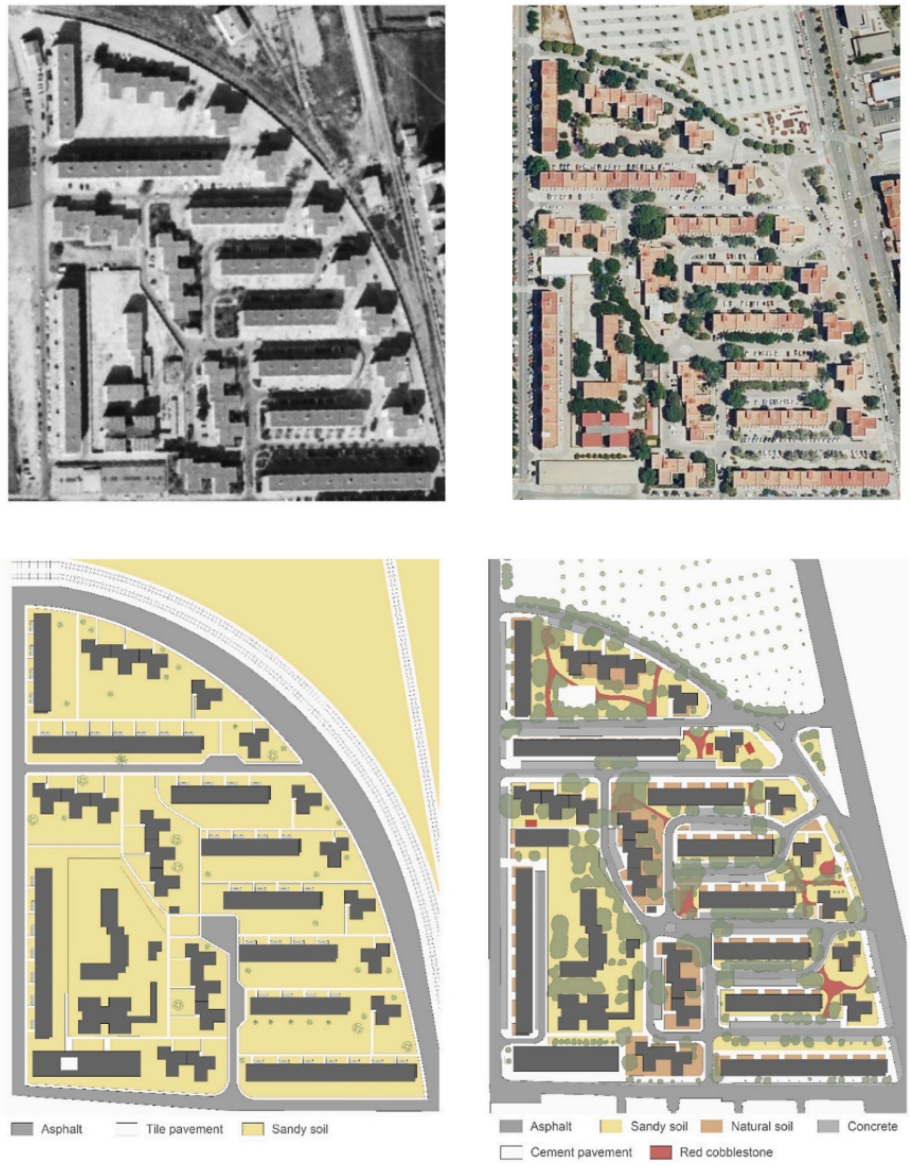

fig. 47- Diverse urban area case study status. (a): First known aerial image, taken in 1980 with the urban configuration still very similar to original one. (b): Current satellite image taken by PNOA. (c): Architectural plan of SC-1 in 1960, original configuration with the project just ended. (d): Architectural plan of SC-2 and SC-3, current urban configuration in 2020. Sources: (MITMA, Plan Nacional de Ortografía Aérea; Caraballo et al., 2024)

The proportion of each surface material in the urban area has been measured. The observed materials are shown in Table 3 for each individual scenario studied.

Materials % presence per each scenario

Pavement material	Scenario 1	Scenario 2/3	Scenario 4/5
Asphalt	17%	30%	--
Tile Pavement	5%	--	--
Sandy Soil	78%	20%	19%
Natural Soil	0%	6%	--
Concrete	0%	6%	--
Cement Pavement	0%	35%	--
Red Cobble	0%	2%	--
Clear permeable Asphalt	--	--	26%
Clear walkway Pavement	--	--	29%
Grass	--	--	7%
Paved Grass	--	--	19%

	Surface Covering		**Shadow covering summary**		
	Imprevious	previous	Green cover	Shade sail cover	Total shadowed Area
Sc. 1	22%	78%	1%	--	1%
Sc. 2/3	74%	26%	13%	--	13%
Sc. 4	29%	71%	13%	--	13%
Sc. 5	29%	71%	13%	6%	20%

Table 3 Materials % presence per each scenario. Source: Caraballo et al., (2024)

Results

Analysis of SC-1, SC-2 and SC-3

The following passive cooling strategies were implemented in this research to counteract the consequences of climate change in the Virgen del Carmen neighborhood: cooling pavements; adding green structures, including shading devices; reducing road traffic areas; and replacing hard surfaces with more permeable, heat-mitigating materials. According to the results of the microclimatic simulations using One Click LCA, (shown in Figure 48), such interventions can decrease urban heat stress by up to 6.3°C UTCI even in the worst-case climate scenario projected at the end of the century.

These strategies were different when selected hours of the day were analyzed. The results show that the performance of SC-2 exceeds SC-1 at 12:00 and 16:00 due to the presence of shade by vegetation and new buildings, which reduces the mean radiant temperature, giving better thermal comfort. For 6:00 and 22:00 hours, on the other hand, SC-1 shows slightly better thermal conditions since vegetation blocks radiation to the sky at night and limits ventilation, thus slightly worsening comfort.

Further analysis concerning SC-2 versus SC-3, using future climate projections, continually showed that SC-3 had higher UTCI values, ranging from 2°C to 7°C, noticeably at 22:00 in the southwest area. The surface materials greatly influence the variation, with asphalt generating extremely high heat stress compared to materials such as soil or concrete, particularly during peak heat hours.

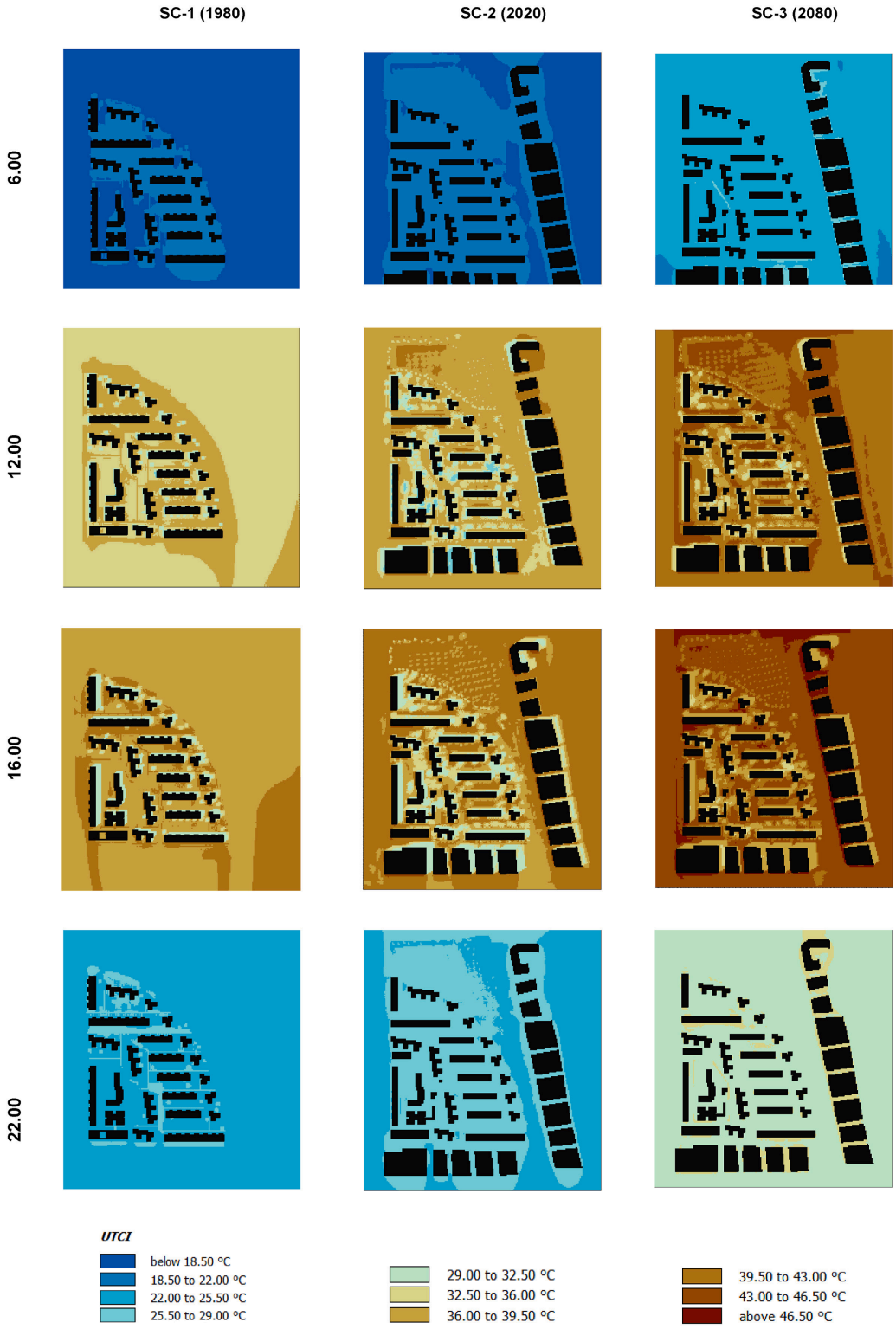

Fig. 48 UTCI maps for the scenarios SC-1, SC-2 and SC-3 at different hours of July 17th. Source: Caraballo et al., (2024)

Scenarios SC-4 and SC-5 proposals

Scenario SC-4 returns to the original concept of the MoMo neighbourhood. In the areas between blocks, roads are eliminated almost completely, and the public spaces are re-established for pedestrians. The MoMo open spaces are recovered but adapting to the future extreme climatic conditions. New materials are used for pavements and soils. The remaining asphalt is replaced with a clear permeable asphalt. The pavement of the walkways is changed to a new clear stone paving with a medium albedo and a lower thermal inertia than the previous cement pavement.

Furthermore, a new walkway material, paved grass, is added to create a walkable pavement that combines clear porous cement and small cavities of grass. This material, based on resistance grass species, has a higher albedo than regular grass, reflects more radiation, allows direct heat transmission to the soil, and is a rigid pavement that produces evapotranspiration, therefore helping to reduce temperatures.

In addition, previous natural soil areas and other new ones are transformed into wild grass zones, providing green soils that improve comfort. Finally, the original sandy soil is maintained but adapted to the new urban configuration. When considering soil characteristics, SC-4 returns to the percentage of pervious surfaces observed in SC-1 (71%), while 45% of the total is natural or semi-natural soil. Furthermore, the albedo of all new pavements has increased or maintained.

scenario SC-5 incorporates new textile shading elements (figure 49) in the form of free-standing awnings into the previous SC-4 design. The advantage of this kind of shading element is that it can be removed in the cold season and enables the creation of new covered areas without increasing RH. In the proposal, the awnings are placed at different heights, creating a non-uniform surface that does not obstruct ventilation. Considering the total shaded areas of public space (plants and awnings), up to 20% of the area of SC-5 is covered, increasing 7% from the original shaded area in SC-2 and SC-3 (3).

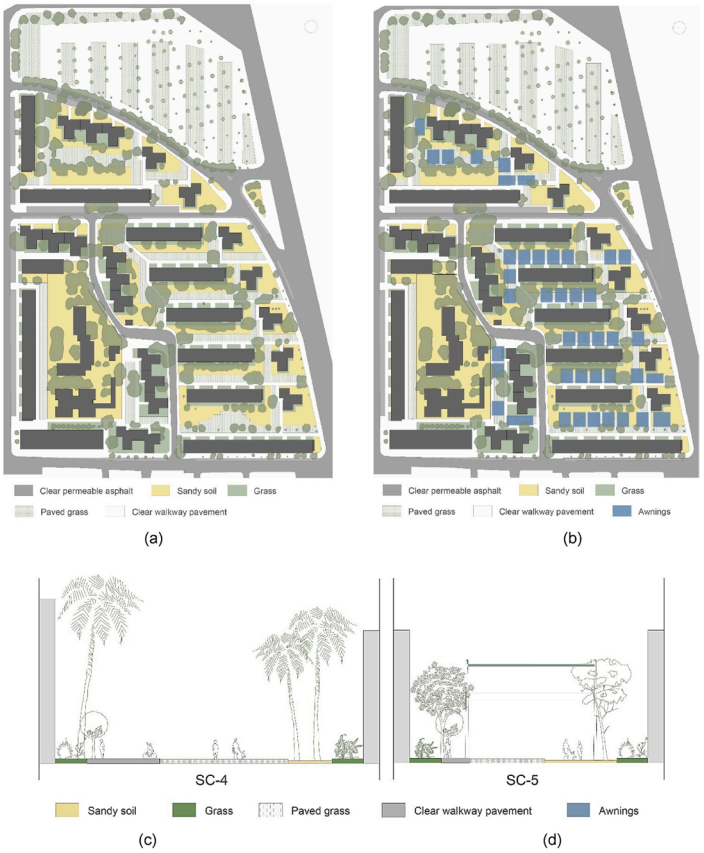

Fig. 49 (a - c) SC-4. (b - d) SC-5, new urban configuration proposals. Source: Caraballo et al., (2024)

Results

Analysis of SC-4 and SC-5

The calculated UTCI result maps for the SC-3, SC-4 and SC-5 are shown in Figure 50 and Figure 51.

Figure 50, shows the UTCI difference between SC-3 and SC-4 at different times of day. In general, better performance was observed at all hours in all areas where the materials had been replaced. The most notable improvement in UTCI values (up to 4.3 °C) occurs at noon, in the streets between the longitudinal blocks, where the asphalt road has been replaced with natural materials and paved grass. The reduction of UTCI in the north area outside the blocks is also worth noting, given that is not shaded, so all improvement is the exclusive result of the change of material. During night-time the UTCI reduction in the area is lower, around 1 °C, but still noticeable.

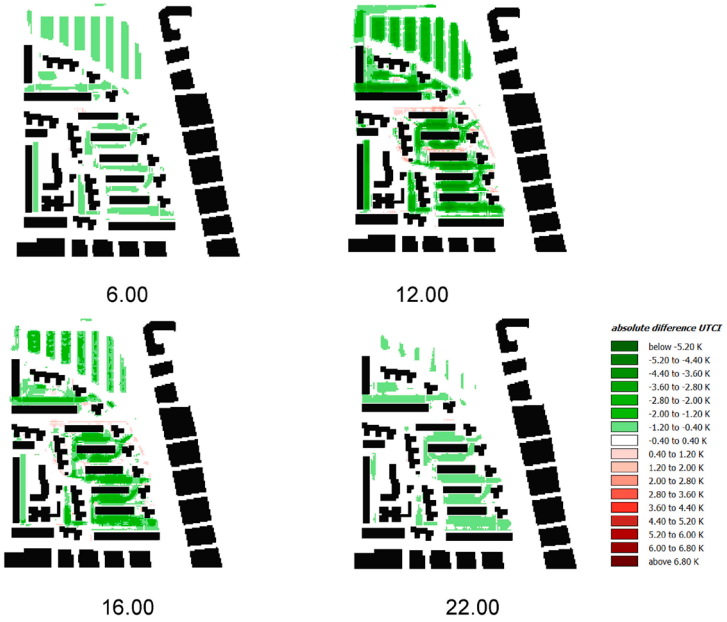

Fig. 50 UTCI difference between SC-3 and SC-4.
Source: Caraballo et al., (2024)

Figure 51, shows the UTCI difference results between SC-3 and SC-5, where the introduction of additional shading using awnings has been considered, in addition to the previous strategy regarding materials. In this case, the UTCI reduction at noon is even higher, reaching 6.4 °C, where the shading is installed. However, during the night (6:00 and 22:00 h), the areas under the shading provide a higher UTCI value than the SC-3 with no shading installed (around 2.4 °C higher). This effect is the result of the shading blocking the night radiation to the sky of the pavement, preventing it from cooling down during the night.

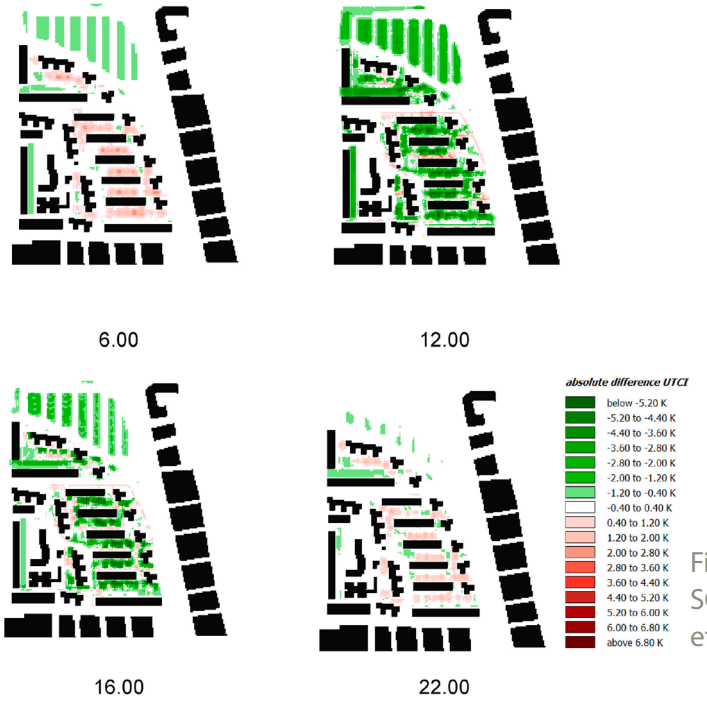

Fig. 51 UTCI difference between SC-3 and SC-5. Source: Caraballo et al., (2024)

2.2 Overview

To identify the most effective microclimate mitigation strategies applicable to my project site, the four case studies presented in Section 2.1 were analyzed in Table 4. Each project demonstrates different approaches to reduce urban heat stress ranging from material substitution and shading systems to vegetation-based cooling and urban-layout modifications. Table 4 provides a comparative summary of these case studies, outlining the strategies employed, the microclimatic indicators assessed, and the quantified improvements achieved.

Case Study	Main Strategies	Most Effective Strategy
Superblocks, Barcelona (Sant Antoni area)	Pedestrianization high-albedo pavements shading structures vegetation modular street furniture	Shading + vegetation + cool materials
Viale Carlo Felice Gardens, Rome	Increasing vegetation Cool pavements Shading structures Water features optimized tree placement	Combination of shading + vegetation
Historical Center of Teramo	Cool roofs Green roofs	Green roofs
Virgen del Carmen Neighborhood, Valencia	Cool pavements Vegetation shading devices permeable materials	SC-5: materials + shading

Microclimate Indicators Used	Key Results
Air Temp, Surface Temp, Wind, Humidity, PET	**Air temperature –0.6 K:** average air temprature decreased by 0.6°C **Surface temperature –10 to –20 K:** shaded/light pavements reduced ground temps up to 20°C **PET –12 K:** thermal comfort improved by up to 12°C **RH +3.8%:** vegetation increased humidity **Wind slightly reduced:** due to added trees
PET, PMV, PPD, Air Temp	**PET –4°C :** thermal comfort improved **PPD reduced by ~30% :** fewer people experiencing discomfort **PMV –2 :** lower perceived heat **Hot-stress areas reduced:** qualitatively shown in maps
Air Temp, MRT, RH, Wind	**Cool roofs: Air temp –0.5K:** reflective roofs cooled air slightly **Green roofs: Air temp –1.2K:** evapotranspiration cooled air more effectively **Night cooling:** slight (few tenths of a degree)
UTCI	**SC-4: UTCI –4.3°C:** better comfort due to new pavements **SC-5: UTCI –6.4°C at noon:** shading + materials was most effective

Table 4 Comparison of Strategies and Climate Outcomes Across Case Studies

Chapter 03

Turin Case Study

3.1 Turin Urban Condition

3.1.1 Climatic Context in Turin

Prior to examining how urban form influences microclimatic behavior, it is essential to first gain a comprehensive understanding of Turin's overall climatic characteristics, particularly its environmental vulnerabilities. For this reason, part of the literature review has been devoted to exploring the insights and research findings presented by the scientific community on this subject.

Turin, capital of the Piedmont region in northwestern Italy, lies between the Po River plain and the first range of the Alps. The city's elevation ranges from approximately 220 to 280 meters above sea level, reaching its highest point of 715 meters at Colle della Maddalena (Geoportale Piemonte, 2024). Its location in the Po Valley, surrounded by mountains, limits natural ventilation and favors the accumulation of heat and pollutants, particularly in summer and winter inversion periods.

ARPA Piemonte is the regional environmental protection agency of Piedmont. It monitors air, water, soil, and environmental risks to support public health and environmental policies. According to ARPA Piemonte, Turin has a humid subtropical climate (Cfa) with cold, foggy winters and hot, humid summers. The Turin Centro (Giardini Reali) station reported average monthly temperatures of +0.9°C in January and +23.1°C in July, with annual precipitation of around 804mm across 79 rainy days (ARPA Piemonte, 2023).

In the long-term climate analysis (1958–2022), ARPA recorded a steady warming: maximum daily temperatures increased by ~0.4°C per decade, while minimum temperatures increased by ~0.3°C per decade, resulting in +2.0°C overall warming in maximums over the past 60 years (ARPA Piemonte, 2023).

In its annual report, ARPA states that 2023 was the second-warmest year on record in Piedmont, with a regional mean temperature of 11.2°C, which is +1.3°C above the 1991–2020 climatological average. The city also experienced a marked increase in extreme heat events, especially during July and August (ARPA Piemonte, 2024).

December, however, proved to be the driest, with 13.3 mm, a significant reduction that continues to raise concerns. Rainfall days across the region totaled 88, compared to 54 in the 1991-2020 period.

Fig. 52 Map of Turin Urban and Principal Road Network, source for base map: Q-GIS

The latest Climate Analysis in Turin

The latest analysis of Piedmont's climate reveals a significant sign: 2024 was the fourth year with the highest temperatures in the region. Temperatures, despite some exceptions in May, June, and September, have shown an upward trend that shows no signs of slowing. Experts from Arpa Piemonte have released this data, highlighting temperatures that are 1.1°C above the 1991-2020 average. The information collected also indicates a significant increase in thunderstorms, rainfall concentrated in certain periods, and a total absence of snow in the plains (ARPA Piemonte, UNO SGUARDO ALL'ARIA anteprima, 2025).

Based on the latest analysis on climatic data in Turin, the hottest days fell in the second half of the summer, with August 11th being the hottest day of the year, while the highest temperature in the plains was recorded on August 13th in Sezzadio, at 37.8°C. (ARPA Piemonte, 2025).

In parallel with severe summer heat spells, Turin occasionally experiences extremely cold events. Based on the datas recorded at Giardini Reali station, the lowest minimum temperatures were recorded in January, between the 21st and 22nd in almost all cities. However during 2024 Turin experienced the coldest day on 23 November around -°6C February, May, and June also contributed significantly to the overall increase in rainfall. (ARPA Piemonte 2025).

The table 5 indicates the average monthly temprature in turin in 2024, and has compared it with average temprature recorded in the years 2014-2023. (ARPA Piemonte, UNO SGUARDO ALL'ARIA anteprima, 2025).

	Temprature (°C)		Rainy days (num)	
	2024	Avrage 2013-2024	2024	Avrage 2013-2024
Jan.	4.7	3.7	4	4
Feb.	8.7	6.3	9	6
Mar.	10.8	10.1	14	5
Apr.	13.8	14.0	9	7
May	16.5	17.7	16	12
Jun.	21.2	22.8	10	9
Jul.	25.6	25.2	5	7
Aug.	25.8	24.2	6	6
Sep.	18.6	19.7	9	5
Oct.	15.3	14.3	15	5
Nov.	8.0	8.5	1	8
Dec.	4.4	4.3	1	5
Year	14.4	14.2	99	78

Table 5 Temperature and precipitation. Comparison between 2024 and the previousdecade, (ARPA Piemonte, UNO SGUARDO ALL'ARIA 2024, 2025).

3.1.2 Urban Vulnerabilities

The city of Turin has suffered from the impacts of climate change in recent years. In fact, every year, there are extreme climatic phenomena that occur with increasing frequency and intensity, causing great damage to the city and its economy. The image shown in Figure 53, displays the complexity of a region that is highly exposed to extreme climatic events aggravated by climate change. In fact, Turin's urban area is the epicentre of a complex hydrological system and presents a hilly area within its region with strong criticalities in terms of hydrology due to the numerous landslides, both active and dormant, that affect that portion of the city (Città di Torino, 2020).

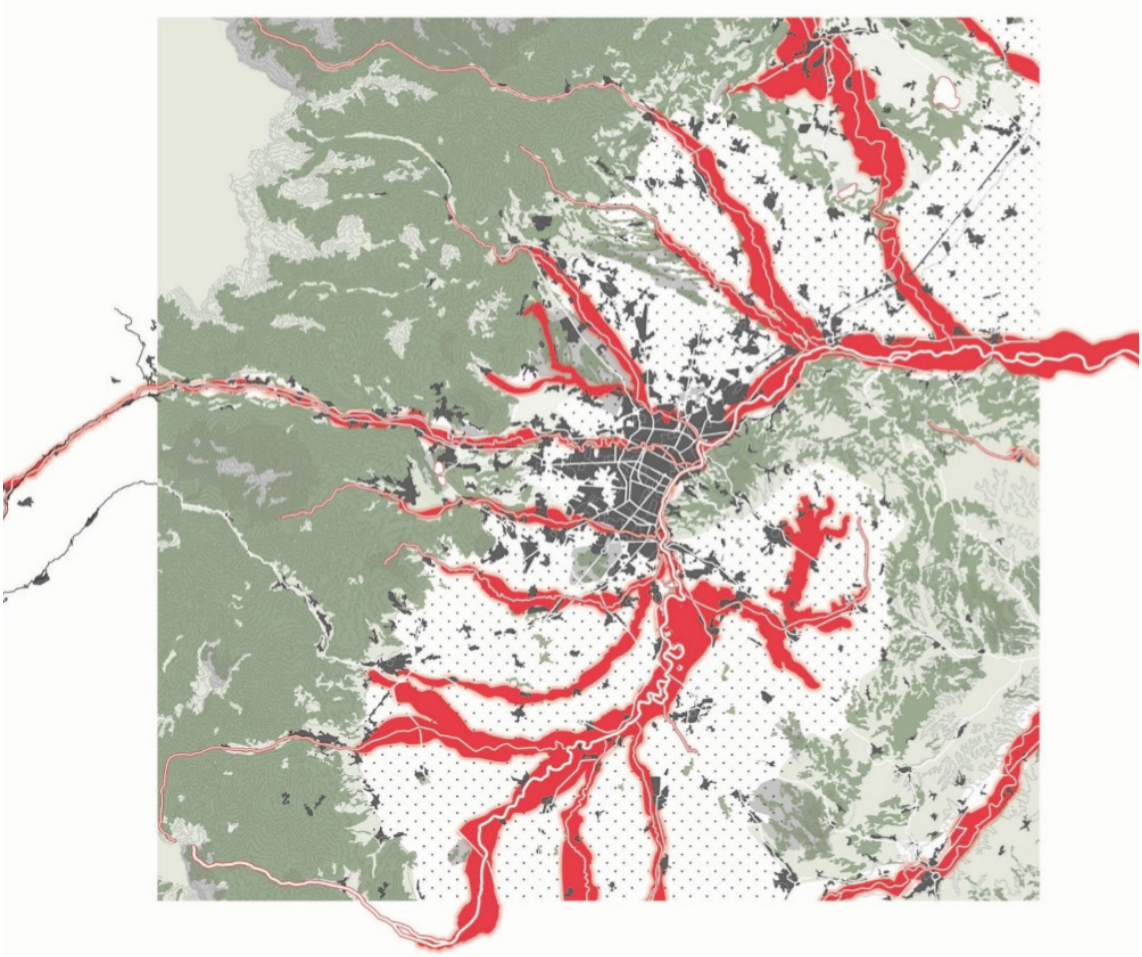

Fig 53 The region of the Municipality of Turin in the surrounding hydrological context. Source: Turin - Towards the metropolitan regional strategy (G. Pasqui - Politecnico di Milano and C. Calvaresi – IRS: Institute for Social Research) - Torino Strategica (Strategic Turin)

Turin has already had to cope with particularly acute episodes of flooding and heat waves. In 1994, 2000, and 2016, the city suffered considerable damage due to the flooding of rivers that cross it, and in 2003, it recorded the first emergency situation linked to heat waves-a phenomenon that has been increasing in recent years, with a sharp rise in the city's mortality rate (Città di Torino, 2020).

Moreover, the analyses done by the municipality on Climatic Vulnerabilities in Turin show that temperatures have increased in the city by up to 5°C over the average from 1971 to 2000 in the last twenty years. This increase approaches the peak values observed during the notoriously hot summers of 2003, 2015, and 2017 (Arpa Piemonte Dipartimento Rischi Naturali e Ambientali & Città di Torino, 2020).

The same report also points out the increase in frequency of tropical days and nights. Tropical days are considered to be days when the maximum temperatures exceed 30°C (Arpa Piemonte Dipartimento Rischi Naturali e Ambientali & Città di Torino, 2020), while tropical nights are nights in which the temperature remains above 20°C (European Commission & European Environment Agency, n.d.).

To contextualize the recent trend, the study evaluated the number of days characterised by physiological thermal discomfort in two time frames: 1989–2016 and 2001–2016. This was to determine if there had been a statistically significant change over the past 15 years. When these data were plotted with the tropical days and nights' trends, the result indicated a marked rise in the number of days of discomfort in the second period (2001–2016), except for those of tropical nights, which remained stable (Arpa Piemonte Dipartimento Rischi Naturali e Ambientali & Città di Torino, 2020).

3.1.3 UHI in Turin

Turin's urban structure also contributes significantly to Urban Heat Island formation. Over 65% of the municipal area is urbanized, much of it with impervious surfaces and low vegetation coverage. This morphological nature of the urban areas increases daytime heat absorption and nighttime heat retention, especially in areas with dense buildings and brownfield zones. (Climaborough.eu)
This orographic enclosure results in poor air circulation on most occasions, which contributes to the accumulation of heat and humidity in the summer and cold air stagnation in the winter. These climatic conditions enhance the city's vulnerability to extreme weather events, especially heat waves, which have become more frequent and intense in recent decades.
In 2024, Turin had about 870,000 inhabitants, being the fourth most populous city in Italy. More than 65% of its area is urbanized, much with impermeable surfaces and scarce vegetation coverage, especially in the older industrial areas and densely residential parts of the city (FutureHubs.eu). This urban configuration contributes significantly to the Urban Heat Island (UHI) phenomenon, as it limits natural cooling and heat dissipation during hot days and nights (Climaborough.eu).

The average temperature of the city has a constant or slightly decreasing trend, while the values of the rural stations show a clearly positive trend. The temperature increase at rural stations may be attributable to several factors, including the increasing urbanisation of rural areas and an increase in the size of the area affected by the Turin UHI. It is well known that even a minimally-sized urban settlement develops its own UHI (Heino, 1999; Soux et al., 2004) and that the UHI of a big city can affect the temperature measurements at surrounding rural stations (Sovrano Pangallo, 1998).

The annual mean temperature for Turin are shown alongside local rural tempera-ture data in Figure 54, highlighting an important aspect of the evolution of the climate over the period under consideration (2000–2016).

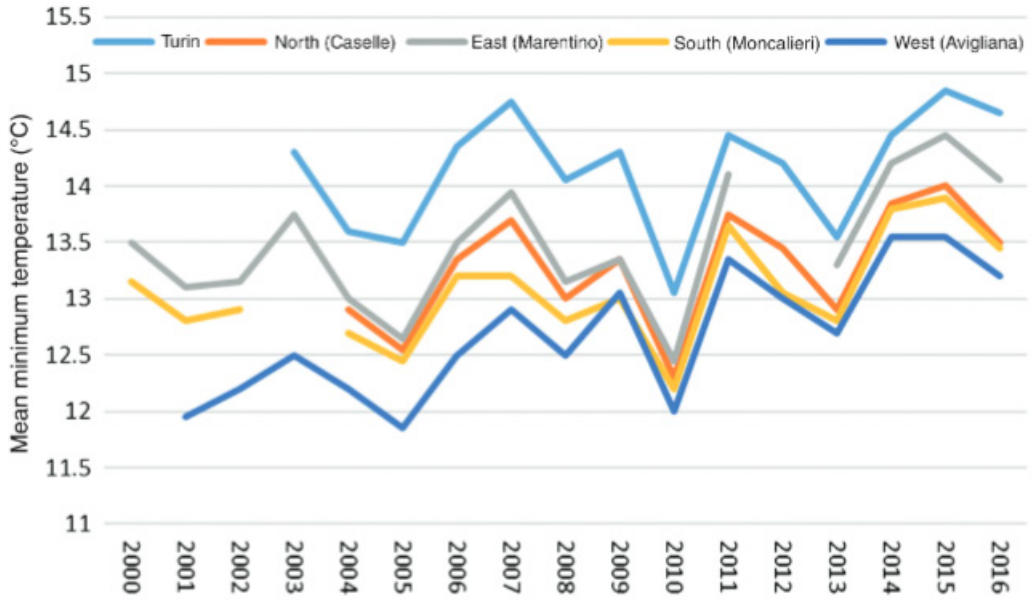

Fig. 54 Annual mean temprature for Turin and four nearby rural stations since 2000. Source: Garzena et al. (2018)

Ellena et al. (2023) introduced a micro-scale risk assessment model integrating climatic hazard, demographic exposure, and social vulnerability indicators for each census tract. The analysis showed that areas with a high proportion of elderly residents, poor housing conditions, and low educational levels are particularly at risk (Ellena et al., 2023). In contrast, industrial areas, though thermally intense, showed lower overall risk because they are sparsely inhabited. The research emphasizes that UHI risk in Turin is strongly shaped by socio-spatial inequalities inherited from the city's industrial past.
figure 55, shows the micro-scale Urban Heat Island risk distribution and prioritised intervention areas in the city of Turin developed in Ellena et al., 2023. The maps, obtained by a risk assessment performed at the census-tract scale, merge three fundamental components: hazard, exposure, and vulnerability.
The R.02 map represents the synthetic risk index, obtained through normalization and aggregation of all indicators, while the R.03 map identifies the zones requiring priority intervention based on the intersection of high hazard levels, socio-demographic fragility, and low adaptive capacity.
The spatial distribution clearly highlights how the most critical zones are concentrated in the densely populated northern and southern peripheries particularly in the neighborhoods of Barriera di Milano, Mirafiori Nord, Mirafiori Sud, Parella, Pozzo Strada, and Vanchiglietta.

These districts exhibit both higher UHI intensity and a higher presence of elderly and socio-economically disadvantaged residents, resulting in elevated composite risk values. In contrast, the hilly southeastern areas of Turin, characterized by abundant vegetation and lower population density, show the lowest risk scores due to their significant cooling effect and greater adaptive capacity.

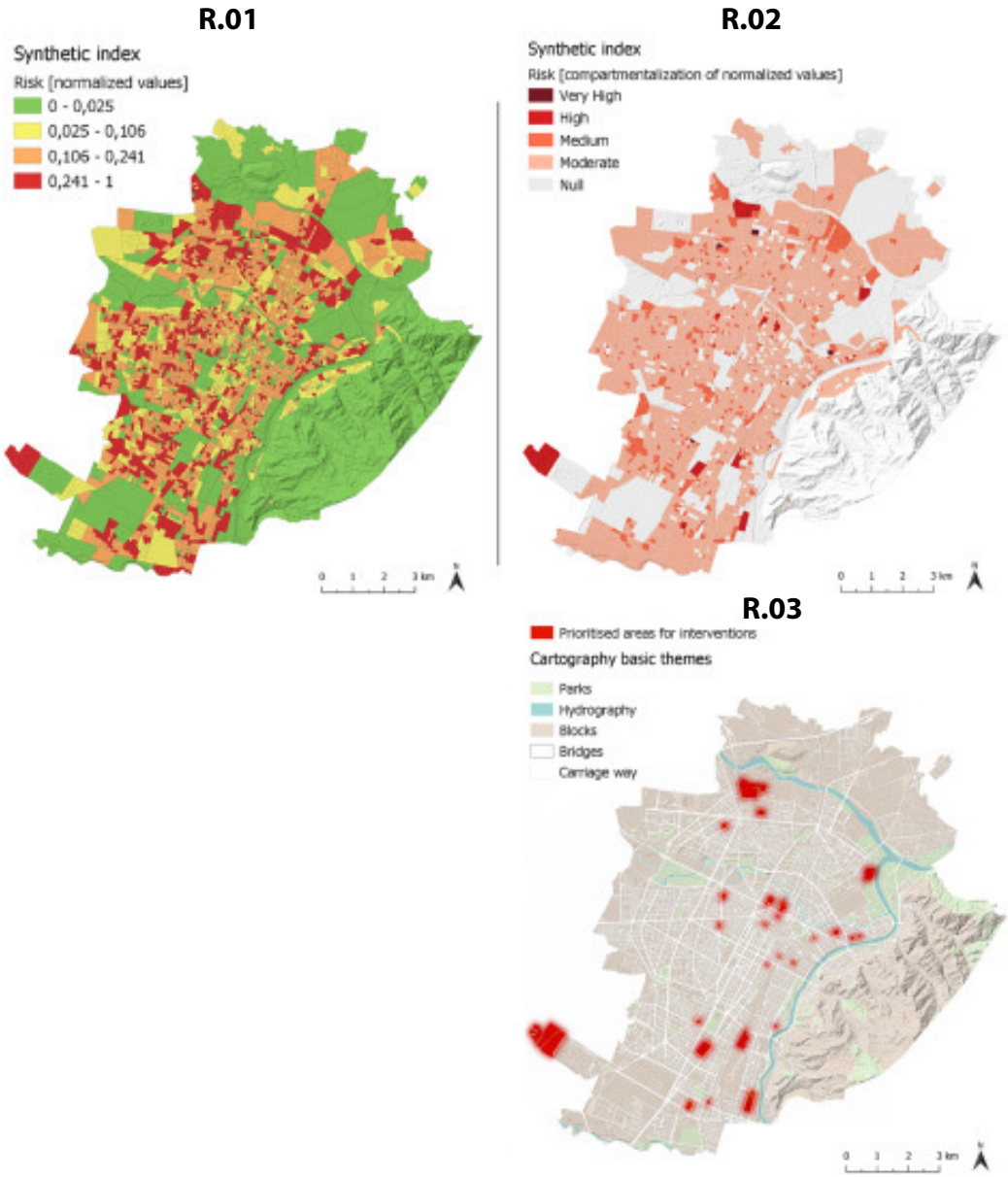

Fig. 55 Mapping the UHI risks (R.01; R.02) and the prioritized areas for intervention (R.03)
Source: Ellena et al. (2023)

3.2 Mapping the zone

3.2.1 The study area

This analysis will focus on a defined urban zone within the Aurora district of Turin, one of the most historically pivotal areas for Turin's industrial identity and among the most dynamic at the moment, undergoing deep transformation.

The Study Area is an historical and contemporary hub situated north of Turin's historic city center. During the Industrial Revolution, Aurora developed as the main working-class district, featuring a high concentration of factories and a large number of workers' homes along the Dora river. After peaking in the period following WWII, the area started to decline with the closure of major industries in the 1980s, such as the Fiat Grandi Motori plant. However, its proximity to the city center and the river has fired intensive recent urban regeneration processes (Quartieri Torino – Storia di Aurora).

The area today embodies an interesting collision of historic layers and modern urbanism. It houses some city landmarks that anchor the precinct's character: the Museo Lavazza and old Flower shop. Based on the maps shown in figure 55, this area is among the medium to high areas in terms of UHI risk and one of the main reasons for choosing this area as the case study.

Crucially, Aurora is currently the object of a major integrated urban renewal program, partly funded by the PN Metro Plus 2021-2027, focused on integral regeneration to ensure environmental sustainability, social inclusion, and greener public space creation, notably along Corso Palermo. Based on Comune di Torino (2025) and PN Metro Plus - Aurora - Barriera project, this ongoing transformation makes the area a prime case study for assessing rapid urban change. Figure 56, illustrates the isometric view of the case study area.

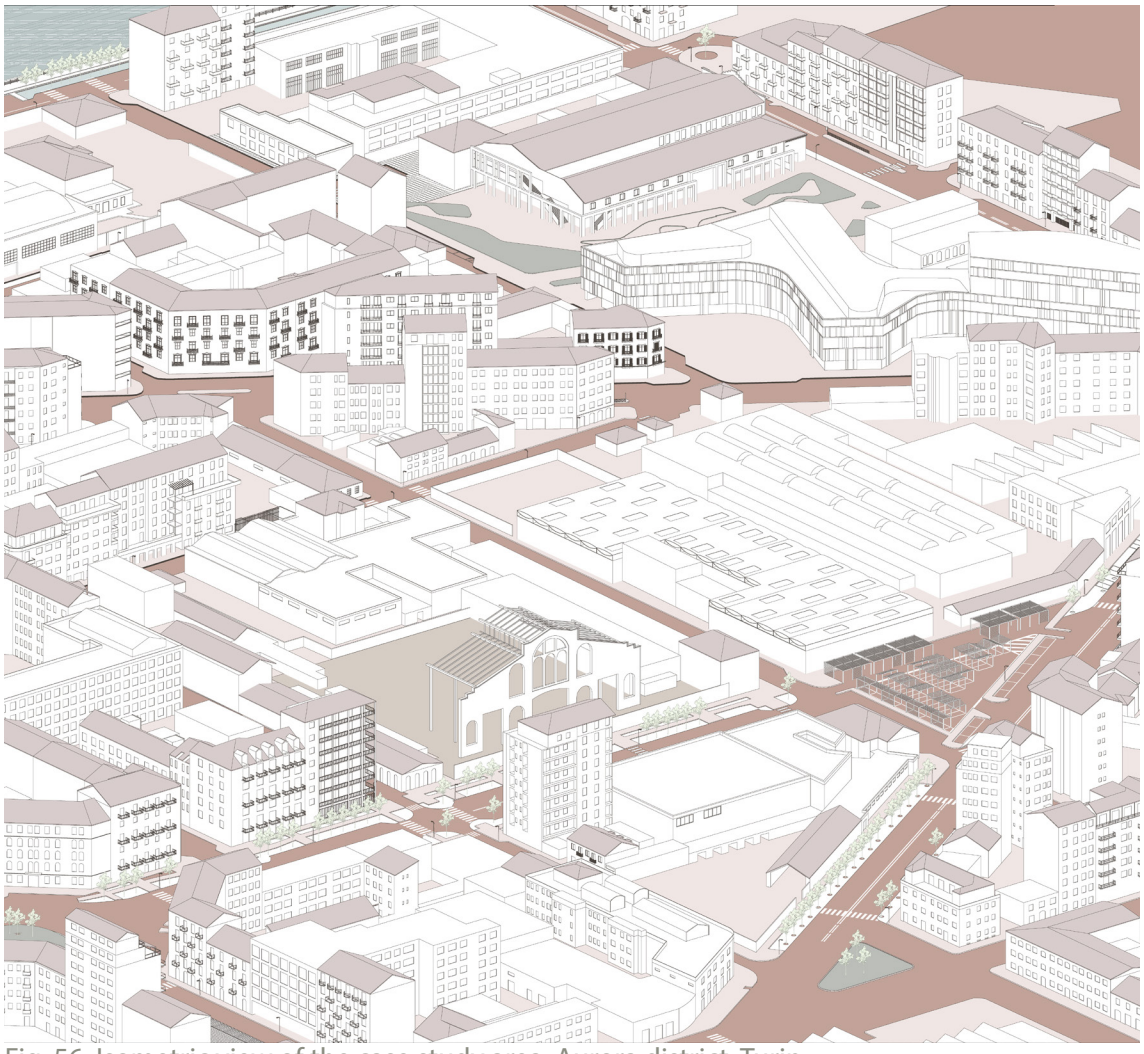

Fig. 56 Isometric view of the case study area, Aurora district, Turin

3.2.2 Analysing the zone

Land use

Land-use patterns have a direct impact on local temperature variations due to differences in material reflectivity, vegetation cover, and anthropogenic heat sources (Oke, 1987). Understanding land use is essential in assessing urban heat distribution because different functions and surface materials influence energy absorption, ventilation, and microclimatic behavior (Oke, 1987).

In this study area, which covers approximately 398,950 m^2, residential buildings occupy the largest area, which is 10.28% of the total surface. Commercial and industrial uses represent 8.60% and 7.69%, respectively. Administrative and public service buildings together make up around 3.3% of the total area. Minor buildings are 4.93%, and educational facilities represent 0.70%. The remaining 0.61% includes other land uses.

Overall, the analysis shown in Figure 57, indicates a predominance of built-up surfaces (around 36% of the total area), with a relatively limited presence of open or vegetated spaces. This high degree of land sealing and functional mix suggests a significant potential for localized heat accumulation, particularly in the dense residential and industrial clusters where vegetation and permeable surfaces are scarce.

Residential Land use: 28.47 %
Total area: 41,015 m^2

Industrial Land use: 21.30 %
Total area: 30,700 m^2

Commercial Land use: 23.83 %
Total area: 34,340 m^2

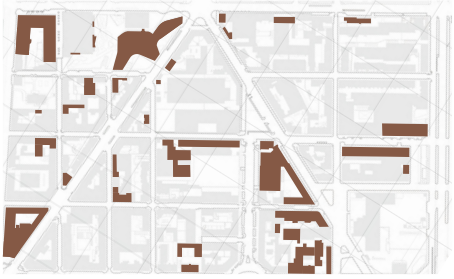

Minor buildings Land use: 13.63 %
Total area: 19,647 m^2

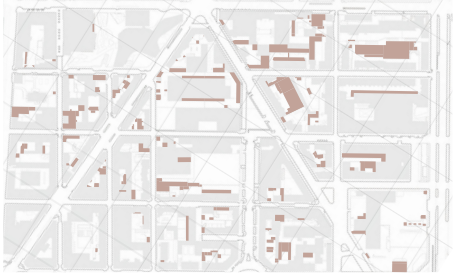

Fig. 57 Land use and buildings' function in the area, Source for base map: Geoportale Comune di Torino

Public Services Land use: 5.04 %
Total area: 7,269 m²

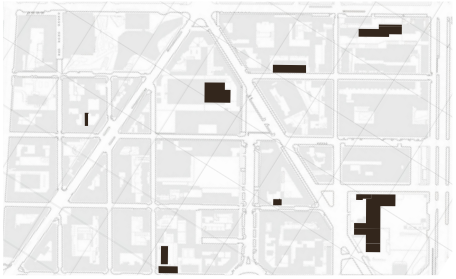

Administrative Land use: 4.10 %
Total area: 5,914 m²

Educational Land use: 1.94 %
Total area: 2,795 m²

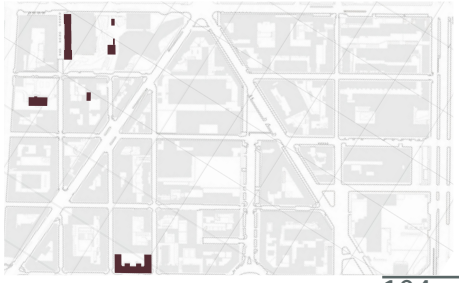

Vegetation

Vegetation has a fundamental role in forming microclimatic conditions and in the mitigation of the heat island effect. Green surfaces in this study area cover an area of 27,538 m^2 (6.9% of the total area) and are mostly concentrated along the main streets Corso Palermo, Via Bologna, and Corso Regio Parco, and in a few small internal courtyards (Figure 58).

Based on the data extracted from Geoportale del Comune di Torino, 597 trees were identified in this study area, the most dominant tree is Fraxinus excelsior (34.7%), while the second and third most abundant trees of the zone are Tilia × europaea (17.7%) and Platanus orientalis (17.6%), respectively. Conifers are less common, with only Pinus nigra var. austriaca at 11.9% of the total. This was joined by small amounts of Pseudotsuga menziesii at 0.5%. The rest of the trees arer Corylus colurna and Ostrya carpinifolia (both 3.7%), followed by Acer platanoides and Carpinus betulus at 2.3%, Celtis australis at 1.5%, and ornamental species representing less than 1% each. The average tree height in the area is from 10 to 18 meters, with mostly mature species exceeding 40 years of age, forming a continuous canopy along the main streets (Geoportale del Comune di Torino).

Fig. 58 Greenery in the case study area, Source for base map: Geoportale Comune di Torino

Surfaces Covered with vegetation

Trees

Building Height Distribution

The dominant architectural profile is low-to-moderate rise, with buildings of 4 stories or less estimated to cover approximately 75% of the built environment. This prevalent fabric is contrasted by distinct clusters of mid-to-high-rise buildings (5 to 10+ stories), which occupy the remaining 25% of the footprint, notably concentrated in the northern and eastern sections of the area (Figure 59).

This variance in vertical profile is key to understanding the Urban Heat Island effect. Taller structures create an urban canyon effect, defined by the building height-to-street-width aspect ratio. High H/W ratios significantly alter the local energy balance by reducing the Sky View Factor (SVF), which limits the escape of longwave radiation (Oke, 1988). This results in heat being trapped within the urban canopy layer, intensifying the nocturnal UHI effect (Oke, 1988).

The aspect ratio is a fundamental indicator of heat accumulation in cities, as it governs the microscale exchange of energy.

The effect of the modulation of urban morphology on the Urban Heat Island exhibits distinct spatiotemporal dependence, with the ratio of building height to street width (H/W) being a primary control on thermal radiation emitted and solar radiation absorbed within the urban canyon (Adapted from Levermore and Cheung, 2012).

Higher building-height-to-street-width ratios, where taller buildings create shade for narrower adjacent streets, have been shown to lead to lower mean radiant temperature and greater thermal comfort levels during the day due to shadowing effects (Chi et al., 2023).

Fig. 59 Building's height map, Source for base map: Geoportale Comune di Torino

1-story buildings
2-stories buildings
3-stories buildings
4-stories buildings
5-stories buildings
6-stories buildings
7-stories buildings
8-stories buildings
9-stories buildings
More than 10 stories buildings

Building's Age

The thermal behavior of buildings varies significantly with their construction period, as older urban fabrics tend to store more heat due to higher thermal mass and compact morphology" (Santamouris, 2014).

The age of buildings provides valuable insight into the evolution of construction techniques, materials, and their interaction with the urban microclimate. In the study area, the majority of the building stock (≈67%) dates from 1960 to 1980, corresponding to Turin's post-industrial expansion phase characterized by reinforced concrete structures and limited thermal insulation.

Earlier constructions, built before 1940, represent roughly 7% of the total, mainly masonry buildings with high thermal mass that store heat during the day and release it at night. Only a minimal share of the stock (<1%) corresponds to new buildings constructed after 2000 (Figure 60).

This temporal pattern indicates that most of the area consists of mid-20th-century buildings, which are highly relevant to UHI analysis because of their low reflectivity surfaces. This map was therefore produced not only to understand the thermal behavior of the existing building stock but also to identify which buildings may structurally support green roof interventions.

By combining this dataset with the roof typology map, it becomes possible to identify the newer flat-roofed buildings that have the greatest potential for green roof implementation as a climate mitigation measure.

Fig. 60 Buildings' age in the case study zone, Source for base map: Geoportale Comune di Torino

Before 1900
1900 - 1920
1920 - 1940
1940 - 1960
1960 - 1980
1980 - 2000
2000 - 2010
2010 - Present
Not Registered
Minor buildings/ shaders

Roof Typology

Geometry and surface material are strong factors that control heat gain and rooftop surface temperature, thereby affecting building energy use and the immediately surrounding microclimate (Li et al., 2014).

The roof typologies analyzed in the study area show a balanced distribution between flat and sloped roofs, with flat roofs covering about 42% of the total roof surface, and sloped roofs around 36% (Figure 61). Flat roofs are typically from mid-20th-century and newer constructions, usually covered with dark bituminous membranes or concrete, materials that have a low reflectivity and high capacity for heat retention. These make them significant contributors to local heat accumulation and promising candidates for green roof retrofitting due to their structural capacity and accessibility.

Sloped roofs are mainly found in older residential and mixed-use buildings, generally covered by clay tiles or traditional materials featuring moderate thermal inertia and emissivity. Partial shading due to their inclined geometry and the ease of rainwater drainage tends to decrease the surface temperature with respect to flat roofs. However, steepness and construction details usually restrain their suitability for green roof installation.Existing green roofs already cover about 21% of the total roof surface, which is a very high integration of nature-based solutions into the existing fabric.Such installations contribute to localized cooling, stormwater retention, and improved visual quality, therefore presenting the positive impact of urban greening strategies. Curved roofs account for less than 1% of the total and are primarily located on public or industrial buildings, mostly made with reflective metallic materials that temper surface heating but have limited greening potential.

Fig. 61 Roof typology in the case study zone, Source for base map: Geoportale Comune di Torino

Sloped Roofs

Green Roofs

Flat Roofs

Curved Roofs

Potential Buildings for green roof

Flat roofs in dense urban areas present the greatest opportunity for extensive green roof retrofitting due to their accessibility and structural feasibility" (Berardi et al., 2014). By combining the data on building age and roof type, three key building categories were identified in figure 62, in terms of their suitability for green roof implementation:

Newly constructed buildings with flat roofs that provide optimal structural and spatial conditions for green roof installation.

Buildings that already have green roofs contribute to existing local cooling and storm-water retention.

New buildings with sloped roofs, which impose limitations in terms of structure for implementing green roofs.

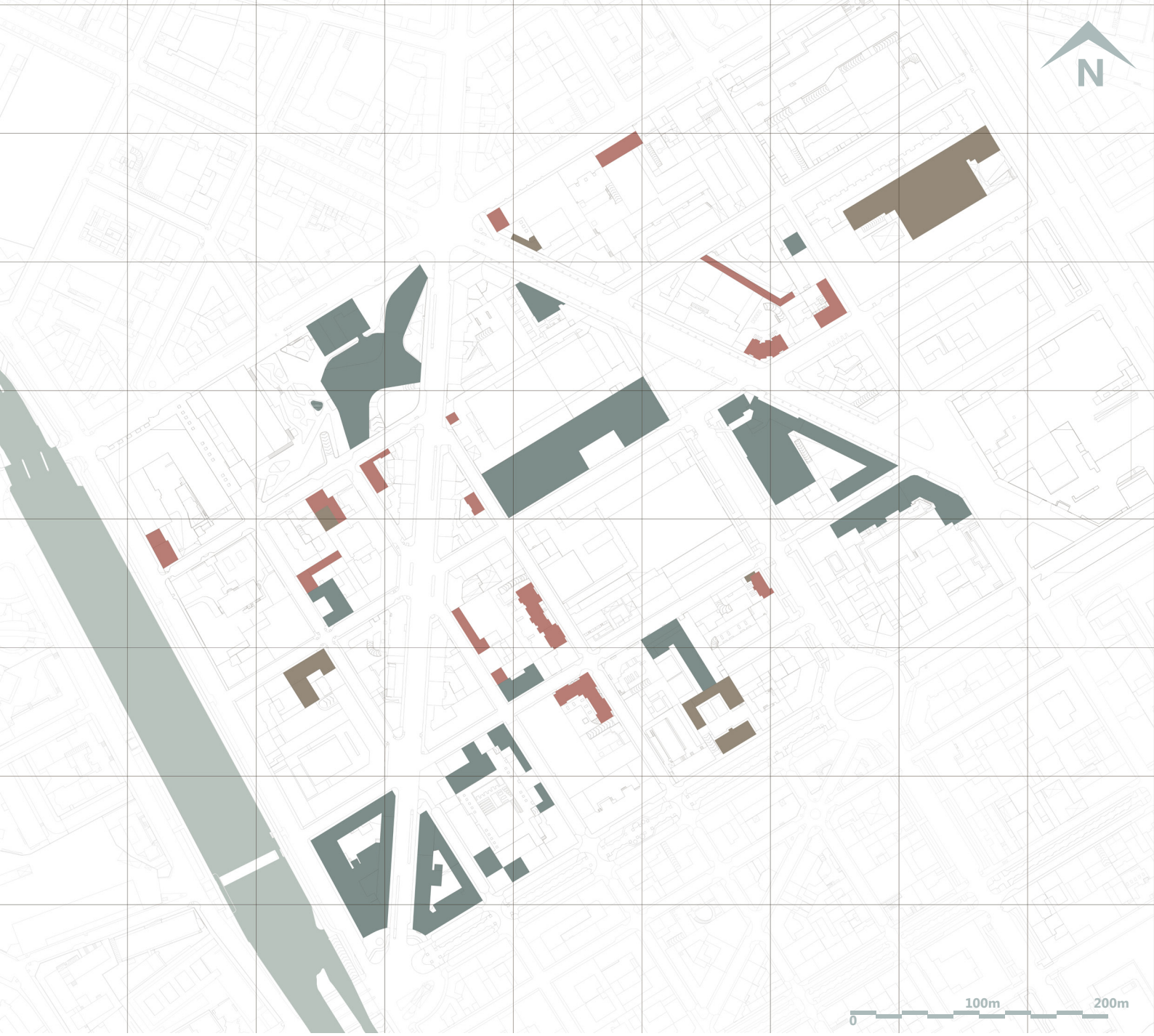

Fig. 62 Potential buildings for green roof implimentation , Source for base map: Geoportale Comune di Torino

Newly constructed buildings with sloped roof

Newly constructed buildings with flat roof (target buildings)

Buildings with green roof

Urban Fabric

Urban morphology defines and represents the main character of the city. Microclimate, thermal comfort, vegetation, density and urban quality are the main components that shape urban morphology (Özalp, 2022).

The configuration of the urban fabric plays a decisive role in shaping microclimatic conditions and the intensity of the urban heat island effect. Compact and continuous fabrics such as the continuous-regular and continuous-irregular typologies tend to trap heat due to reduced ventilation and high built density, yet they can also provide self-shading that slightly mitigates surface temperature in dense blocks(Kouklis et al., 2021). In contrast, discontinuous or irregular fabrics allow better air circulation but are often characterized by higher surface exposure and limited shading, which leads to higher heat accumulation during daytime.

As analyzed by Özalp (2022), In the study area, the urban fabric is composed of continuous-regular and continuous-irregular types dominating the residential core, while discontinuous-irregular and no-order fabrics appear along the borders. The industrial complex mass occupies a limited but climatically significant portion, contributing to local heat retention due to large impervious surfaces and low albedo materials. In figure 63, the urban fabric distributed in the case study area is shown.

Fig. 63 Urban fabric classifications, Source for base map: Geoportale Comune di Torino

Type 1: Continuous–Regular

Type 2: Continuous–Irregular

Type 4: Discontinuous–Irregular

Type 7: No Order

Type 10: Industrial Complex Mass

Local Climate Zone (LCZ)

Figure 65 shows Lcal Climate Zone classifications in the study area. The area is predominantly classified by Built Land Cover Types, reflecting its high-density urban setting. The largest and most widespread classification is LCZ 2: Compact midrise (brighter red). This zone consists of dense blocks of midrise buildings (3–9 stories), characterized by mostly paved surfaces and a few or no trees.

The next most significant classification is LCZ 1: Compact highrise (darker red), which occupies the upper right corner of the zone. This area is characterized by the highest density, featuring tall buildings (ten or more stories) and little pervious land cover.

Smaller, distinct zones are also present:

LCZ 10: Heavy industry is centrally located within the zone, indicating the presence of large industrial structures, power plants, and associated infrastructure.

A small portion of LCZ 8: Large lowrise is observed in the bottom right corner, which is characterized by open arrangements of large lowrise buildings (1–3 stories) with a mix of pervious and impervious surfaces. All the classifications are based on figure 64, provided by World Urban Database.

Fig. 64 Local Climate Zone Classifications, Source: World Urban Database

Fig. 65 LCZ in the case study area, Source for base map: Geoportale Comune di Torino

1 Dense mix of tall buildings to tens of stories. Few or no trees. Land cover mostly paved. Stone, brick , tile, and concrete construction material.

2 Dense mix of midrise buildings (3-9) stories. Few or no trees. Land cover mostly paved. Stone, brick , tile, and concrete construction material.

5 Open arrangement of midrise buildings (3-9) Abundance of pervious land cover (low plants, scattered trees). Concrete, Stone, steel and glass construction materials.

8 Open arrangement of Large lowrise buildings (1-3 stories). Fewor no trees. Land cover mosty paved. Steel, concrete, metal and stone construction materials.

10 Lowrise and midrise industrial structures (towers, tanks, stacks). Fewor no trees. Land cover mosty paved or hard-packed. Metal, steel and concrete construction materials.

3.2.3 Analysing the streets

The intensity and spatial distribution of the UHI effect are fundamentally controlled by immutable characteristics of the built environment. In order to go beyond generalized assumptions, a granular, data-driven baseline was established for the Aurora district through a rigorous morphological analysis of the fourteen primary street segments within the study area. The specific, non-negotiable parameters that govern the local exchange of energy, momentum, and radiation and thus dictate microclimatic conditions were mapped and quantified.

As illustrated in the following drawings and pages, the analyses cover the most crucial parameters for each street:
Urban Canyon Geometry: A critical parameter determining the Sky View Factor ,
Street Length: The extent of the thermal corridor.
Street Width: A direct input into the H/W ratio, influencing solar penetration and potential ventilation.
Average Building Height: The numerator in the H/W ratio, representing the capacity for heat storage and shadowing.
Surface Characteristics:which represent the albedo and heat capacity of the paving and
Orientation: The alignment of the street axis, which dictates the daily solar exposure patterns and the efficacy of natural cooling through wind.

This detailed geometric and material dissection is essential for understanding the intrinsic spatial and material factors influencing UHI in the district. It is through this comprehensive measurement that we can predict and understand where thermal vulnerabilities are greatest.

The analysis is structured in a manner that allows for a comparative microclimatic assessment, grouping the fourteen streets based on their prevailing orientation. We start with the Northeast-Southwest axis, opening with the major corridor of Via Bologna, then continuing with its internal parallel arteries: Via Ancona, Via Perugia, Via Foggia, and Corso Regio Parco. This grouping enables direct comparison of H/W effects under similar solar exposure conditions.

The structure then moves to the singular, strong North-South orientation of Corso Palermo, and the separate segment of Corso Brescia (Northeast-Southwest).

The final and largest group is that of the streets aligned along the Northwest-Southeast axis. These include Lungo Dora Firenze, Via Pisa, Via Parma, Via Modena, Corso Verona, Via Padova, and Corso Novara. In ordering the streets in this way, the subsequent microclimatic simulations (presented in table 6) can be directly related back to these base urban morphological characteristics. This detailed procedure ensures that any suggested climate-responsive design strategy is not only based on theoretical principles but also precisely calibrated to the particular spatial constraints and thermal issues highlighted for the Aurora district.

Table 6- Streets in the case study area

Via Bologna
Orientation

Urban Canyon


=0.74

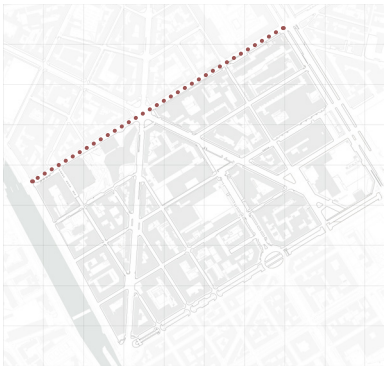

Via Ancona
Orientation

Urban Canyon


=0.99

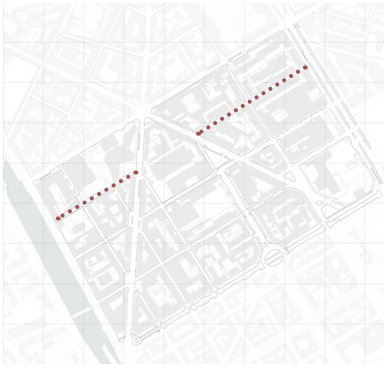

Via Perugia
Orientation

Urban Canyon


=0.61

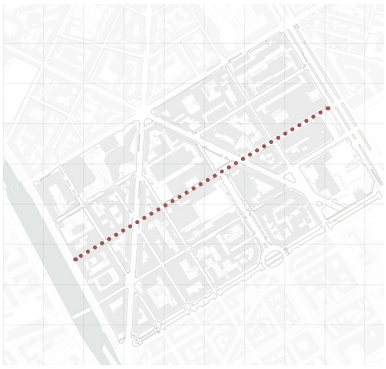

Via Foggia
Orientation

Urban Canyon


=0.81

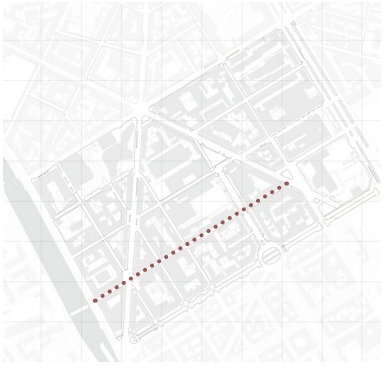

Corso Regio parco
Orientation

Urban Canyon

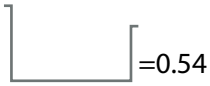

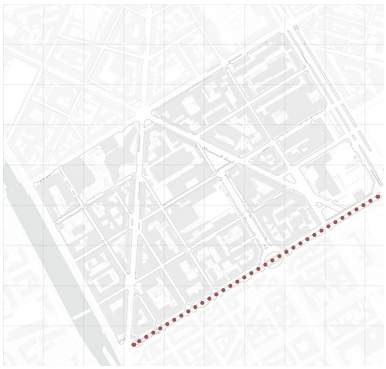

Corso Palermo
Orientation

Urban Canyon

Corso Brescia
Orientation

Urban Canyon

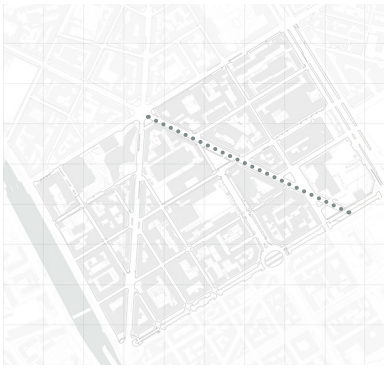

Lungo Dora Firenze
Orientation

Urban Canyon

Table 6- Streets in the case study area

Via Pisa
Orientation

Urban Canyon


=0.85

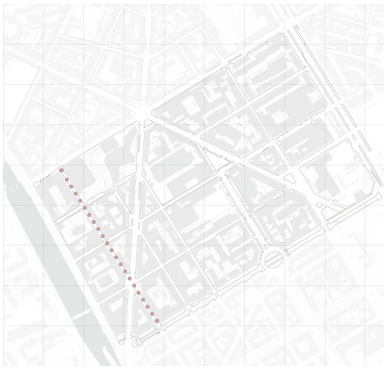

Via Parma
Orientation

Urban Canyon


=1.18

Via Modena
Orientation

Urban Canyon


=1.08

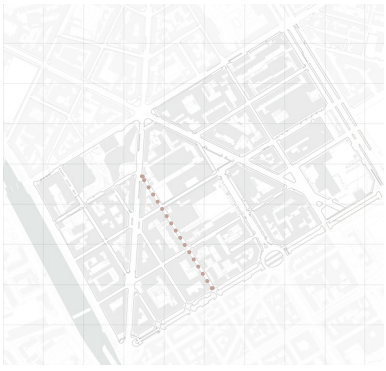

Corso Verona
Orientation

Urban Canyon


=0.37

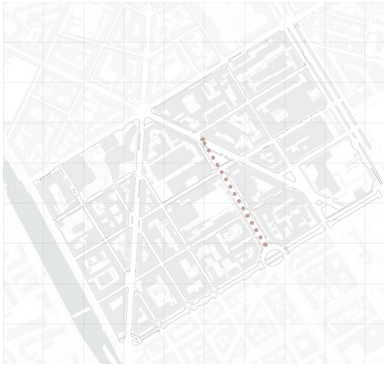

Via Padova
Orientation

Urban Canyon


=1.23

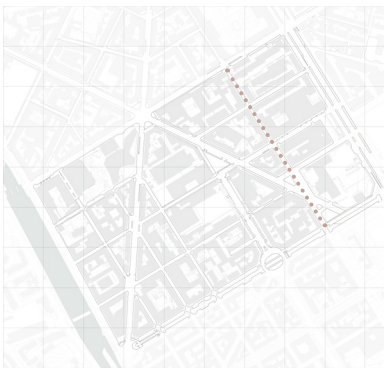

Corso Novara
Orientation

Urban Canyon

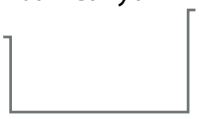
=0.49

Via Bologna

Via Bologna, one of the major streets of the study area, hosts the Museo Lavazza and is an important cultural and mobility axis not only in the area but also in the city. The street is 19–20 meters wide, with average building heights of 16.75 m on the north side and 12.58 m on the south side, that result an urban canyon ratio of 0.74.

This section includes asphalt sidewalks, a 10.5-metre carriageway, parking lanes on both sides of the street (2.5–2.8 m), and a central bus lane, functioning as a corridor of public transportation. The main surface materials in this street are asphalt, bright asphalt and in some parts especially the sidewalks connected to Museo Lavazza granite stones and concrete. The mentioned street characteristics are presented in figures 66 and 67.

Vegetation in this street is very limited, the street itself has only five Crataegus trees, located on the western segment, with a few grass or permeable surfaces.

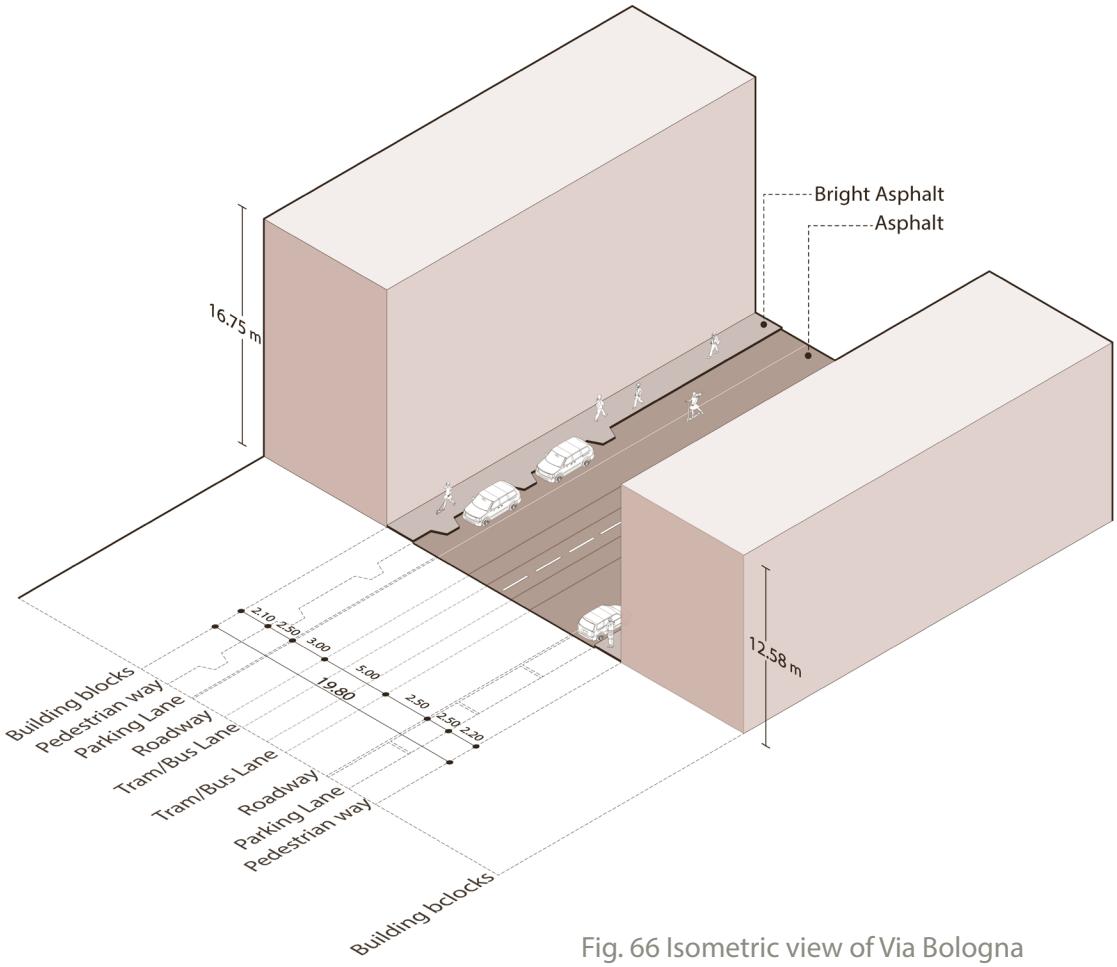

Fig. 66 Isometric view of Via Bologna

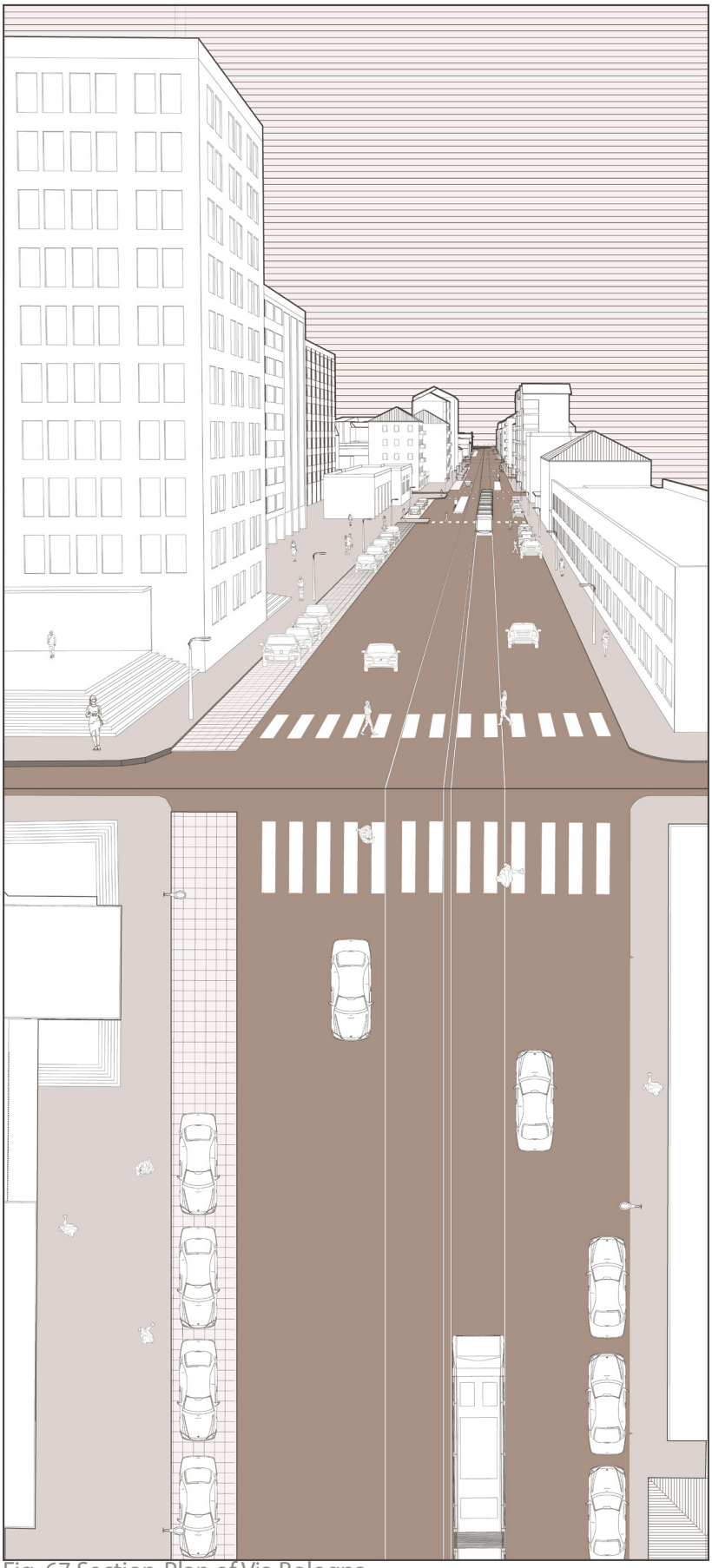

Fig. 67 Section-Plan of Via Bologna

Via Ancona

Via Ancona is a narrow street with a width of 11.90 m including sidewalks with width of 1.5–1.6 m on both sides. Sidewalks are surfaced partly with bright granite stones and partly with asphalt or bright asphalt, and the roadway and parking lanes are completely asphalted.

The average building height in this street is 14.5 meters on the northern side, and 9.5 meters on the southern side, that make an urban canyon ratio of 0.99. Therefore, the street profile is relatively enclosed. The layout of the street is shown in figures 68 and 69.

Via Ancona does not contain street trees, or vegetation pavements, but vegetation from the school courtyard, located on the western side of the street and green elements related to the Museo Lavazza on the opposite side provide a minor influence on microclimatic conditions along this street.

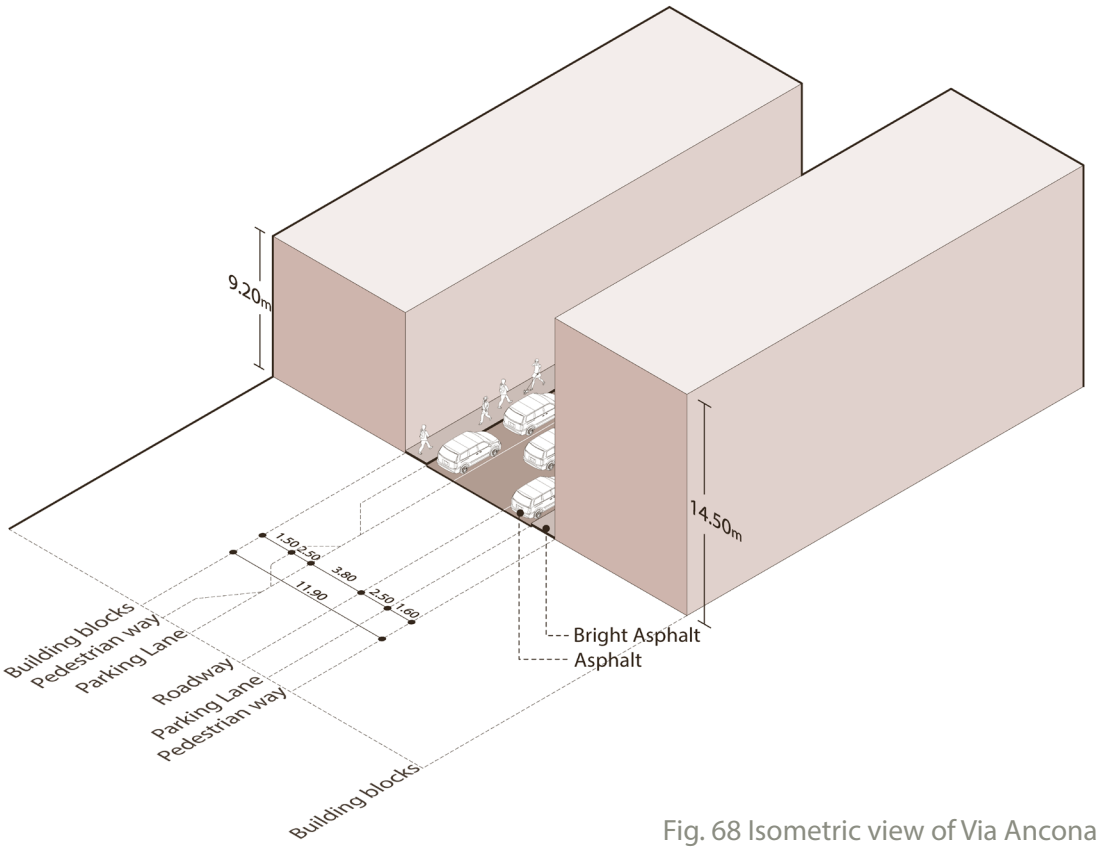

Fig. 68 Isometric view of Via Ancona

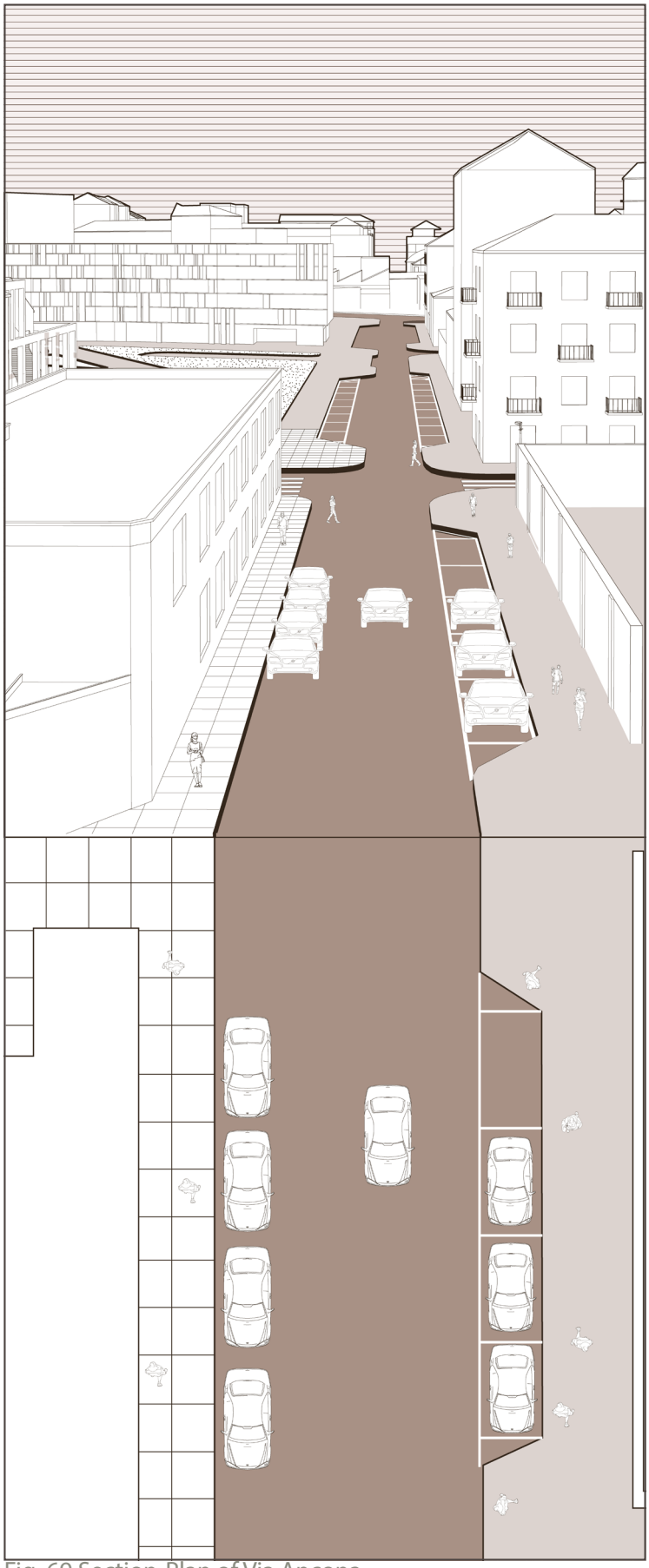

Fig. 69 Section-Plan of Via Ancona

Via Perugia

Via Perugia is a one-way street, 19.10 meters wide. The average building height in the street is 11.8 meters, producing an urban canyon ratio of 0.61. Therefore, the profile of the street is relatively open. The street has wide sidewalks, approximately 2.8 meters on one side and 3.8 meters on the other, and about 90% of the surfaces are paved in asphalt. The rest of the pavements are in bright asphalt or dark granite stones.

The roadway in the street is completely asphalt-paved, and it has parking lanes on both sides. In some parts of this street, Parking lanes perpendicular to the sidewalk. There is no street tree or vegetation in this street along the area. Figures 70 and 71 depict the characteristics of this street.

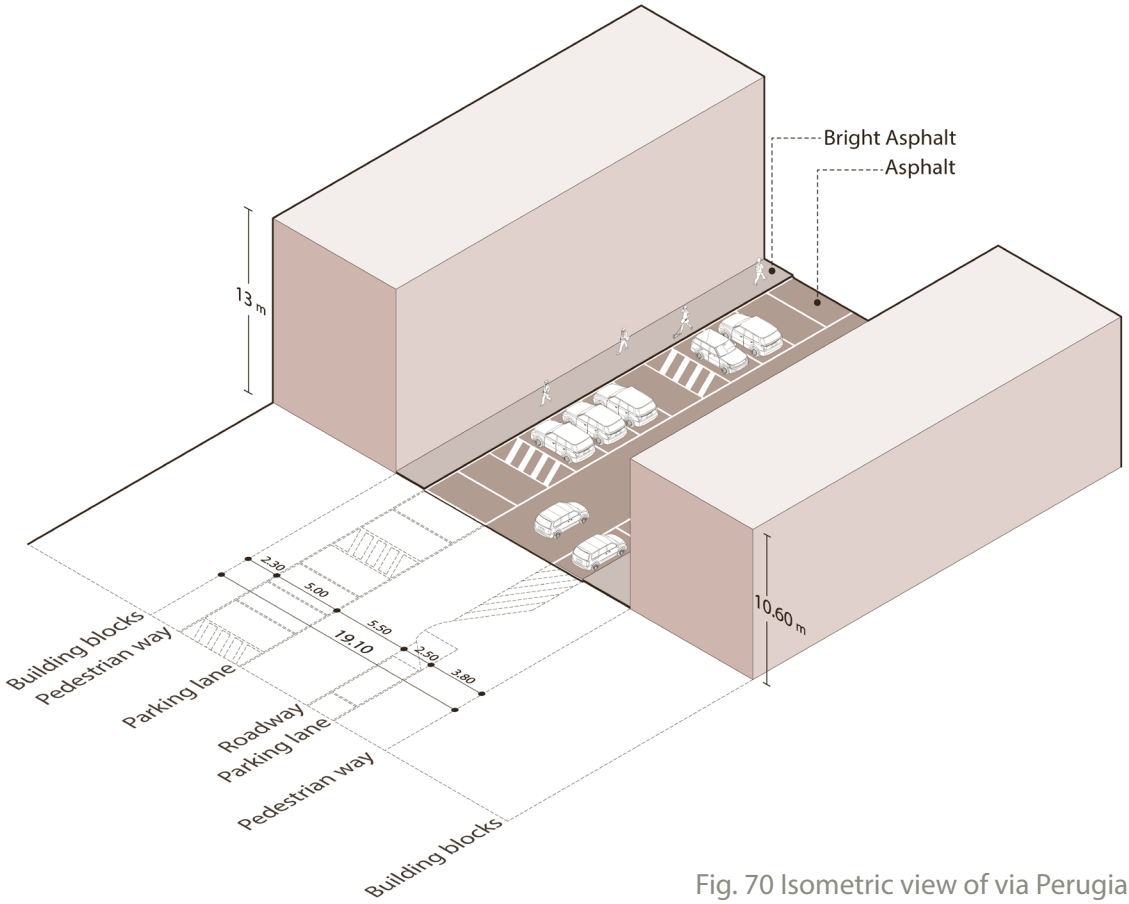

Fig. 70 Isometric view of via Perugia

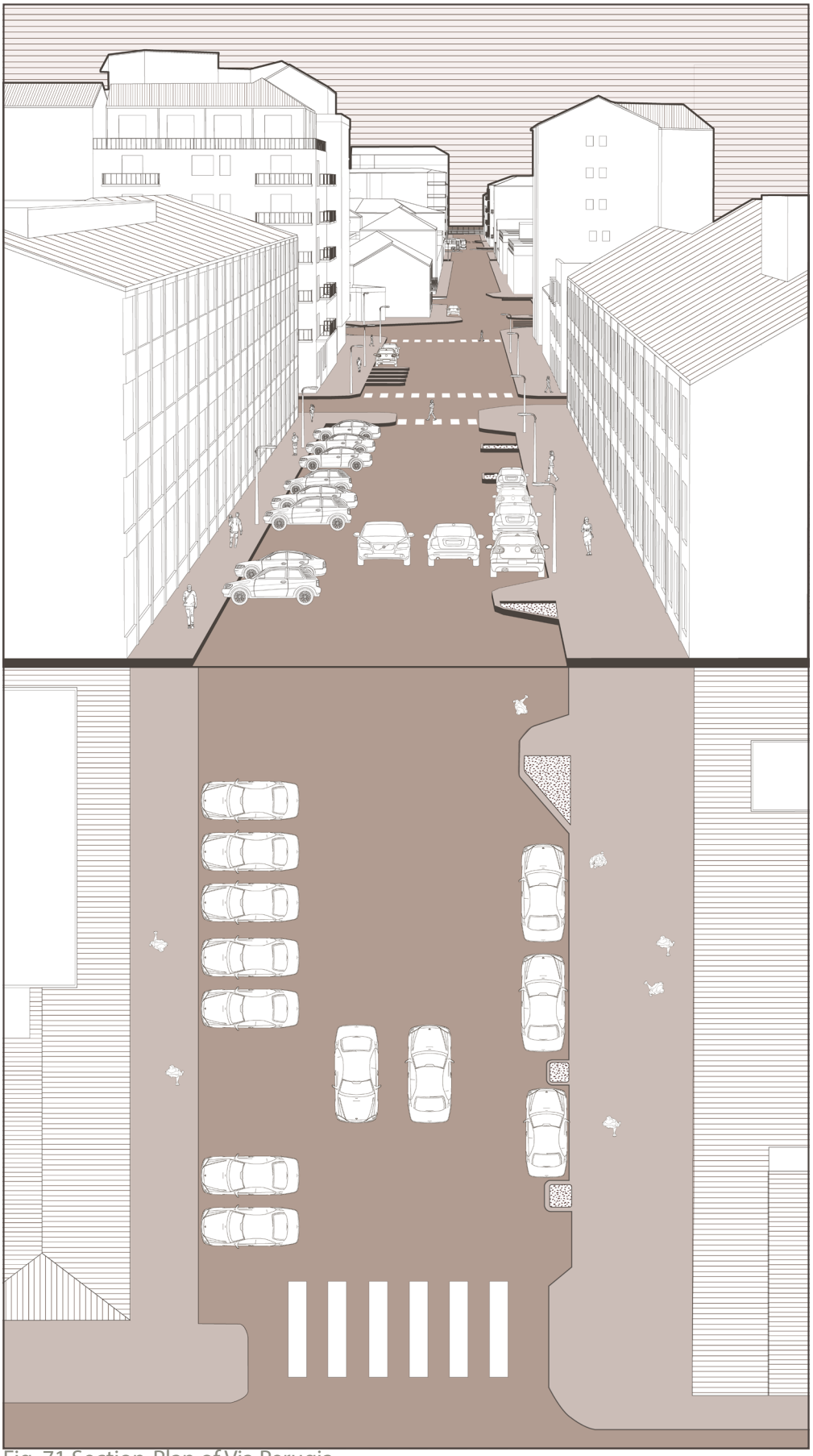

Fig. 71 Section-Plan of Via Perugia

Via Foggia

Via Foggia is a one-way street that is 14.6 meters wide. The average building height in this street is 11.8 meters, and the urban canyon profile is moderately open at 0.81. On the both sides of the street, the width of the sidewalks varies between 2.5 and 5 meters along the street. In sections where the sidewalks are wider, no parking lane is presented, thus allowing space for more pedestrians.

The material distribution for the sidewalks and carriageway is dominated by asphalt or bright asphalt. Moreover, the actual roadway is completely asphalt-paved, and no vegetation is provided along the street in the area. These characteristics are represented in figures 72 and 73.

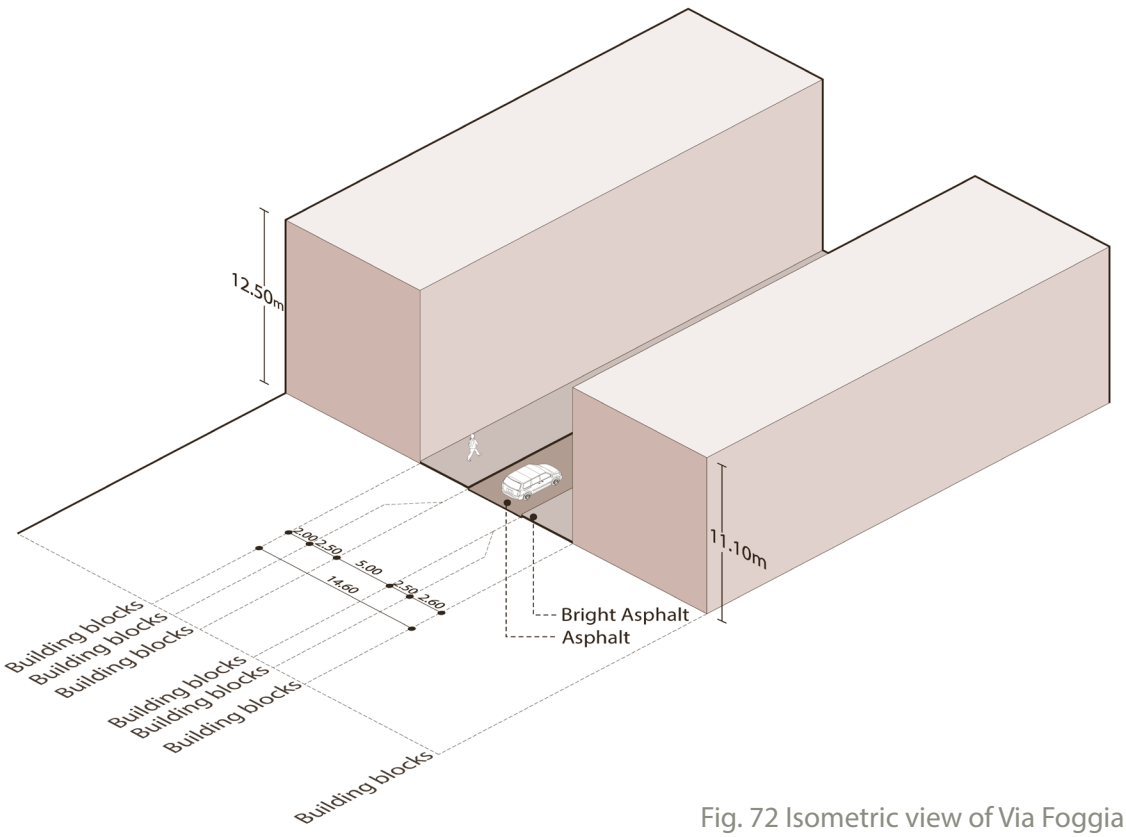

Fig. 72 Isometric view of Via Foggia

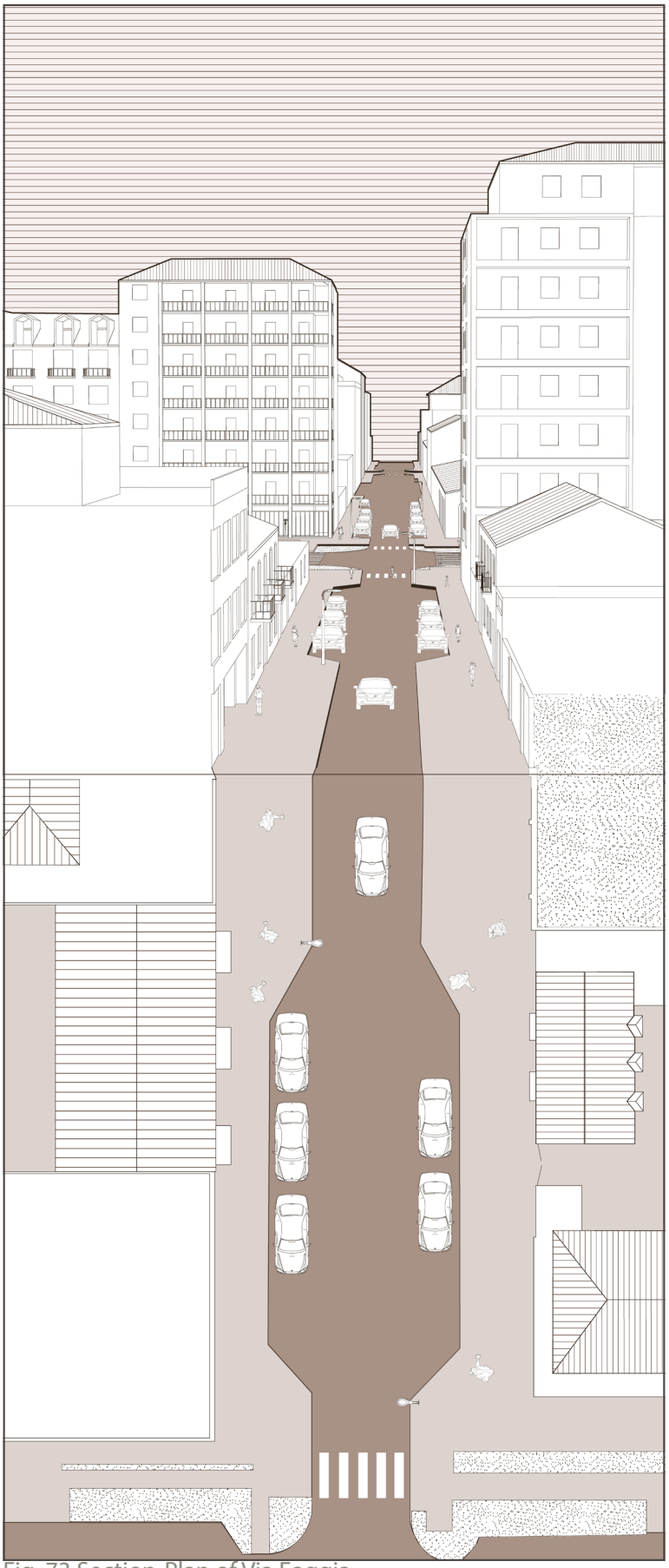

Fig. 73 Section-Plan of Via Foggia

Corso Regio Parco

Corso Regio Parco is one of the main streets in terms of historic corridors and accessibility in the study area and in Turin. Corso Regio Parco is one of the longest streets in the city with a legnth of 2.80 km, but in this area, a 780-meter-long segment is analysed which is the western part of the street. The street has an average width of 32.85. The average building height is 20.60 meters, producing an urban canyon ratio of 0.54. The character of this street is defined by a central pedestrian promenade, 5 meters wide, and paved with granite and in some parts cobblestones. Median strips down the promenade contain rows of mature trees. The parking lanes are perpendicular (with a slight angle) to these strips which are paved with permeable pavement providing both parking and some infiltration in the street. The carriageways are surfaced with asphalt on both sides, with granite surfaces at intersections, while pavements are of bright asphalt and, in places, of concrete-like materials. These trees, combined with the pavements materials, is expected to provide microclimatic comfort. Figures 74 and 75 illustrate features of this street.

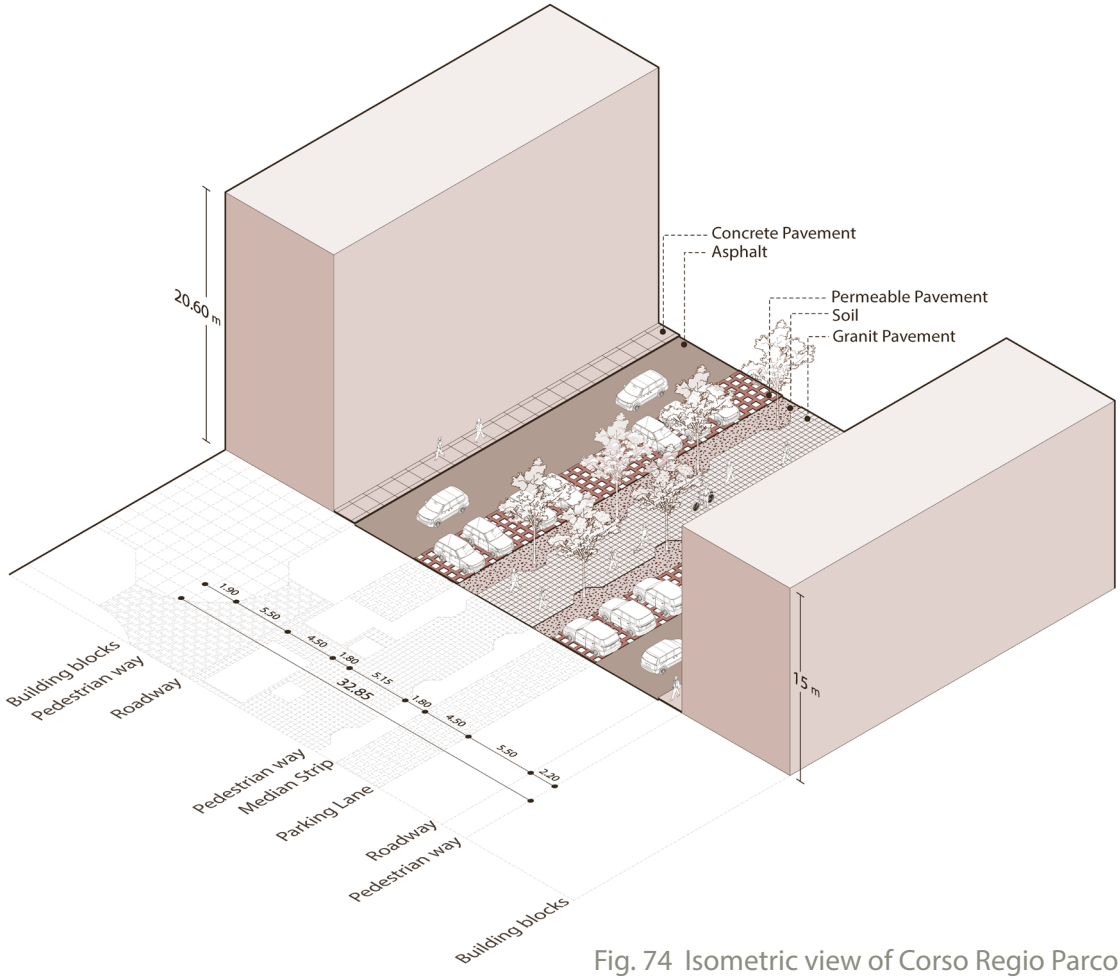

Fig. 74 Isometric view of Corso Regio Parco

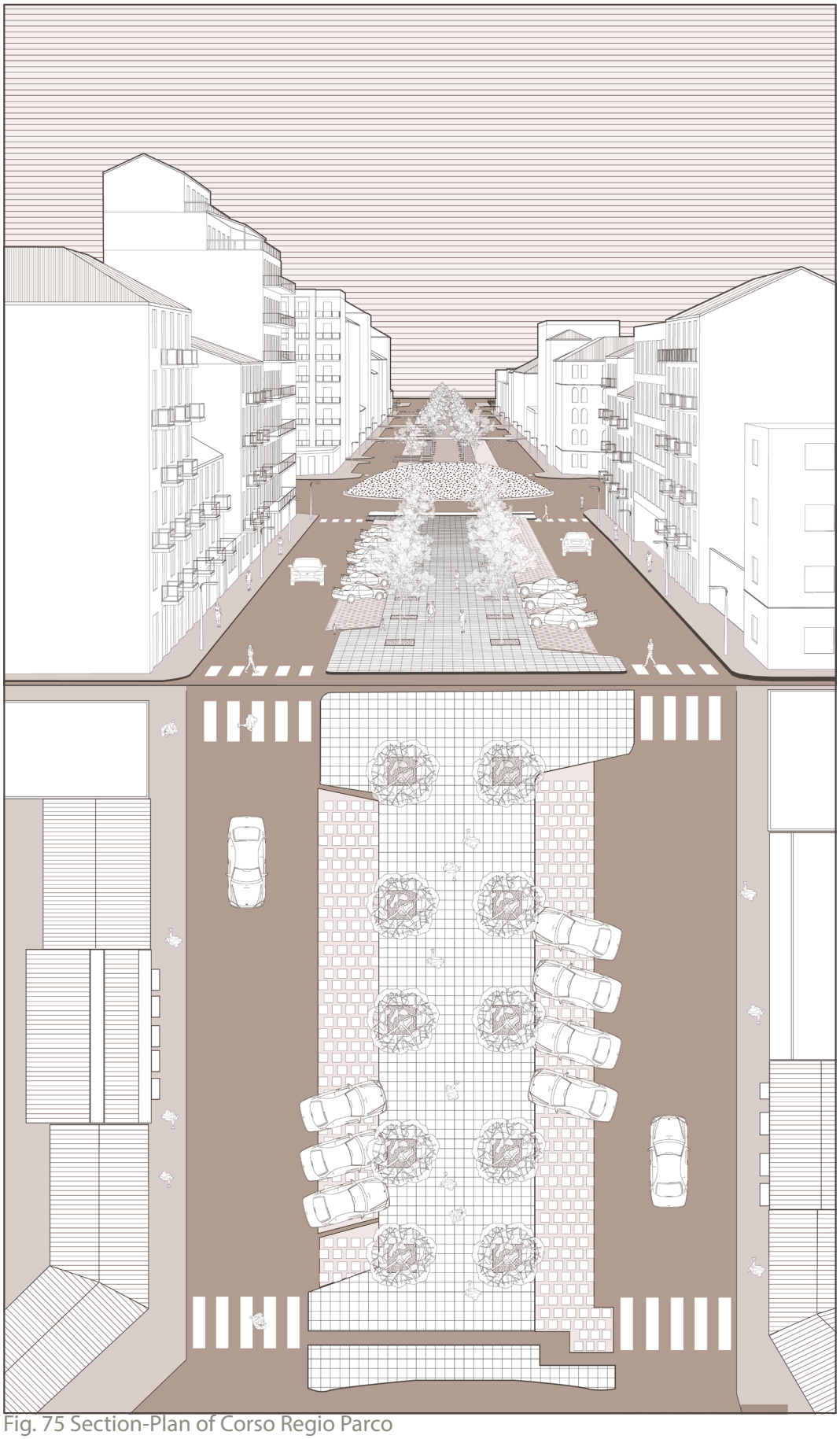

Fig. 75 Section-Plan of Corso Regio Parco

Corso Palermo

Corso Palermo is the only north–south oriented street in the study area, the segment analysed in this zone is 560 meters logn, and the width is 19.90 meters. The average building height is 14.55 meters, resulting to an urban canyon ratio of 0.73.

The street has sidewalks on both sides, partly paved with bright asphalt and partly with concrete, but does not have street trees or any other vegetation. It has a central bus lane along the middle of the street. The parking lanes can be found in sections without bus stops or opposite to the bus stations.

This street contains large intersections with great areas of asphalt, and no vegetation provided. These features have been drawn in figures 76 and 77.

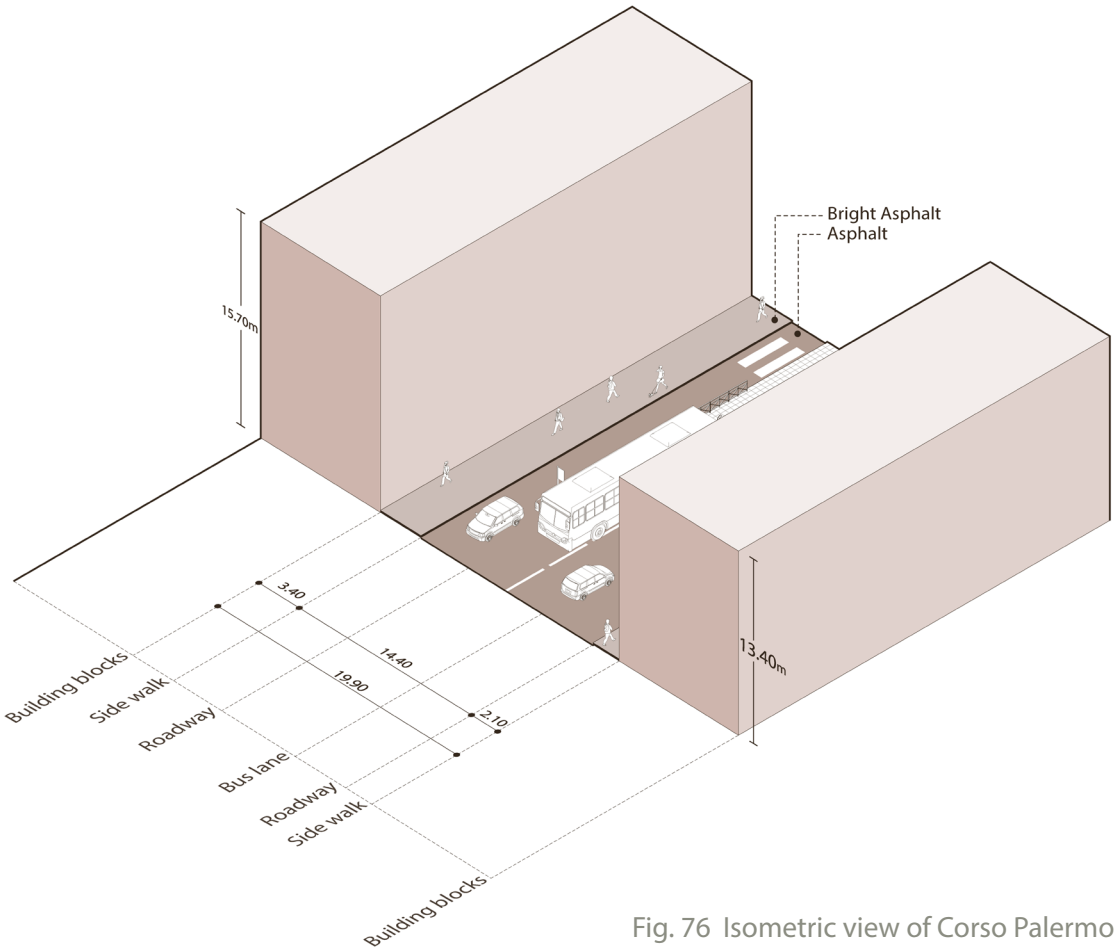

Fig. 76 Isometric view of Corso Palermo

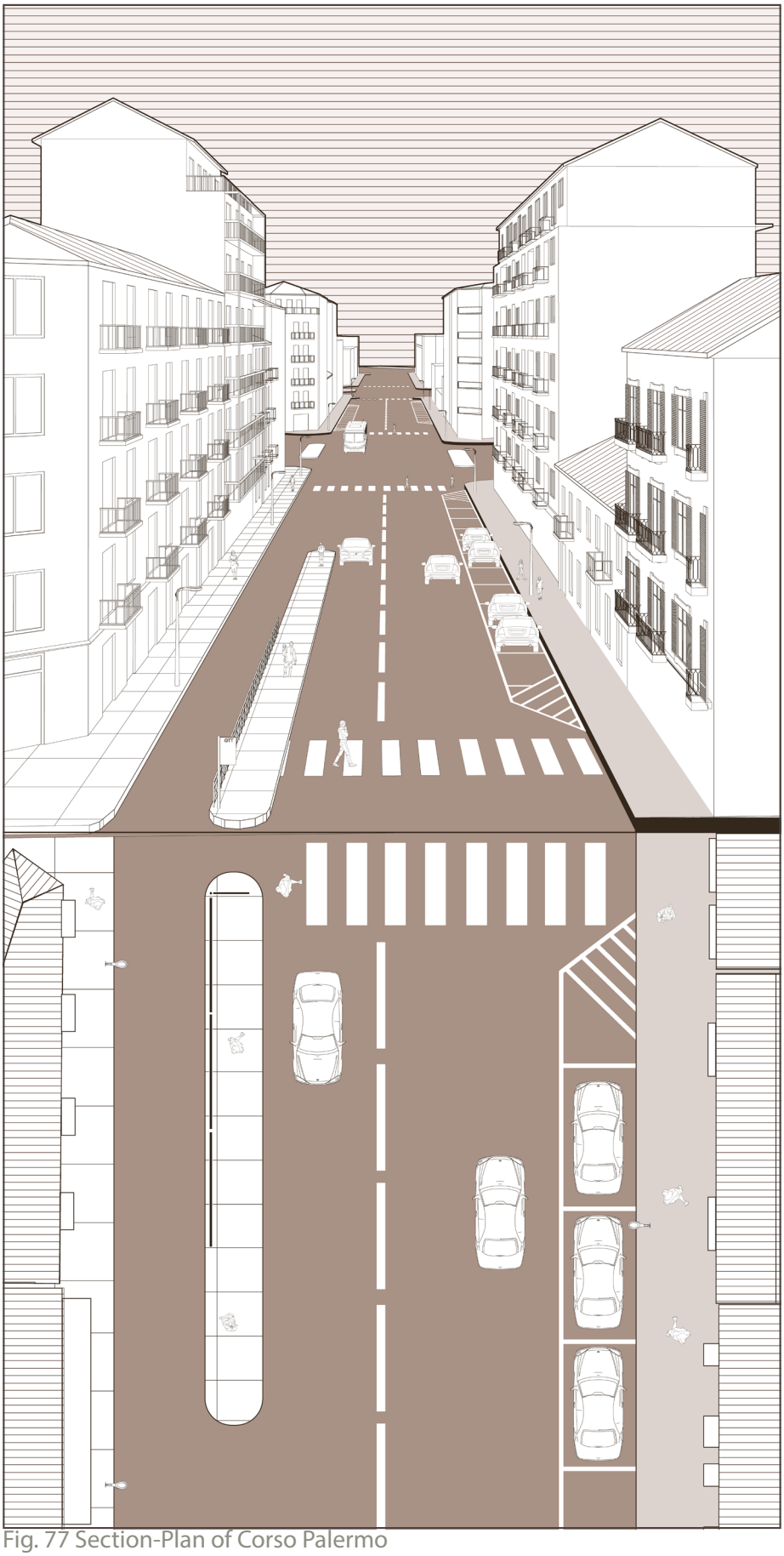

Fig. 77 Section-Plan of Corso Palermo

Corso Brescia

Corso Brescia is a Northeast-Southwest oriented street in the study area and has a width of 25.7 meters. With an average building height of 10.60 meters it results to an Urban Canyon of 0.41.

The materials of the sidewalks are partly concrete and partly of bright asphalt and on both sides.

The street has mature trees on either sides, about 16–20 meters high, providing considerable shading and visual comfort.

The carriageway is about 13.3 meters wide, asphalted, and has slightly angular parking lanes on both sides, increasing its capacity for parking without disrupting the traffic flow. Figures 78 and 79 show the features of the street mentioned above.

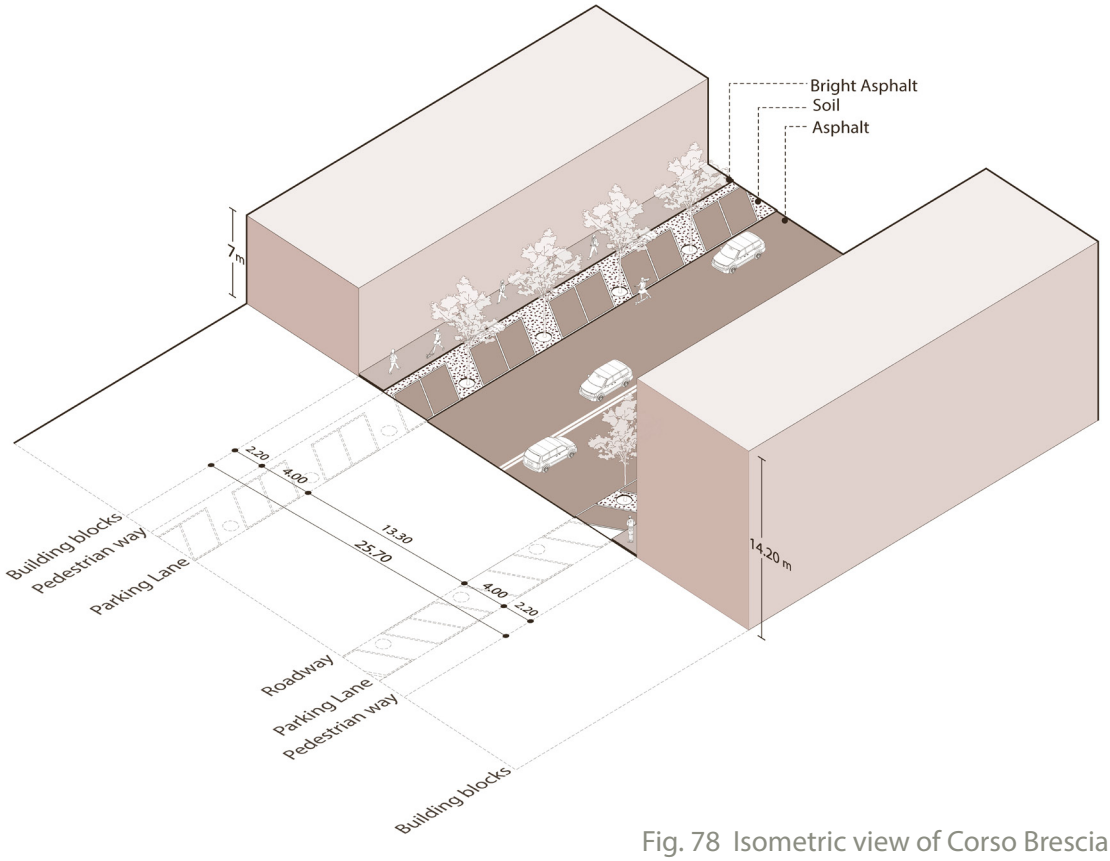

Fig. 78 Isometric view of Corso Brescia

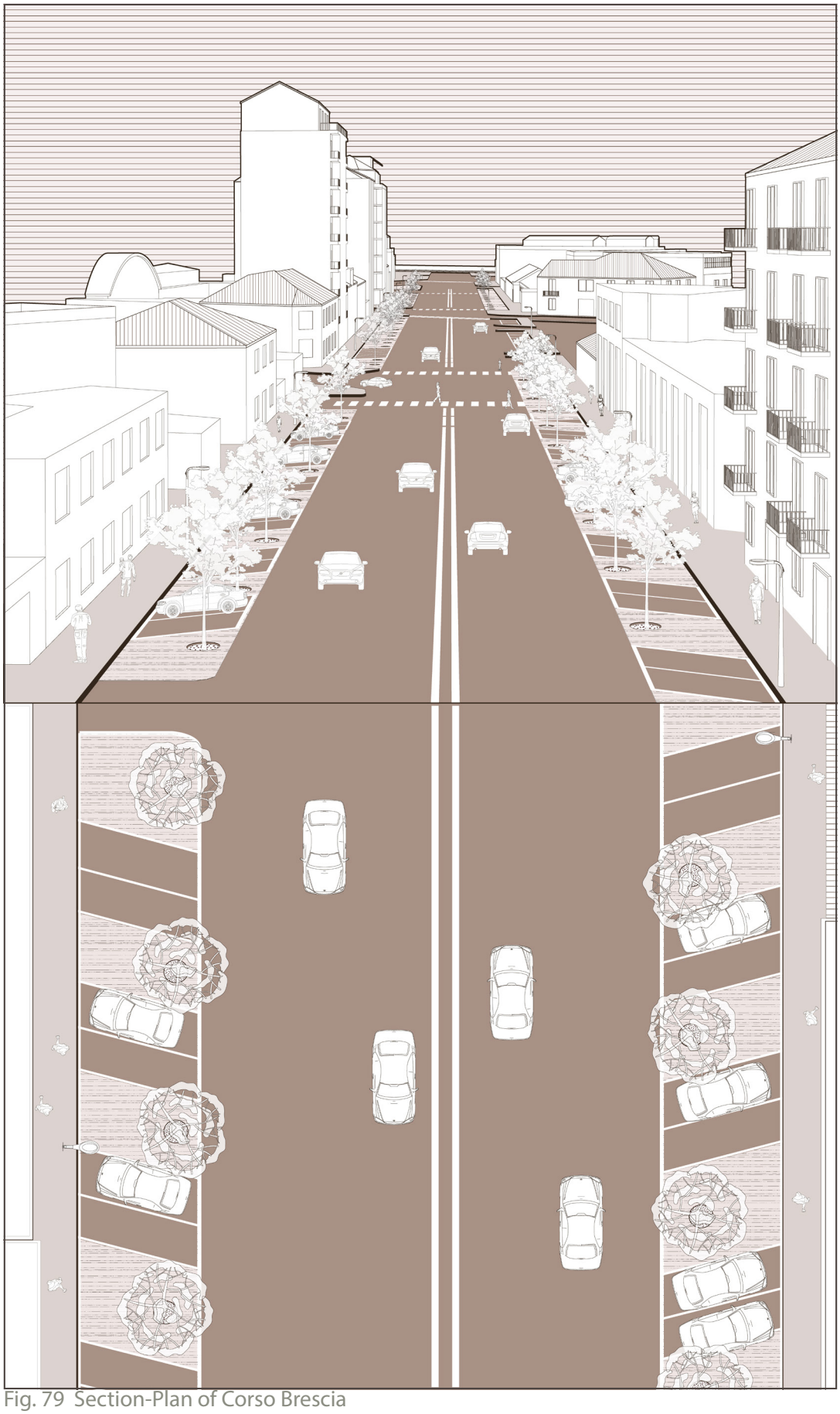

Fig. 79 Section-Plan of Corso Brescia

Lungo Dora Firenze

On the west side of the area, Lungo Dora Firenze goes along the Fiume Dora, with an average building height of 12.85 meters on the opposite side of the river. The street is 22.95 meters wide, giving it an urban canyon ratio of 0.55, that makes an open street profile.

The west side along the river has tall pine trees with an average height of 12 meters that provide shading. Asphalt paved parking lanes are on both sides of the street. On the west side also there is a bike lane with red asphalt coating and a pedestrian path. On the eastern side, the sidewalk is made of bright asphalt. The river along the street which provides water surface, high trees, bike path, and pedestrian areas are expected to make a positive contribution to the microclimatic and street character. The street features can be seen in figures 80 and 81.

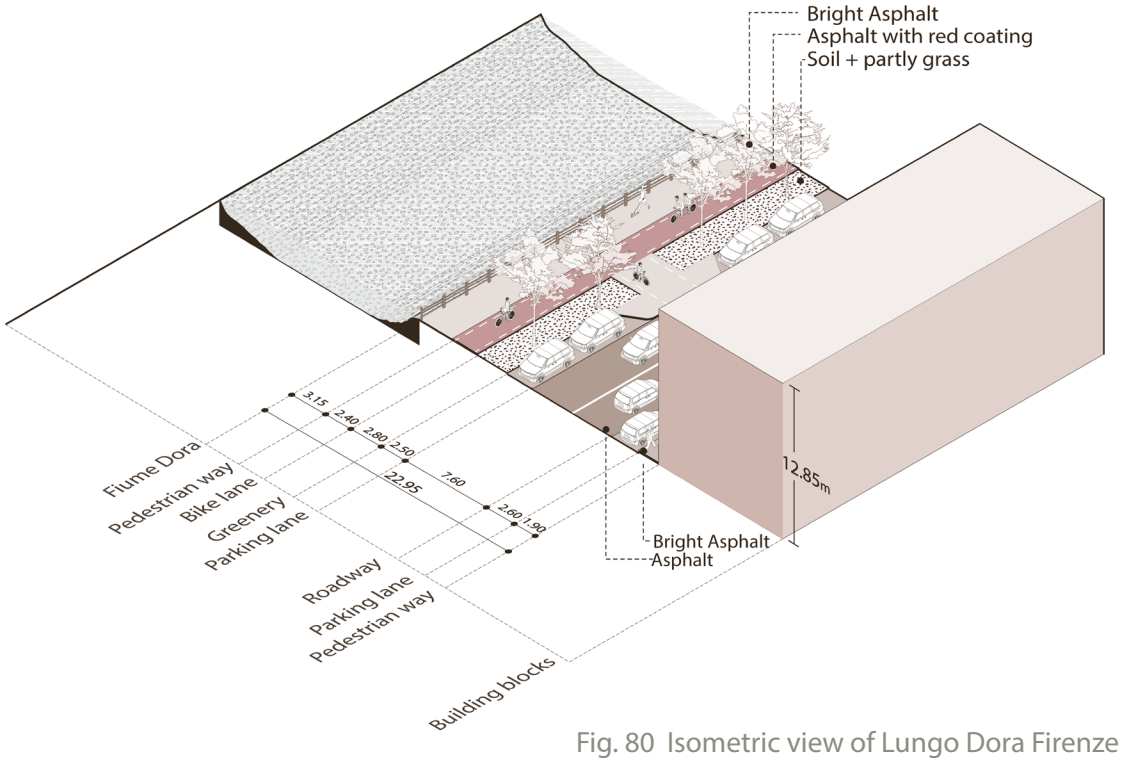

Fig. 80 Isometric view of Lungo Dora Firenze

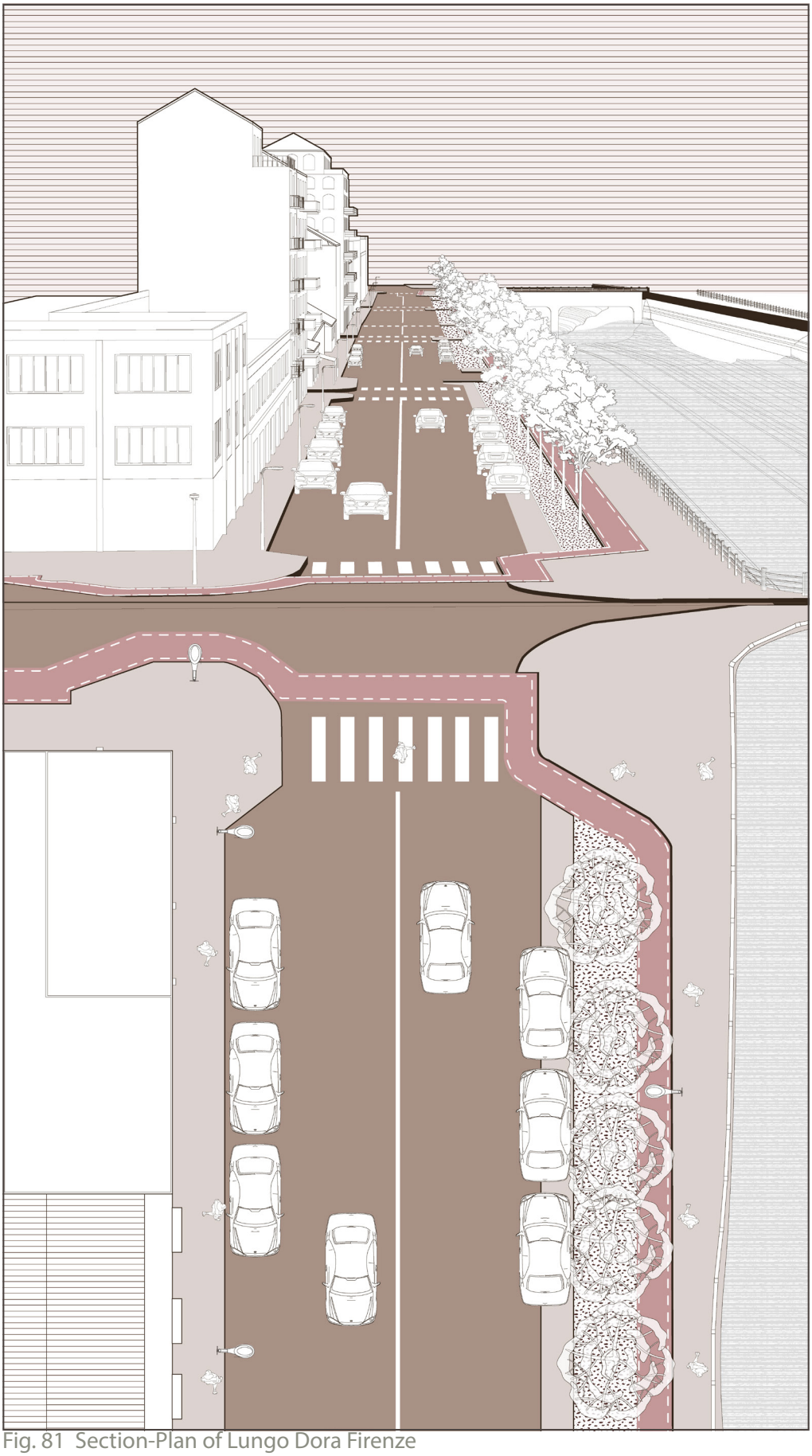

Fig. 81 Section-Plan of Lungo Dora Firenze

Via Pisa

Via Pisa is a street with a width of 11.90 meters and an average Building's height of 10.15 meters. The northern part of the section of the street in the study area is completely pedestrianized, paved with bright granite stones, and lined with 14 young trees that have an average 5 meters height.

In the southern segment, the street is one-way with parking lanes and asphalt sidewalks on both sides. However, the granite pavement from the northern pedestrian segment continues into the sidewalk of southern segment of the street up to a certain point.

In contrast with the north segment, no vegetation is present in the southern part of the street, which is expected to make a difference in terms of shading and microclimatic comfort in the two parts of the street. Via Pisa features are shown in figures 82 and 83.

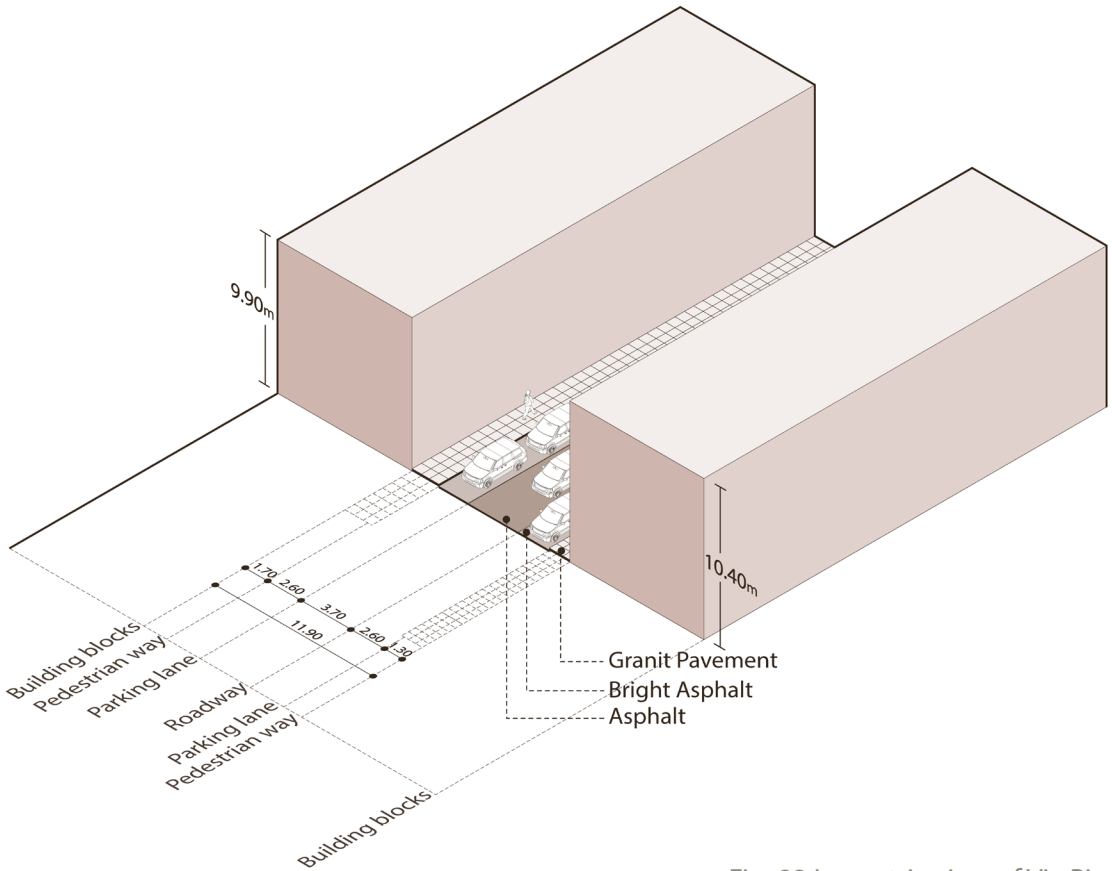

Fig. 82 Isometric view of Via Pisa

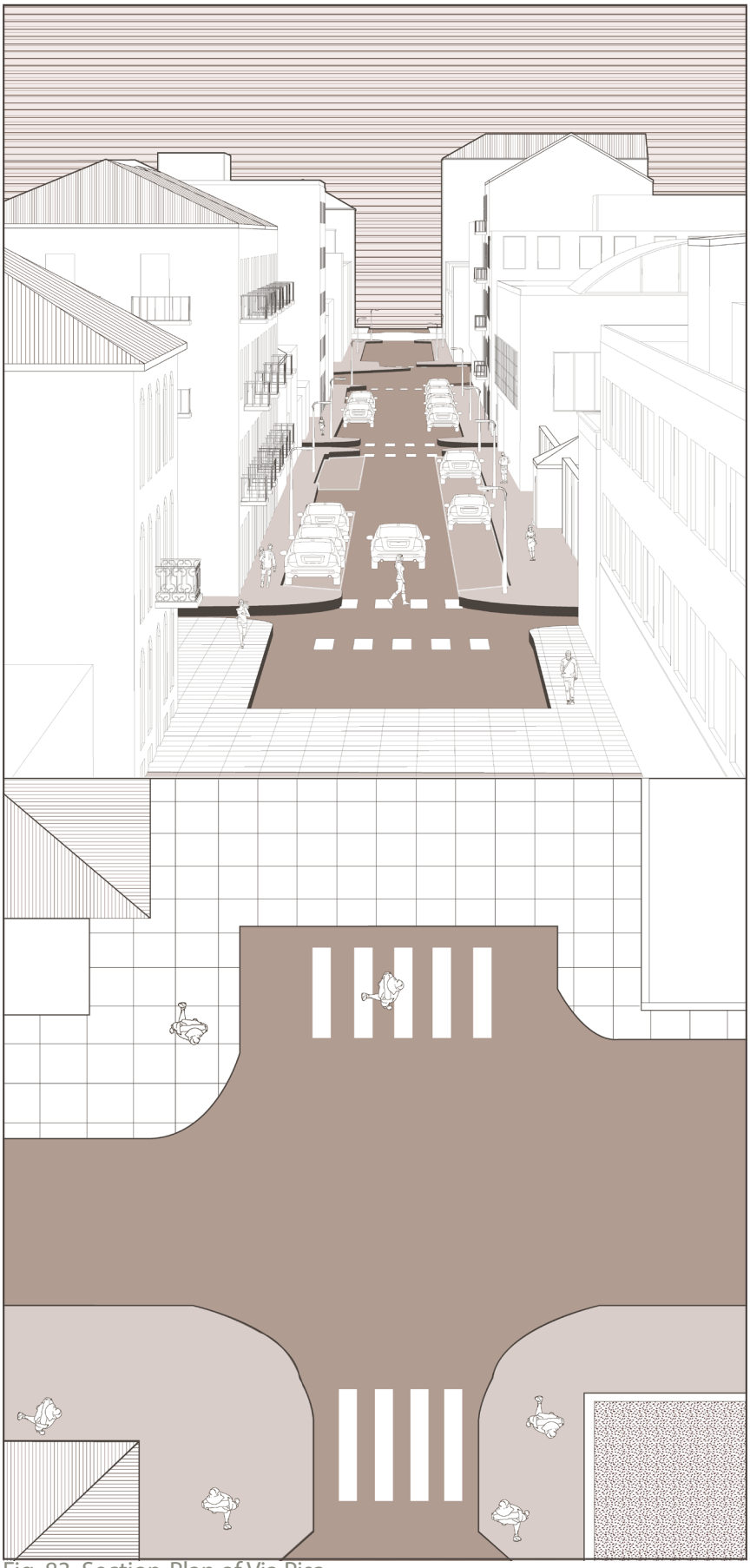

Fig. 83 Section-Plan of Via Pisa

Via Parma

Via Parma is a street with 11.2 meters width and an average building height of 13.25 meters, so it has one of the highest urban canyon ratios in the study area, which is 1.18, and results to an enclosed and deep street profile.

This southern part of the street is paved with cobblestone, but the rest of the street section in the noth part are asphalted. On each side, there are parking lanes, a mix of bright asphalt / normal asphalt pavement. No vegetation is present on this street to provide shading. Figures 84 and 85 illustrate the layout of the street.

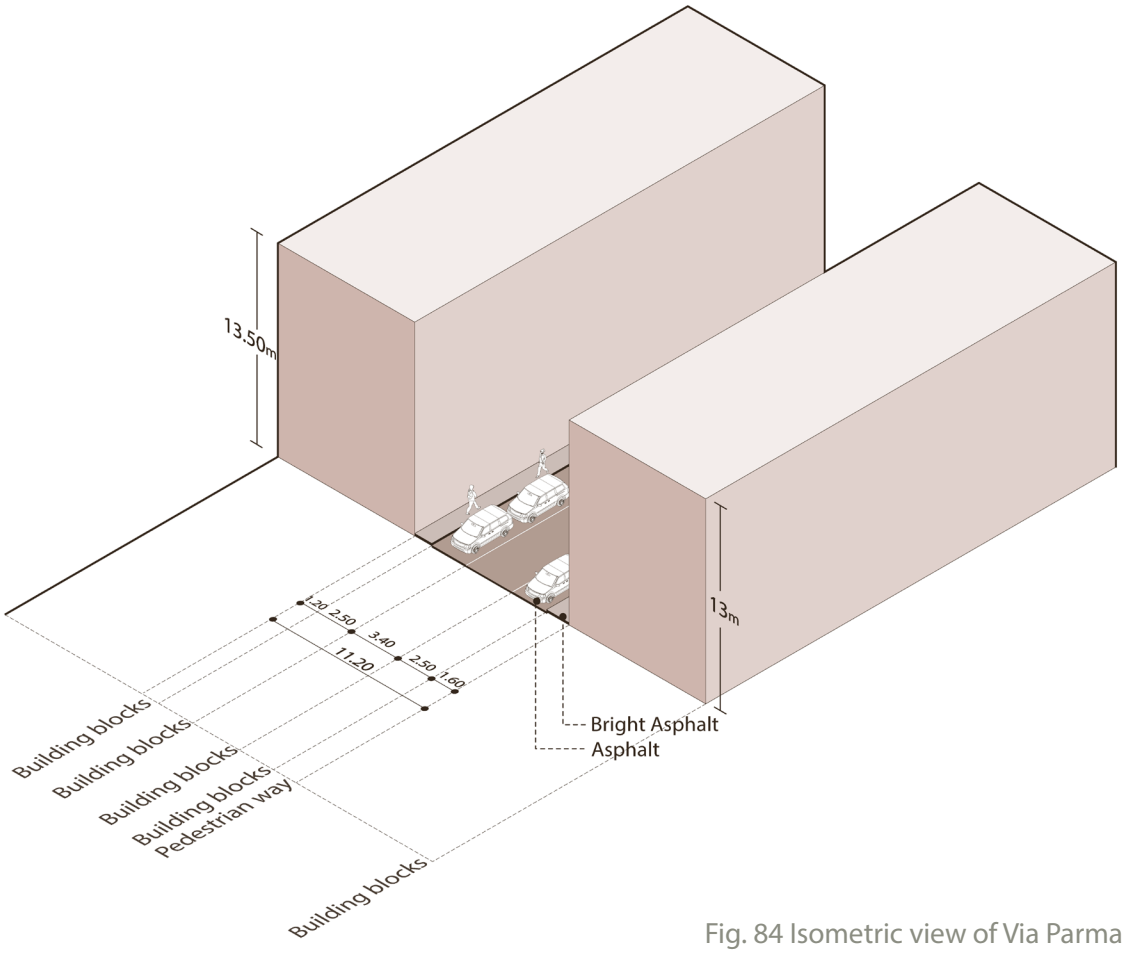

Fig. 84 Isometric view of Via Parma

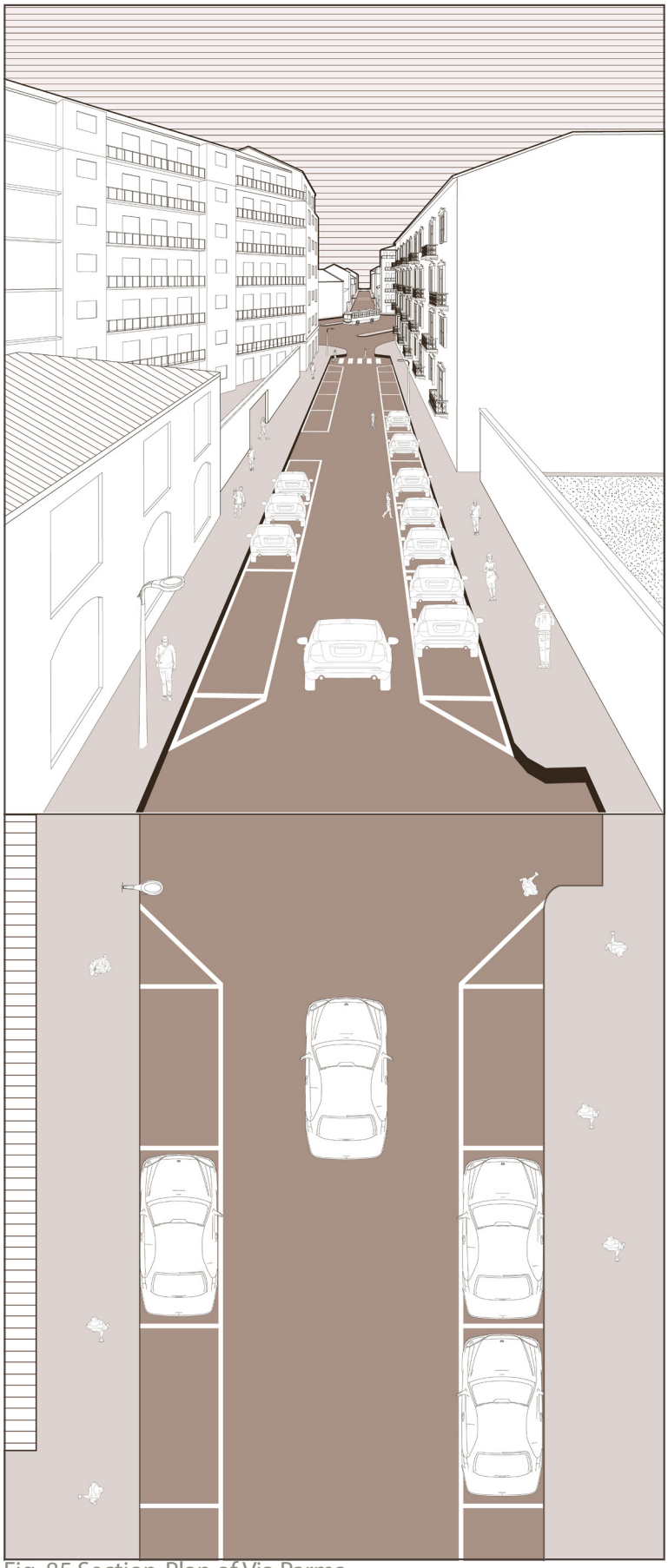

Fig. 85 Section-Plan of Via Parma

Via Modena

Via Modena is a narrow one-sided street with a width of 11.2 meters. The average building height in this street is 12.1 meters, that make the urban canyon ratio 1.08, which is a relatively enclosed street profile.

The street has parking lanes on both sides; sidewalks are paved with bright asphalt along all its length. No vegetation is present which is expected to provide poor shading as well as microclimatic condition. The features of the street are shown in the figures 86 and 87.

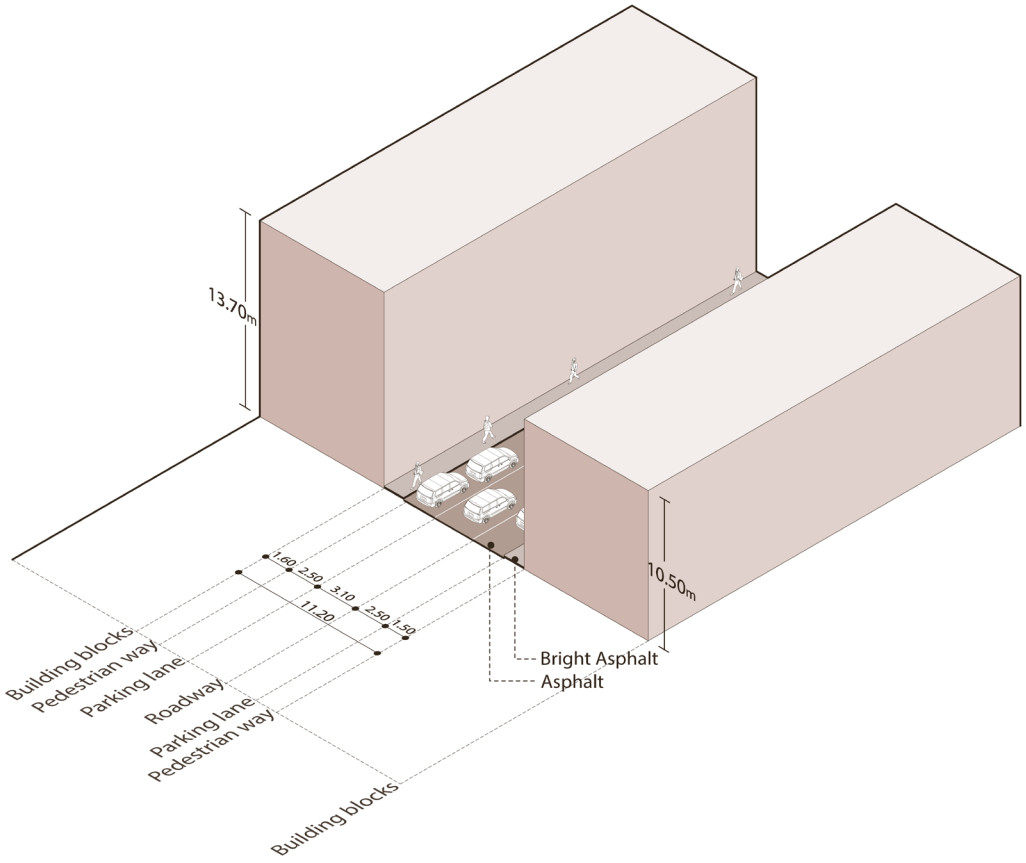

Fig. 86 Isometric view of Via Modena

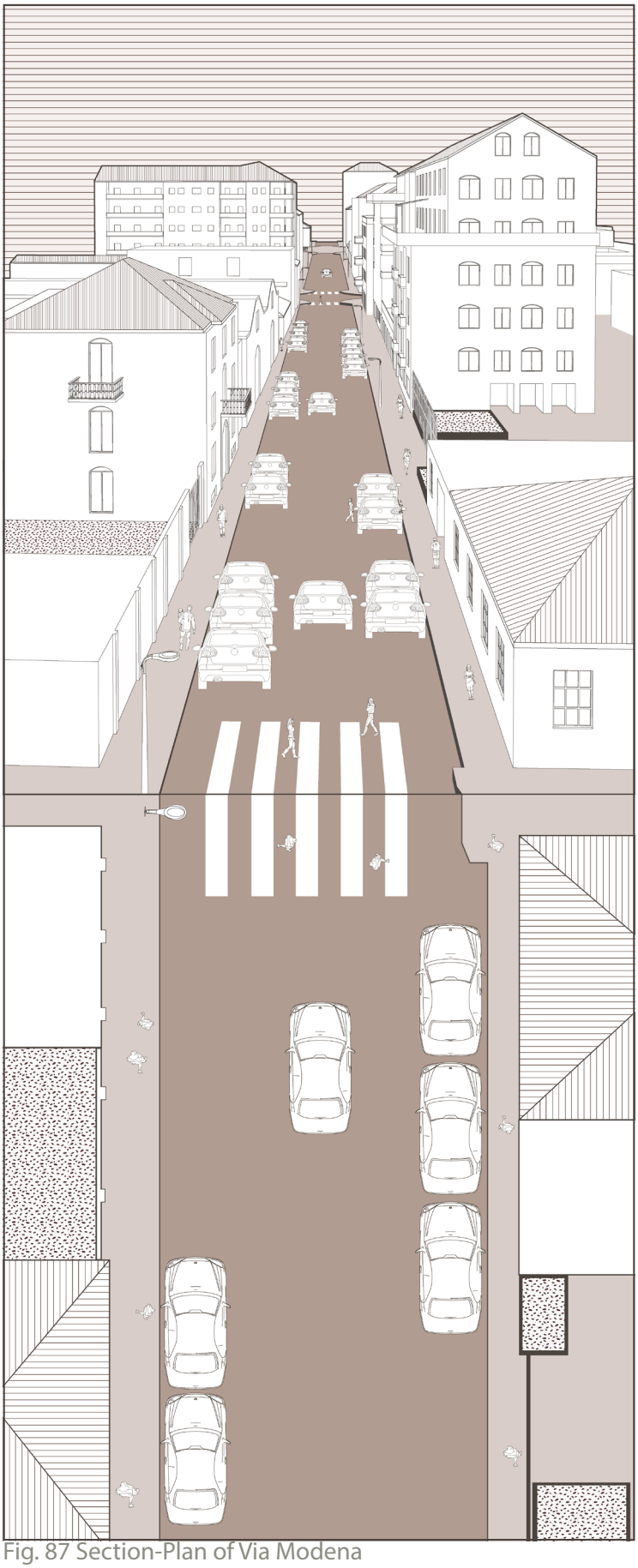

Fig. 87 Section-Plan of Via Modena

Corso Verona

Corso Verona is a 215 meters long street in the area, and is 39 meters wide. Its average height of the buildings is 14.8 m; with higher buildings on western side with an average height of 17.5 m, and on the eastern side, shorter buildings with and average height of 12.10. Therefore, it has the lowest urban canyon ratio compared to the other streets in the area, which is 0.37, that gives an open and expansive character to the street.

On both sides of the street, there are trees that are about 11 meters high on average. They have been planted within median strips incorporated into the sidewalks, made of concrete. The two parking lanes, on either side, are paved with fair-coloured asphalt compared to the carriageway. Large sidewalks, mature trees, and a generous street width contribute to a pleasant, well-shaded, and visually comfortable urban environment. A typical section of this street is shown in figures 88 and 89.

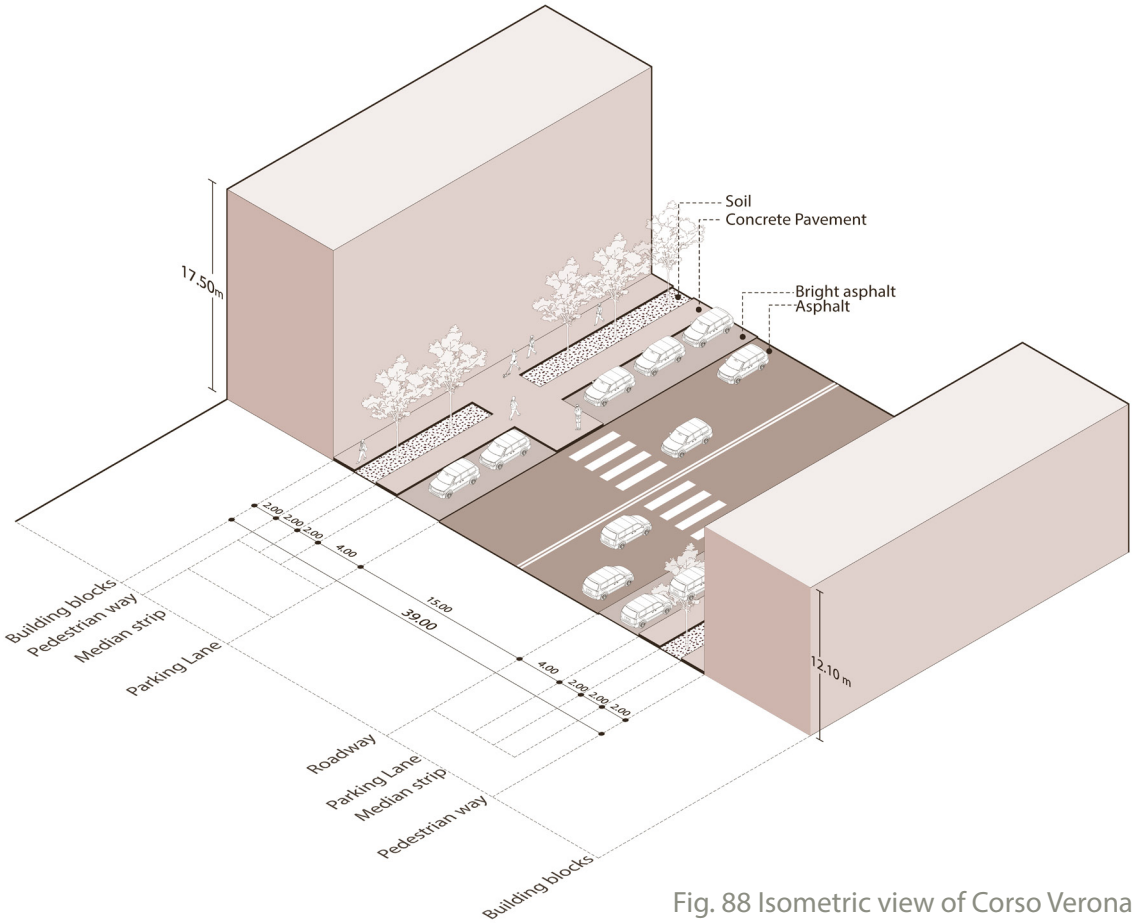

Fig. 88 Isometric view of Corso Verona

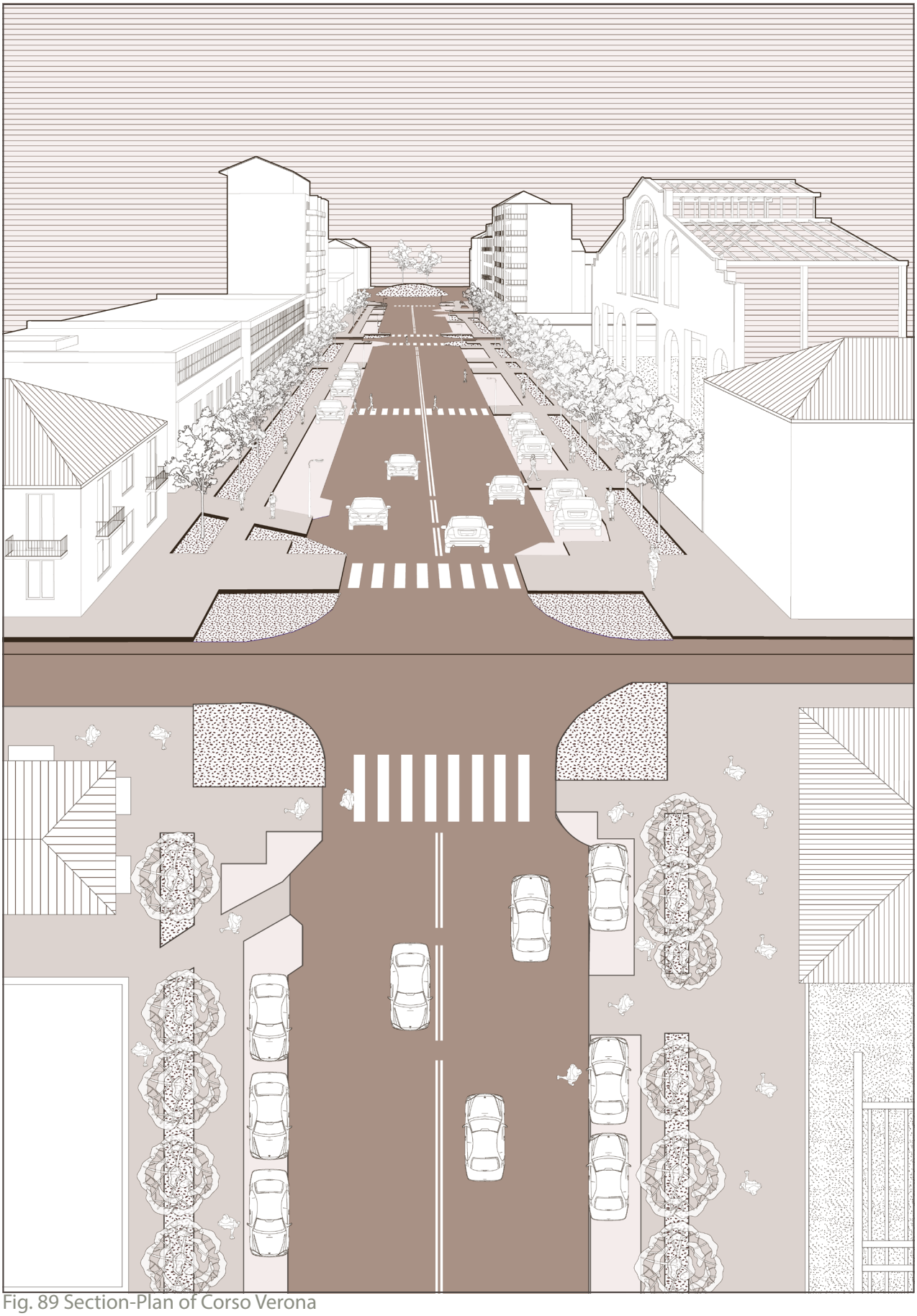

Fig. 89 Section-Plan of Corso Verona

Via Padova

Via Padova is a one-sided street, 14.7 m wide and lined with an average building height of 18.1 m, giving the highest urban canyon ratio among all streets in the study area, 1.23, resulting in a strongly enclosed street profile.

The street section includes a central asphalt-paved carriageway with parking lanes on both sides and sidewalks paved with asphalt and bright asphalt. There is no vegetation provided in the section of the street in this area, therefore, higher surface temperature is expected for this street. The street layout is drawn in the figures 90 and 91.

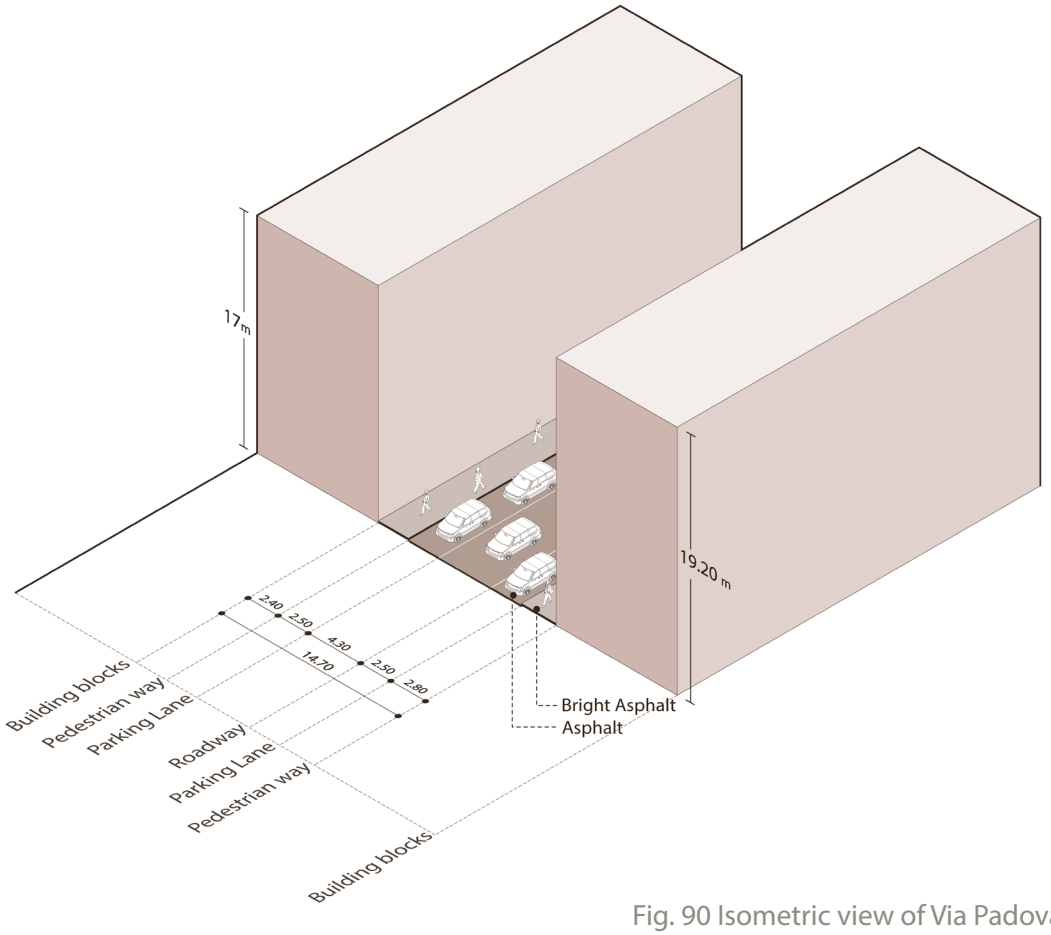

Fig. 90 Isometric view of Via Padova

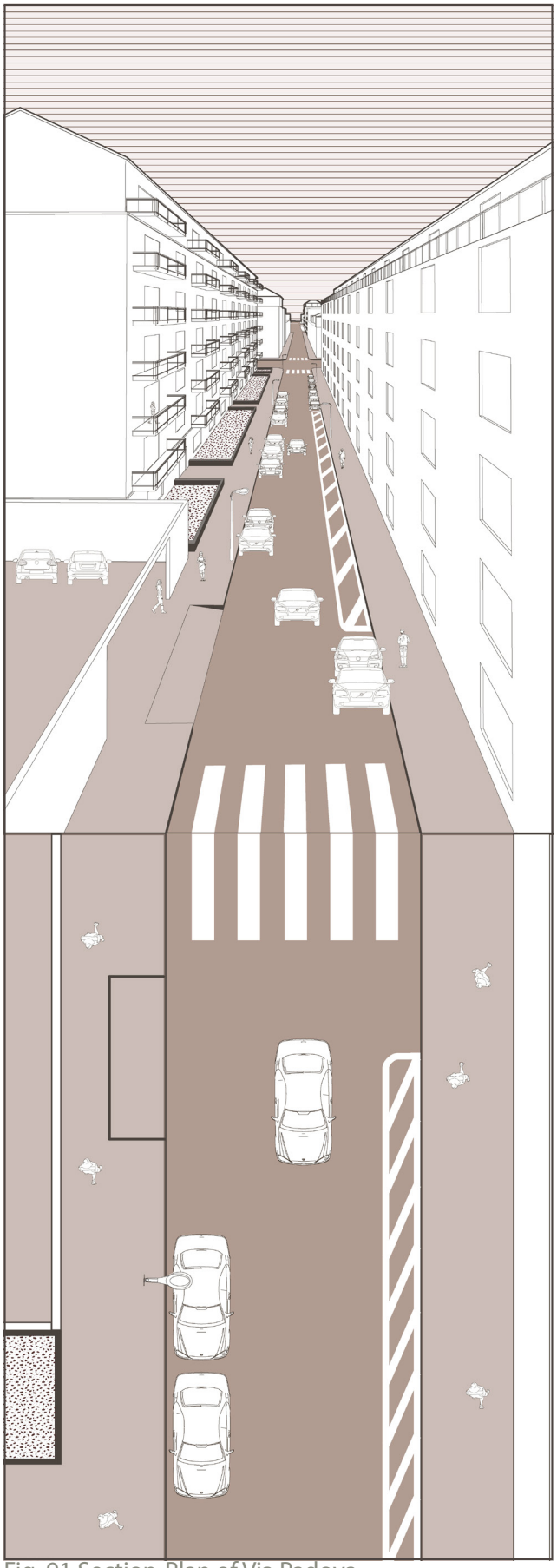

Fig. 91 Section-Plan of Via Padova

Corso Novara

The tallest buildings in the case study area are positioned in Corso Novara, with an average height of 24.3 meters, since the buildings height is higher on the eastern part of the zone rather than the west part (Figure 51). Despite thus fact, the urban canyon ratio is relatively low at 0.49, because Corso Novara is the widest street in the zone with a width of 48.75 meters and makes a spacious and open street profile.

The street has double-sided carriageways, each of two lanes. Between the carriageways and the slower vehicle lanes, median strips of about 4 meters, with tall Platanus orientalis trees averaging 25 meters, offer extensive shading and visual relief. Along both sides of these slower vehicle lanes, parking lanes run, and the sidewalks are in bright asphalt, allowing pedestrian circulation along the full street. The wide medians, together with tall trees and generous street width, create a visually and climatically comfortable urban environment despite high building heights. The characteristics of the Corso Novara are shown in figures 92 and 93.

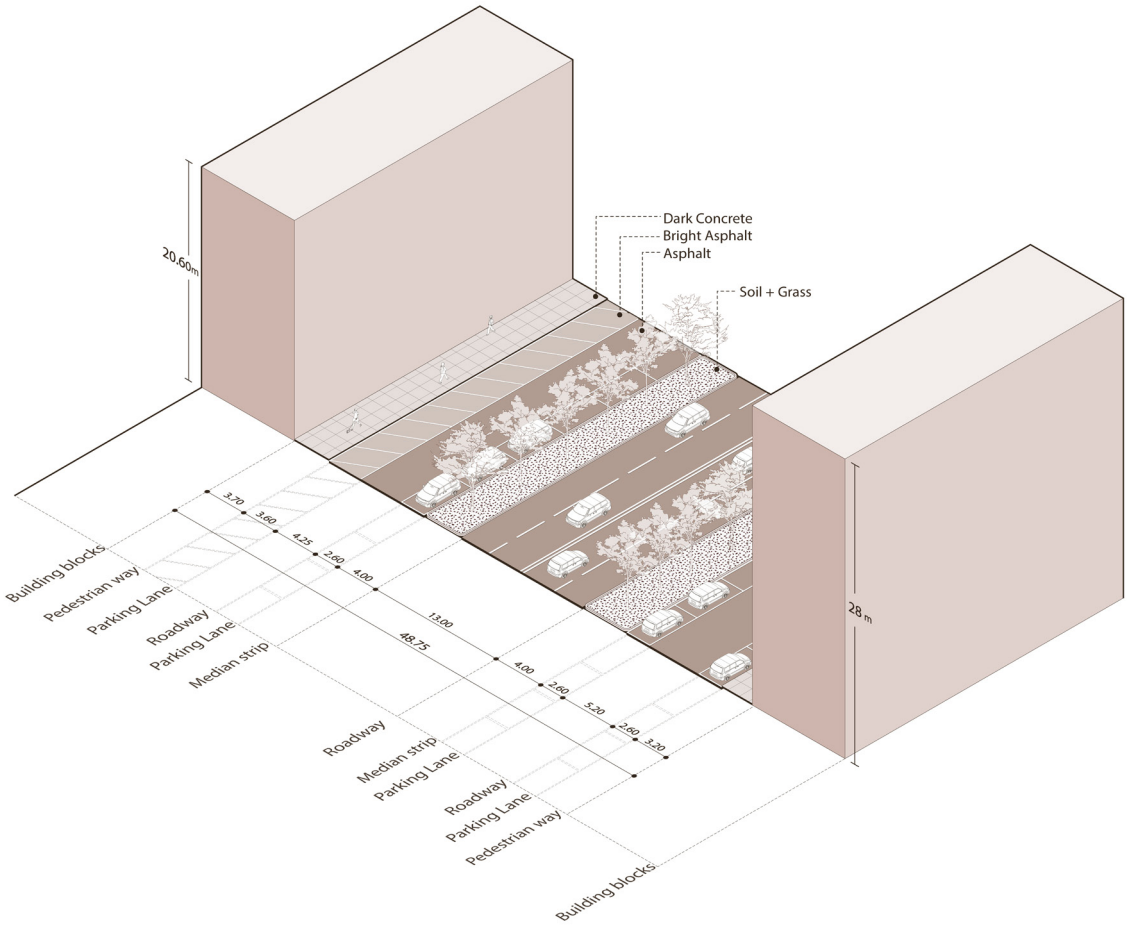

Fig. 92 Isometric view of Corso Novara

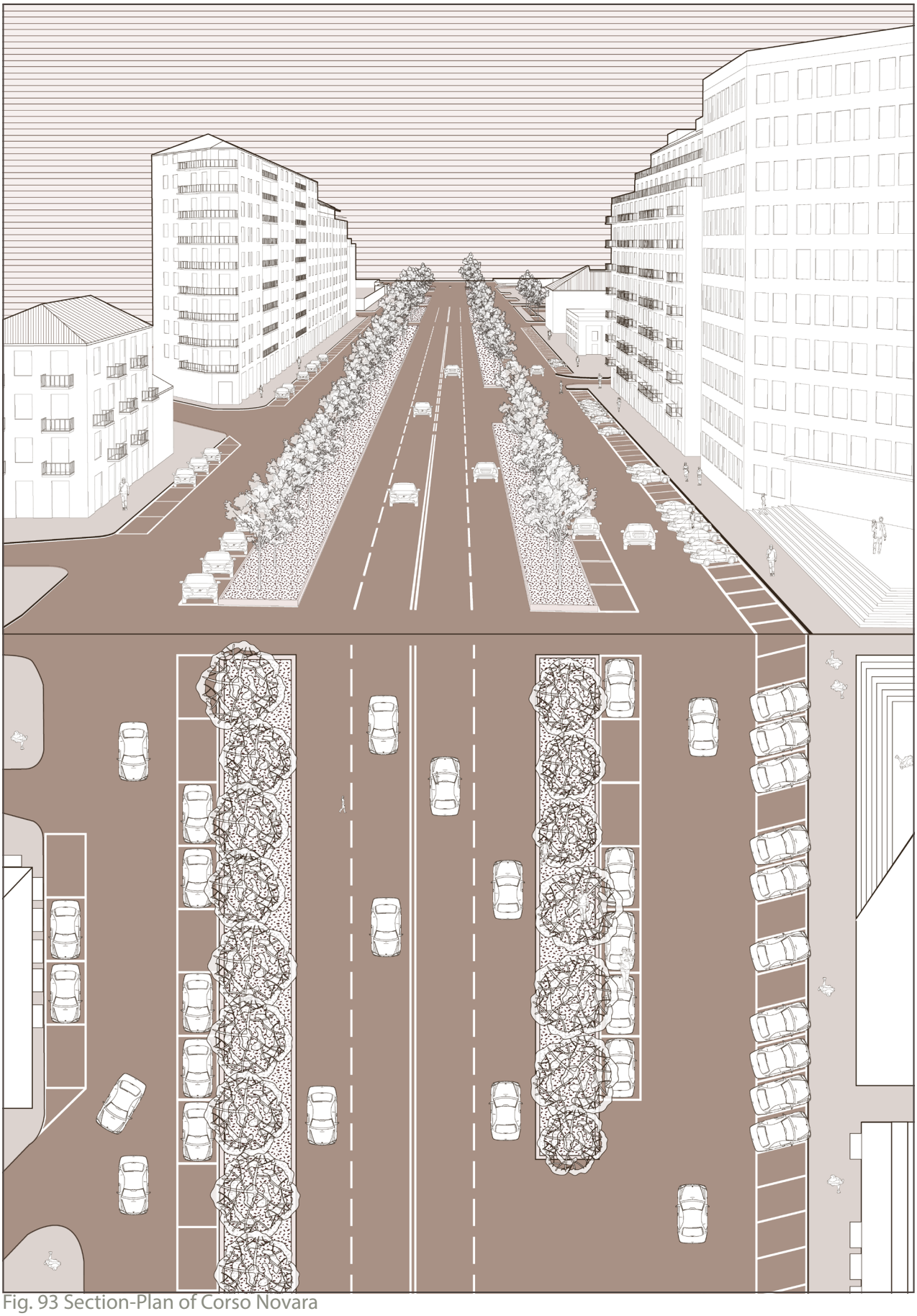

Fig. 93 Section-Plan of Corso Novara

3.3 Microclimate Analysis

3.3.1 Software Information

The main tool used for the microclimatic simulation of the case study area, in this thesis, is the ENVI-met version 5.8.0.

The three-dimensional CFD microclimate model, ENVI-met, is a tool developed to simulate the interaction of surfaces, vegetation, and atmosphere in complex urban environments. It facilitates the investigation into how minor-scale urban design interventions can affect the prevailing microclimatic conditions and assists research in architecture, landscape architecture, environmental planning, and building physics.
ENVI-met is a prognostic model based on the fundamental laws of fluid dynamics and thermodynamics, which enables simulations including:
Airflow around and between buildings
Short- and longwave radiation exchanges
Surface and wall energy balance
Water and heat fluxes between soil, vegetation, and atmosphere
Evapotranspiration processes
Dispersion of gases and particles

Green infrastructure, such as façades, trees, and green roofs significantly influences various biometeorological parameters include PET. The software operates on a grid-based system with high temporal and spatial resolution. Horizontal resolution usually ranges between 1–10 m, while vertical resolution is divided into several layers to handle atmospheric stratification. Simulation duration may range from several hours up to several days, depending on the model size and configuration.

ENVI-met version 5.8.0 includes several integrated modules, each serving specific functions in the modelling workflow:

Manage Projects– for creating model boundaries and global settings

Edit Model Area – for detailed 3D model construction, including buildings, vegetation and surfaces;

Simulation Settings – for defining meteorological and boundary conditions

Start Simulation– the simulation engine responsible for running the model

Simulate Thermal Comfort– for post-processing and calculating biometeorological indicators

Visualize Results – for visualising and analysing the simulation results.

Additionally, **Materials and Objects Library** and **Tree Library** modules are used for editing material and vegetation databases, respectively. From 2022 onwards, ENVI-met also includes TreePass and Projects/Workspaces, which facilitate vegetation calibration and project management (ENVI-met, 2025).

3.3.2 Input Data

The model coordinates were set according to the city's geographical position at latitude 45.07° N and longitude 7.69° E, under the Central European Standard Time zone (reference longitude 15.00°).

The model geometry was defined with the following grid configuration:

x-Grids: 447
y-Grids: 272
z-Grids: 50
Grid size: 2.0 m × 2.0 m × 2.0 m
Vertical generation: the lowest gridbox was divided into five subcells for higher precision near ground level.
Model rotation: 32° from the north, aligning with the street orientation in the real site.

These settings allowed a precise representation of urban morphology, including buildings, streets, and vegetation characteristics. Both built-up zones and green spaces are captured by the model area, allowing the analysis of microclimatic conditions for the simulation.
Meteorological boundary conditions, including air temperature, relative humidity, wind speed, and radiation parameters, were taken from local climate data provided by an ARPA weather station in Turin. The simulation period targeted the hottest day of the year, with a special focus on daily temperature variations and urban heat accumulation.

3.3.3 Modeling Process and Simulation

For the geometric setup, the Carta Tecnica Regionale was downloaded from the Geoportale del Comune di Torino. Since the base map was oriented toward the geographical north, and for higher modeling precision, the map was rotated by 32° to align the street grid with the ENVI-met model axes. This rotation allowed the model to be developed along orthogonal coordinates, simplifying the spatial organization of buildings and surfaces. The adjusted map was then exported as a bitmap file and imported into ENVI-met Spaces to serve as the background and reference layer for area digitization. Based on the scale bar and real-world dimensions of the selected area, the grid resolution was set to 2 × 2 × 2 m, providing a balance between computational efficiency and spatial accuracy. The model was configured with the following parameters:

Parameter	Description
Location	Turin, Italy
Geographic Coordinates	Latitude: 45.07° N, Longitude: 7.69° E
Reference Time Zone	Central European Standard Time (UTC +1)
Number of Grids	447 (x) × 272 (y) × 50 (z)
Nesting Grids	4
Resolution	2 × 2 × 2 m
Model Rotation	32° from North
Wall Material	Default wall – moderate insulation
Roof Material	Roofing tile
Real Dimensions	894m × 544 m
Area	486,336 m^2

Table 7- Model confguration parameters

Soil Profiles

After defining the building geometries and vegetation, appropriate surface materials were assigned to the ground and built elements. Most of the materials were selected directly from the ENVI-met material database, ensuring consistency with standard surface properties. However, for asphalt surfaces, a custom material was created by modifying its emissivity value to achieve more realistic thermal behaviour and enhance the reliability of the simulation results.

The materials used from the ENVI-met database are listed below:

Material	Albedo	Emissivity	Funcion
Default sandy loam	0.20	0.90	Base soil layer under the buildings- Median strips
Asphalt road	0.12	0.90	Car roads - Parking lane
Bright asphalt road	0.25	0.90	Side walks
Brick road (red stones)	0.30	0.90	Courtyards - side walks
Dark granit pavement	0.25	0.90	Courtyards - side walks
Granit pavemet	0.35	0.90	Courtyards - side walks
Concrete pavement light	0.5	0.90	Courtyards - side walks
Concrete pavement dark	0.20	0.90	Courtyards - side walks
Concrete pavement grey	0.30	0.90	Courtyards - side walks
Basalt brick road	0.20	0.90	Courtyards - side walks
Deep water	0.00	0.90	Fiume Dora
Grass 10 cm	0.20	0.97	Greenery

Table 8- Material choices for ENVI-met models

Trees

Looking more closely at the street-by-street distribution, a clear pattern in the clustering of species emerges.

Lungo Dora Firenze is mainly lined with Pinus nigra, forming a typical corridor of conifers.

Via Bologna, for the part included in the study area, has only five Crataegus trees.

Via Pisa has 13 Carpinus betulus trees, creating a uniform row of small–medium deciduous trees.

The Corso Novara plant type is mostly Fraxinus excelsior; it also contains some Ostrya carpinifolia; another segment hosts Platanus orientalis, contributing to the high canopy cover.

Corso Brescia is mainly planted with Tilia × europaea, which forms one of the most continuous and dense avenues in the area.

Corso Regio Parco has mostly Fraxinus excelsior trees, with the company of some Corylus colurna and some isolated Ulmus campestris.

All the other streets in the study area have no trees and therefore do not add to the overall arboreal composition.

In Table 9, all species were studied in relation to their morphological characteristics, such as height range, trunk diameter, growth form, evergreen/deciduous, and coniferous/broadleaf. Next, for each species, the most related tree model was chosen.

The following table summarizes all tree species found in the area, their quantities, physical characteristics, generic/common names, the corresponding ENVI-met model used, and whether they belong to coniferous or broadleaf categories.

Scientific Name	Common Name / Generic Name	Type	N° of Trees
Fraxinus excelsior	European Ash	Broadleaf	207
Tilia x europaea	Common Lime / Linden	Broadleaf	106
Platanus orientalis	Oriental Plane Tree	Broadleaf	105
Pinus nigra var. austriaca	Austrian Black Pine	Conifer	71
Corylus colurna	Turkish Hazel	Broadleaf	22
Ostrya carpinifolia	Hop Hornbeam	Broadleaf	22
Acer platanoides	Norway Maple	Broadleaf	14
Carpinus betulus	European Hornbeam	Broadleaf	14
Celtis australis	Hackberry / Nettle Tree	Broadleaf	9
Betula alba	Silver Birch	Broadleaf	7
Crataegus laevigata	Hawthorn (ornamental)	Broadleaf	5
Juglans nigra	Black Walnut	Broadleaf	5
Prunus spp.	Cherry / Ornamental Plum	Broadleaf	3
Pseudotsuga menziesii	Douglas Fir	Conifer	3
Ulmus campestris	Field Elm	Broadleaf	3
Magnolia grandiflora	Southern Magnolia	Broadleaf	1

Table 9- The species of trees in the case study area. Source for Info. Data: Geoportale Città di Torino

Height (m)	Trunk Diam.	ENVI-met Suggested Tree-Model
5–20	20–70	Ash / Medium–Tall Broadleaf
16–20	40–60	Linden / Tall Broadleaf
25–28	55–70	Plane Tree / Very Tall Broadleaf
10–17	40–50	Pine (Conifer Medium–Tall)
6	25	Small–Medium Broadleaf (rounded crown)
11	37	Medium Broadleaf (hornbeam group)
10–15	40–50	Maple / Medium Broadleaf
5–8	10–15	Hornbeam / Small–Medium Broadleaf
10–15	40–50	Medium Broadleaf (similar to elm)
9	18	Birch / Slender Broadleaf
5	20	Small Ornamental Tree
12	28	Medium–Tall Broadleaf (walnut type)
3	6	Very Small Ornamental Tree
11	27	Conifer / Medium Fir
5	6	Elm / Small–Medium Broadleaf
12	52	Magnolia / Medium Broadleaf Evergreen

Simulation

ENVI-guide is the module where the simulation settings are adjusted. The simulation period was set as 48 hours, starting from 27.06.2019 (the hottest day of the year) at 00:00. The website of Arpa Piemonte was used as a source for the input parameters concerning air temperature, relative humidity, wind speed and wind direction for each hour of the day (see Table 10). Simple forcing was used to feed the software with the information that it needs regarding the meteorological boundary conditions.

The simulation was run through Simulation module with each simulation taking 15 days.

Output

The outputs of the simulation were imported into "Leonardo" section of ENVI-met, which allows exporting plan and section views from any plane of the simulation domain. For potential air temperature and wind speed results, "atmosphere" file has been used as a source, whereas for surface temperature results, "surface" file has been relevant. To analyze the results of physiological equivalent temperature (PET), "BIO-met" module of the software has been used, which allows not only the calculation of PET but also other comfort indexes such as UTCI and PMV. Once the times of the day and the plane height for which the PET value is intended to be examined are chosen, one can calculate the PET value. The results of this calculation creates a folder named "biomet" in the simulation output folder. This data was imported to the Leonardo module to be able to convert the datas into maps.

Hour	T air °C	Wind speed (m/s)	Wind direction°
00:00:00	25.2	0.0	-
01:00:00	24.6	1.0	308
02:00:00	24.2	0.9	276
03:00:00	23.7	0.3	272
04:00:00	23.5	0.7	323
05:00:00	24	1.5	271
06:00:00	27	1.2	247
07:00:00	30.1	2.2	227
08:00:00	31.1	1.2	254
09:00:00	32.4	2.6	181
10:00:00	32.9	2.0	200
11:00:00	34.1	2.9	173
12:00:00	35.3	1.4	188
13: 00:00	36.3	2.5	184
14:00:00	37.1	3.0	186
15:00:00	37.6	4.0	199
16:00:00	38.2	4.3	201
17:00:00	37.4	2.6	214
18:00:00	34.9	1.9	245
19:00:00	313.1	1.7	327
20:00:00	29.4	2.6	319
21:00:00	27.6	1.6	309
22:00:00	26.6	1.8	267
23:00:00	25.6	1.7	323

Table 10- Input values for the simulation. (Arpa Piemonte, n.d.)

3.3.4 Results

The figures 94-96, show Potential Air Temprature in the area with existing condition at 09:00, 12,00, 15,00 h.

Date: 27.06.2019, x//y cut at K=4 (1.8 meters)

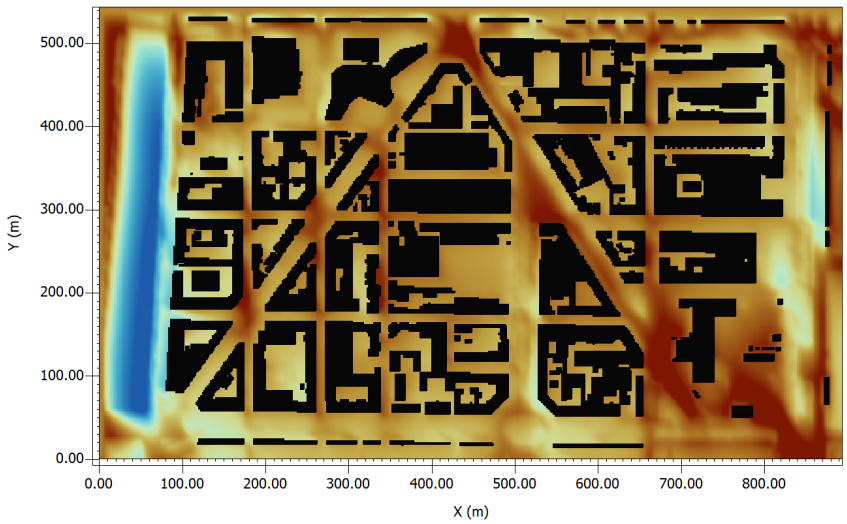

Fig. 94 Existing Potential Air Temprature map at 09:00 h

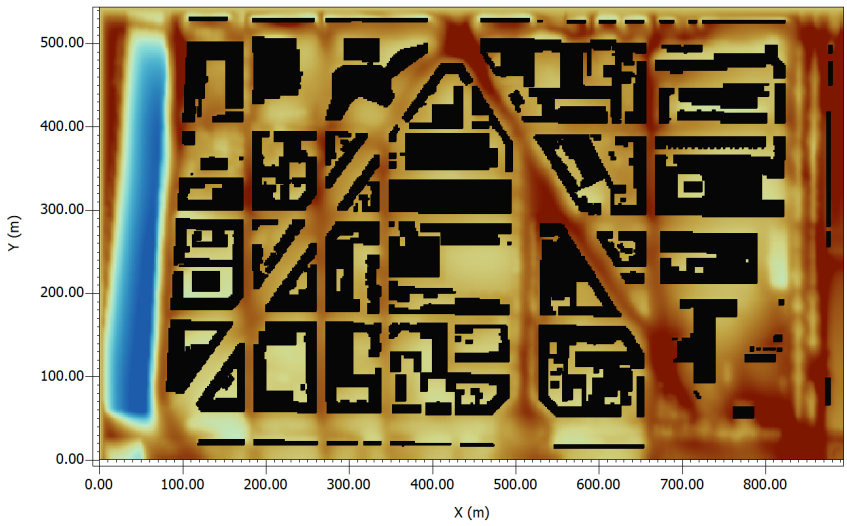

Fig. 95 Existing Potential Air Temprature map at 12:00 h

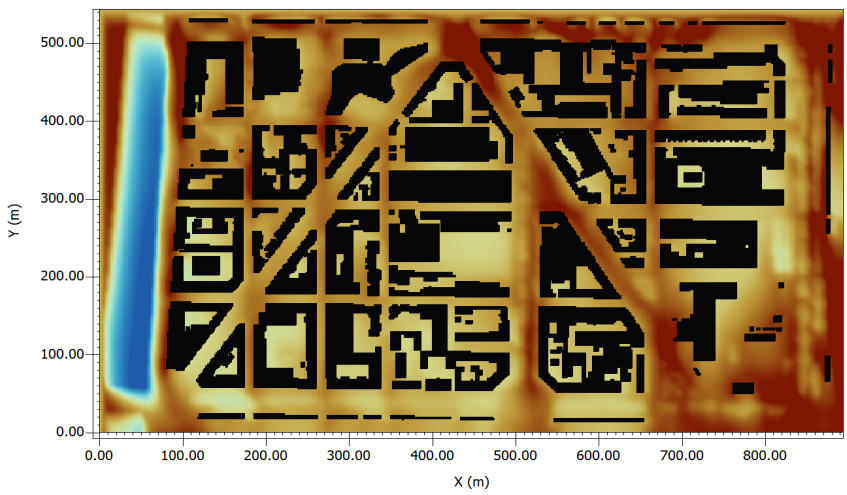

Fig. 96 Existing Potential Air Temprature map at 15:00 h

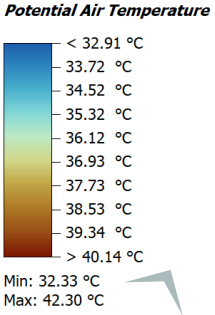

The figures 97-99, show PET with existing condition at 09:00, 12,00, 15,00
Date: 27.06.2019, x//y cut at K=4 (1.8 meters)

Fig. 97 Existing PET-map at 09:00 h

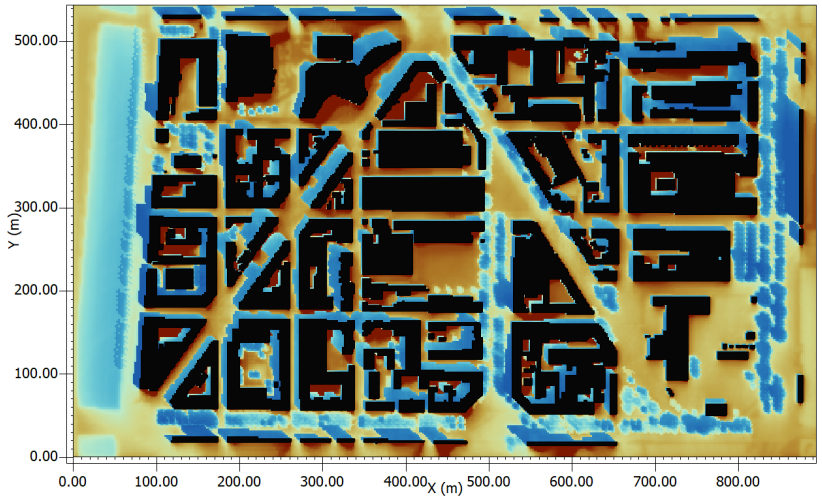

Fig. 98 Existing PET map at 12:00 h

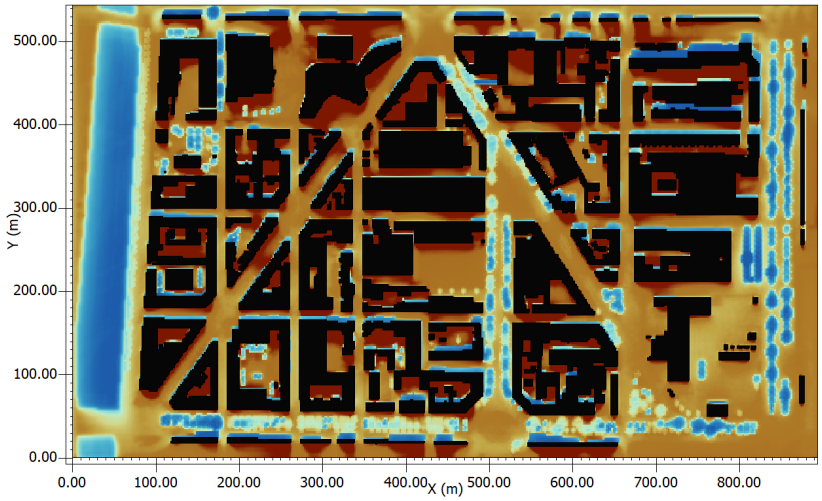

Fig. 99 Existing PET map at 15:00 h

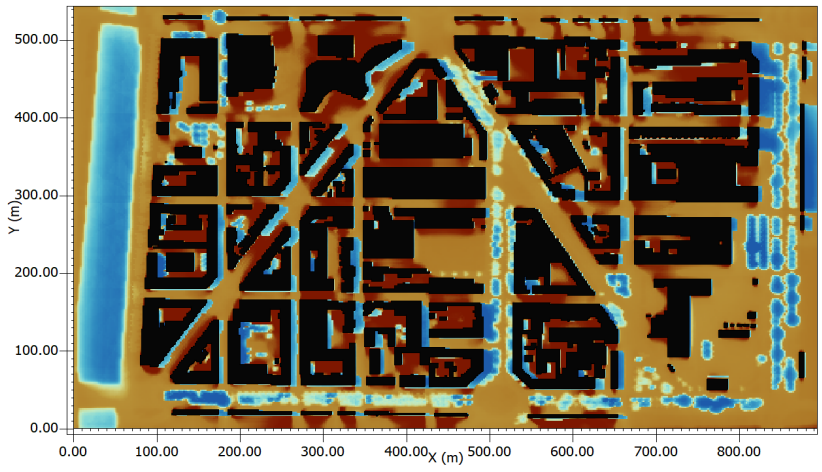

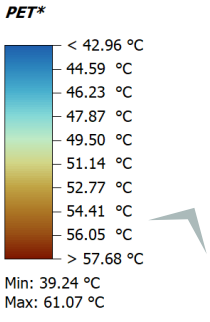

The figures 100-102, show Surface Temprature in the area with existing condition at 09:00, 12,00, 15,00

Date: 27.06.2019, x//y cut at K=4 (1.8 meters)

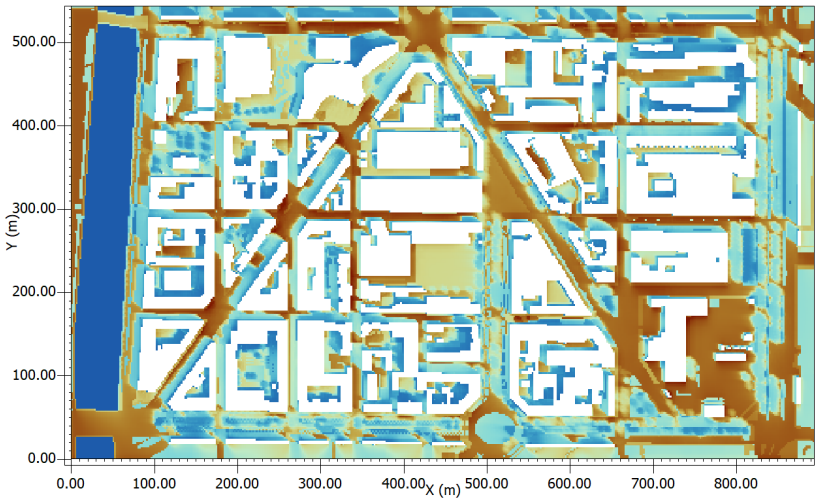

Fig. 100 Existing Surface Temprature map at 09:00 h

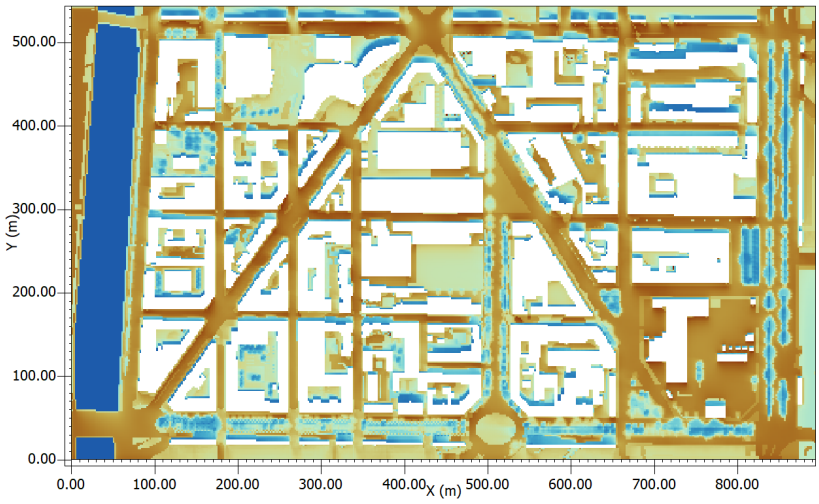

Fig. 101 Existing Surface Temprature map at 12:00 h

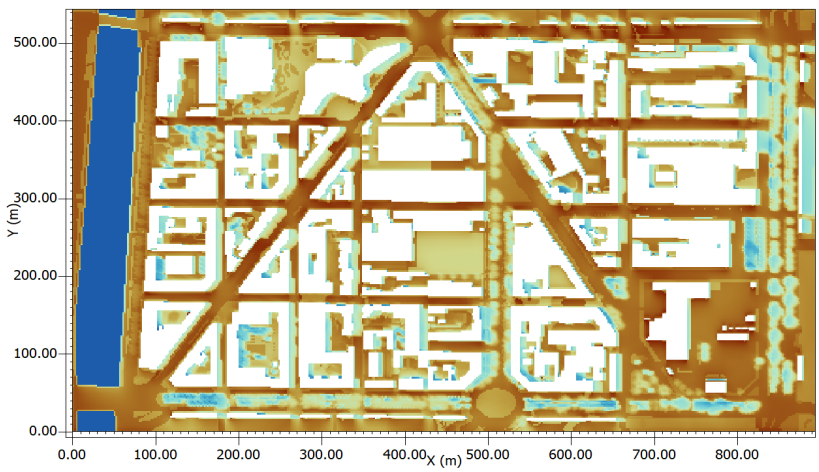

Fig. 102 Existing Surface Temprature map at 15:00 h

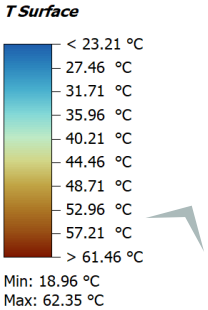

The figures 103-105, show Wind flow with existing condition at 09:00, 12,00, 15,00
Date: 27.06.2019, x//y cut at K=4 (1.8 meters)

Fig. 103 Existing Wind Flow map at 09:00 h

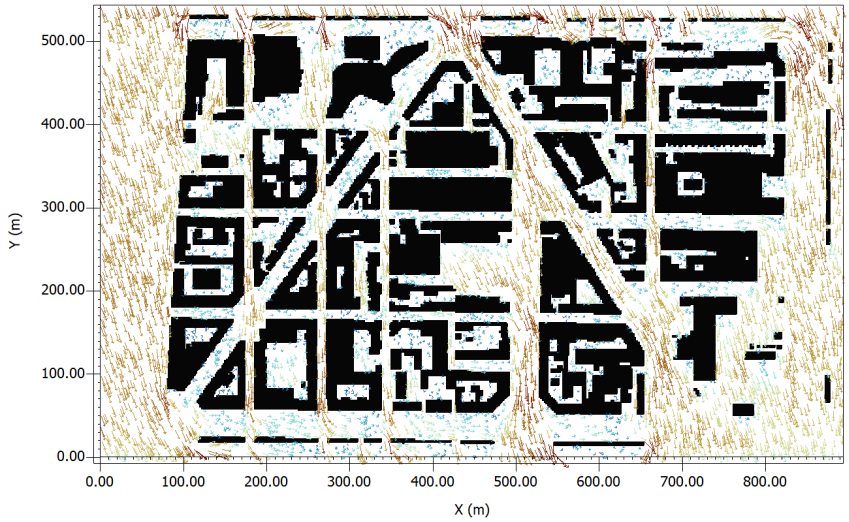

Fig. 104 Existing Wind Flow map at 12:00 h

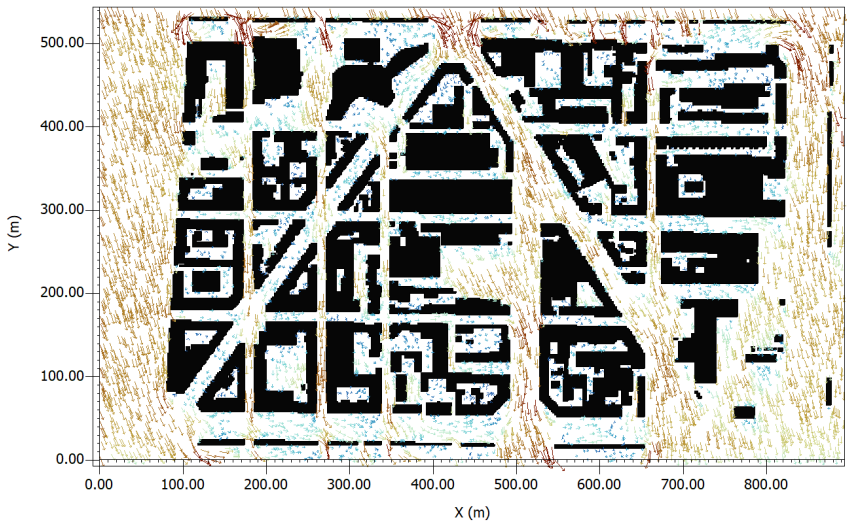

Fig. 105 Existing Wind Flow map at 15:00 h

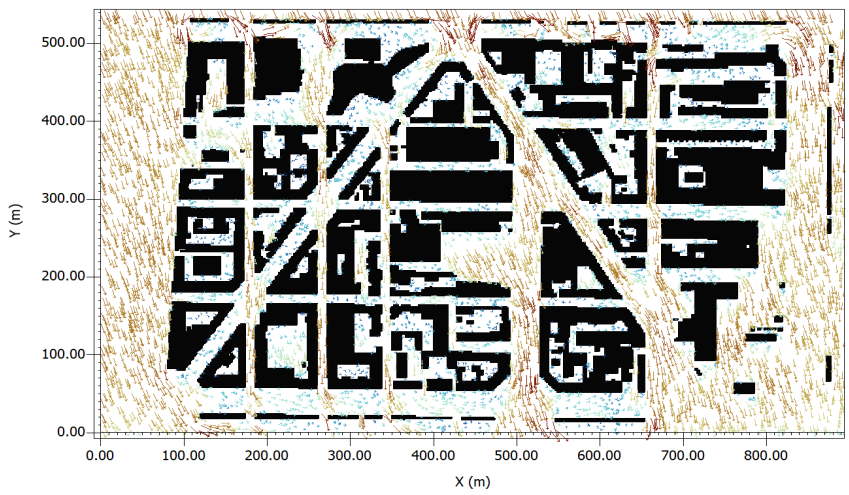

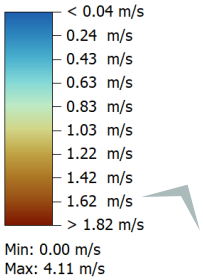

Fig. 106 Identifying the most critical areas based on PET

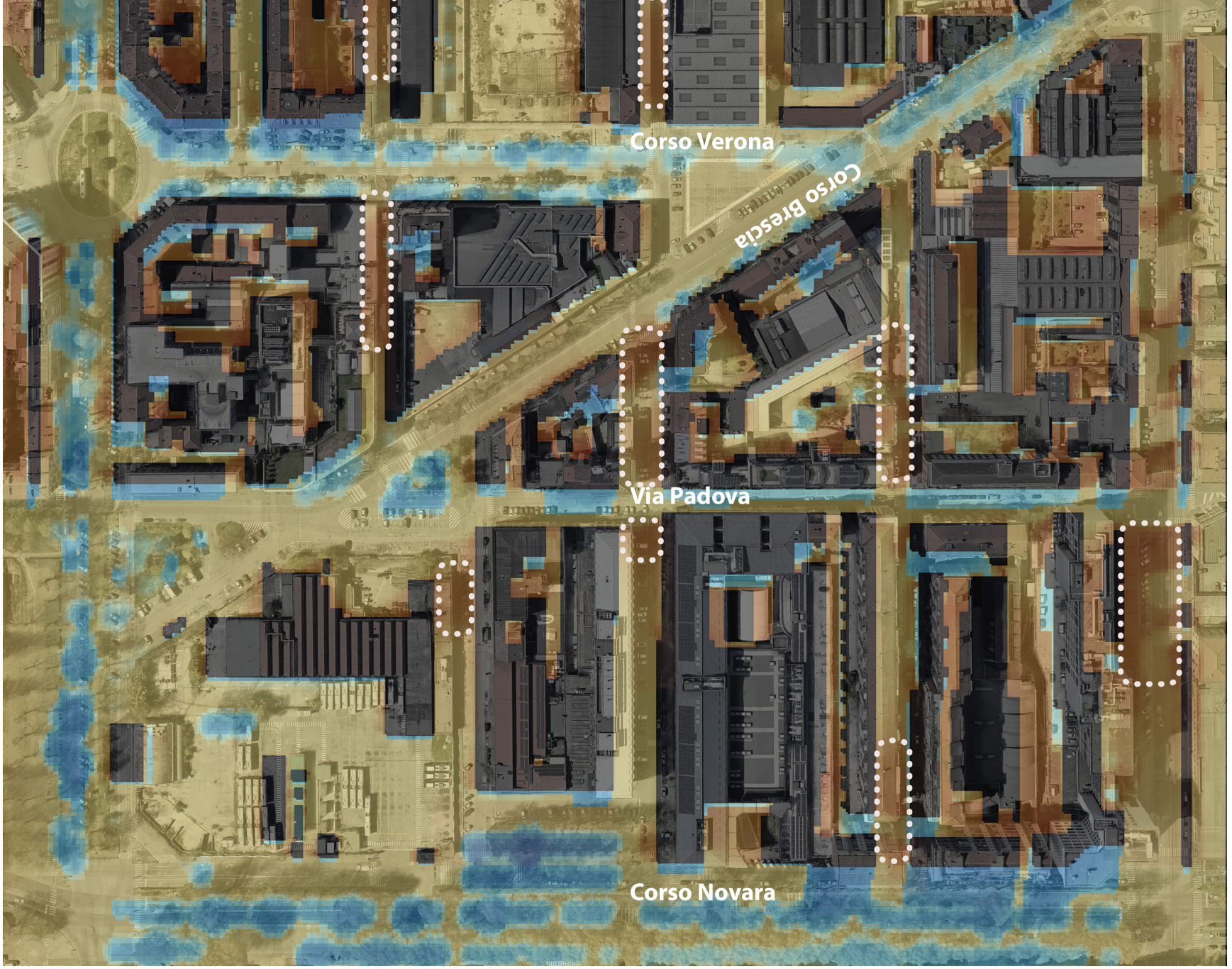
Corso Verona
Corso Brescia
Via Padova
Corso Novara

Fig. 107 Identifying the most critical areas based on Surface Temprature

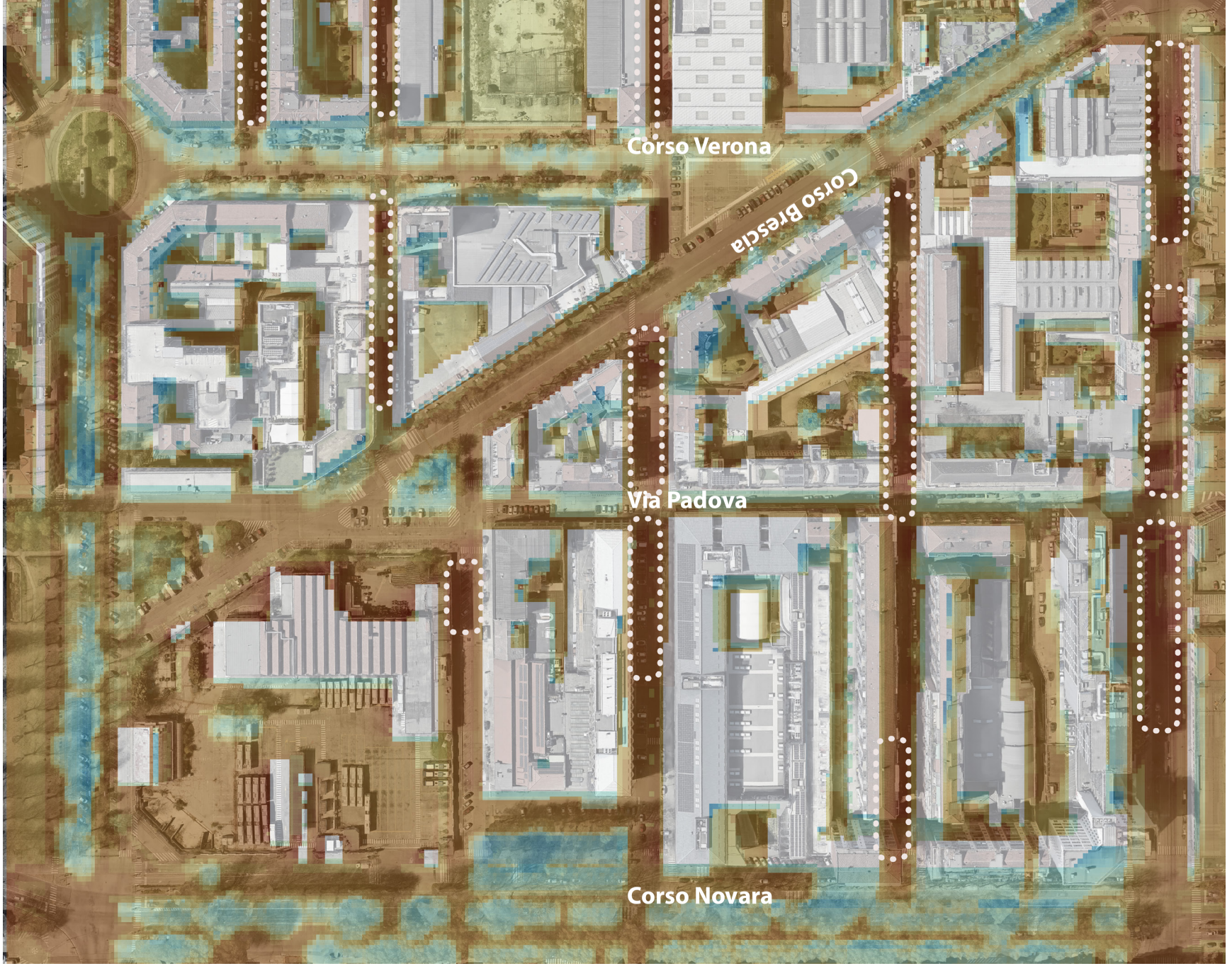
Corso Verona
Corso Brescia
Via Padova
Corso Novara

3.3.5 Discussion

The understanding of how urban form, surface materials, and vegetation shape the microclimate of the study area is achieved using ENVI-met simulations of the existing conditions. The surface temperature maps indicate that streets with a northeast-southwest axis have the highest surface temperatures compared to the streets oriented in different axes, sometimes exceeding 60°C in some instances. This becomes more evident when there is long exposure to direct solar radiation, greatly increasing heat gain during the daytime. On the other hand, streets oriented northwest–southeast have relatively low surface temperatures and PET values, thanks to more favorable sun–street alignment, which decreases peak solar loads. Areas of high surface temperature and greater PETs are represented in Figures 106 and 107.

The north-south oriented and wide section of Corso Palermo provides a less optimal thermal performance, with high intensity of solar exposure and scarce shading resulting in high values both in the PET map and in the surface temperature map. For the narrower and deeper urban canyons, such as Via Pisa, Via Parma, and Via Modena, there is a different thermal behavior; they generally record lower surface temperatures and lower PET values. Their morphology offers considerable shading during almost all daylight hours, greatly decreasing the radiant heat load at pedestrian level. Their limited air circulation, however, determines higher potential air temperatures for these streets, ranging from 38.53°C to 40.14°C, highlighting how canyon depth limits ventilation and traps warm air. From the wind flow charts, it can be seen that the wind flows more moderately in the streets with wider and more open sections like Via Bologna, Corso Palermo, and Corso Regio Parco.

The street sections containing trees and vegetation with permeable surfaces have a visible difference in terms of PET and surface temperature, compared to the streets that lack these elements. It can be understood from the maps, that vegetation and trees contribute positively to thermal comfort. Their combined shading and evapotrant effects outperform the benefits provided by permeable green surfaces. In areas with tree cover, surface temperatures are noticeably different with areas with no trees. For example, in Via Pisa, the vegetated sections recorded temperatures up to 17.52°C lower than adjacent non-vegetated points with otherwise identical characteristics.

The existence of the water surface of the Dora River significantly improves microclimate regulation in the surrounding streets. This aligns with extensive research identifying water bodies as some of the most effective elements for UHI mitigation (Taleghani et al., 2014).

Strategies

Based on previous research and best practice studies, the combined use of cool pavements and vegetation is one of the most effective strategies for microclimate mitigation. In the proposed design, permeable surfaces covered with grass have been introduced along sidewalks (figure 100-103D) to increase vegetation density, support evapotranspiration, and improve thermal comfort. Dark asphalt has been replaced with bright asphalt,(figure 100-103B) which has a higher albedo, reducing heat absorption and lowering surface temperatures. For sidewalks previously covered with asphalt, bright concrete pavements and granite stones have been selected; these materials are highly reflective, durable, and exhibit lower thermal retention compared to traditional asphalt. Granite pavement is also used at selected intersections (figure 102B), following the example of Corso Reggio Parco, where it proved effective in reducing surface temperatures in the existing-condition ENVI-met maps (figure 91). By combining high-albedo pavements with increased vegetation, this strategy provides shading, reduces radiant heat, and creates a complementary cooling effect, enhancing pedestrian comfort and improving the overall microclimate in streets and open areas of the case study.

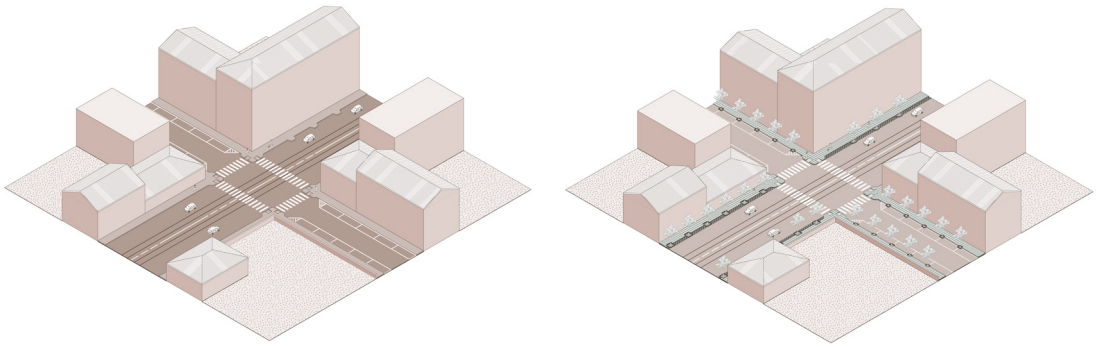

Fig. 108 Isometric View of Cool Pavement + Vegetation Strategy

In the following figures 109-110, the map of the arera is shown before and after interventions containing vegetation surfaces and pavement materials. The numbers on the map refer to the points in which the strategies are done on ENVI-met model and are illustrated in figures 111-114. The point number 2, refers to the second strategy (integrating shaders), which is shown in figure 115.

Fig. 109 The map of the area, with existing pavement materials and vegetation

Fig. 110 The map of the area after interventions

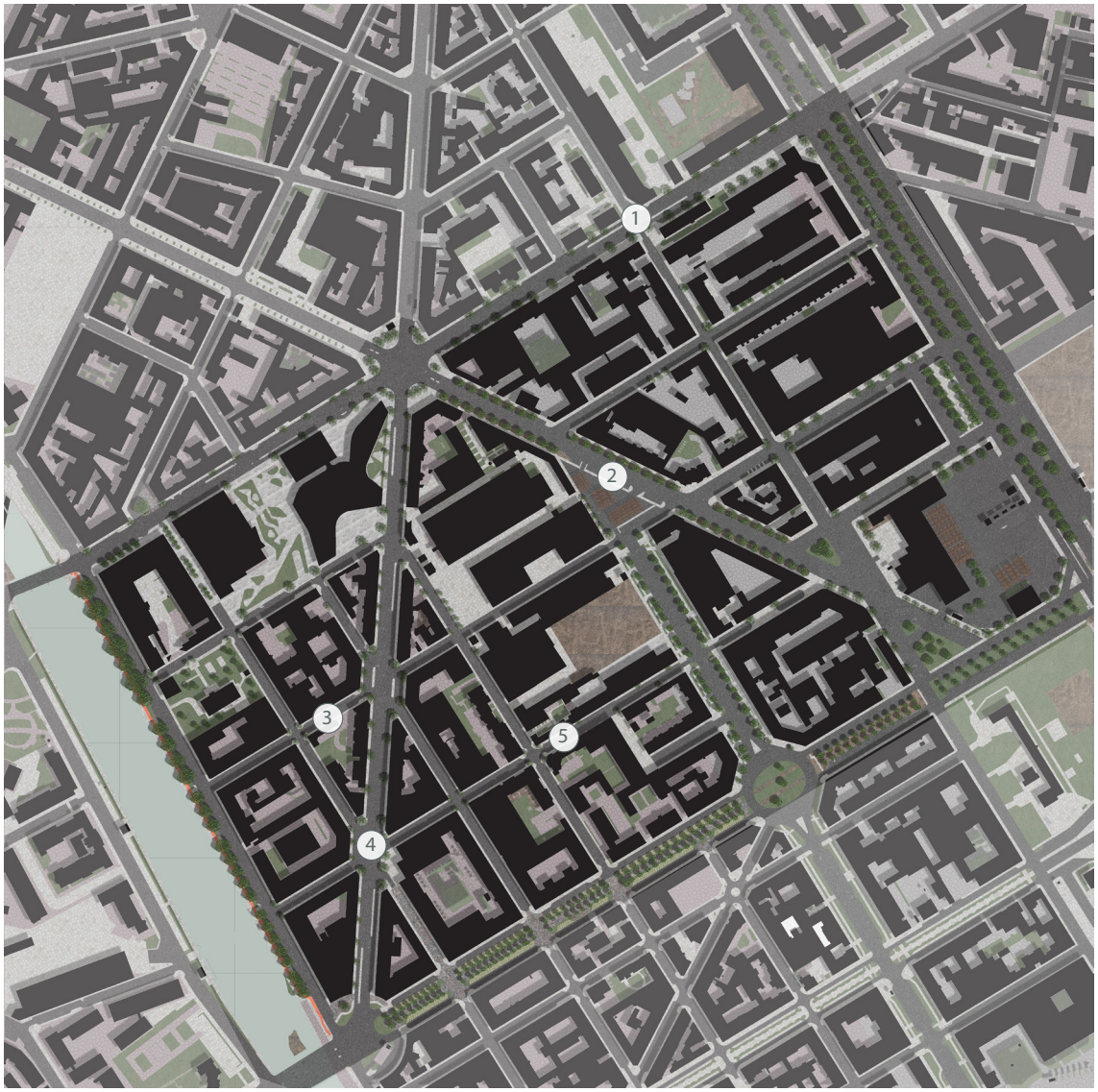

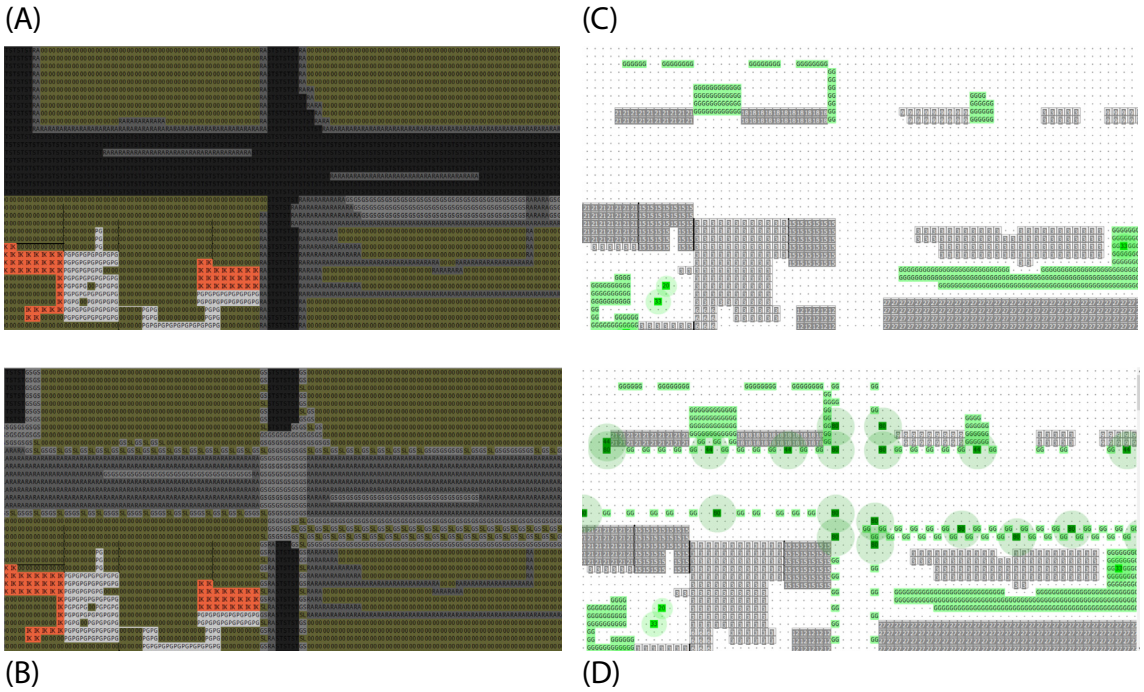

Fig. 111 ENVI-met model of the point 1, Via Bologna shown in figures 109-110 (A): showing the area with the existing surfaces (B): showing the same area with proposed Pavement material replacements (C): Existing vegetation coverage of the area (D): Proposed vegetation coverage for the referred area

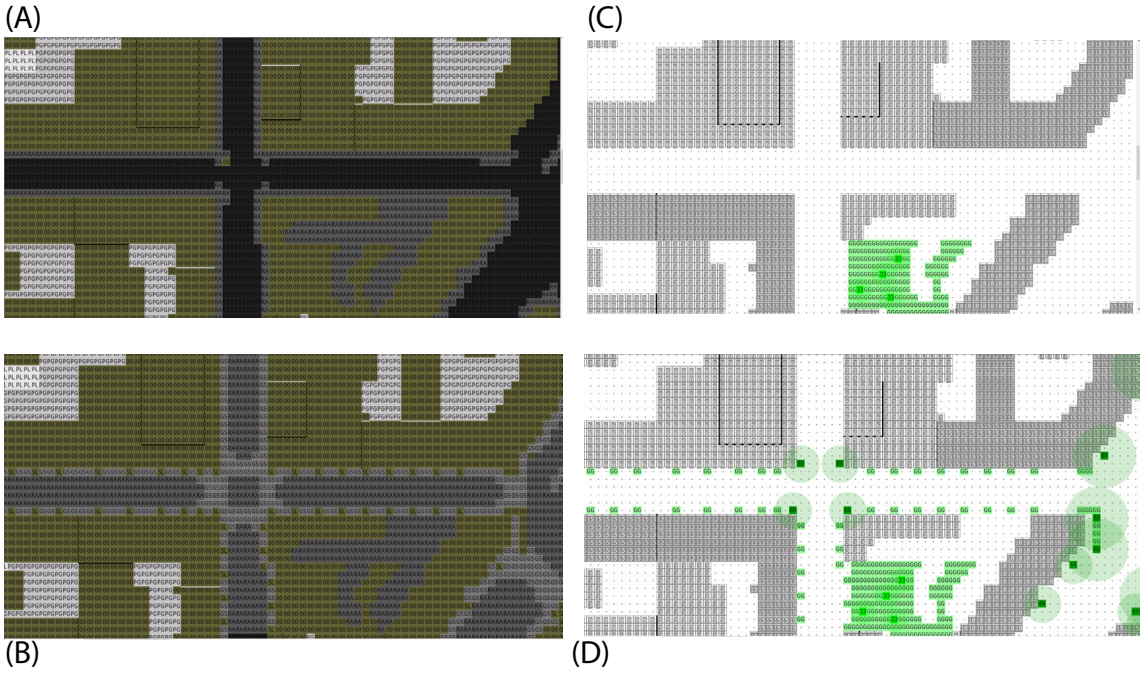

Fig. 112 ENVI-met model at point 3 shown in figures 109-110, the intersection of via Perugia and Via Pisa (A): showing the referred area with the existing surfaces, (B): showing the same study area with proposed Pavement material replacements, (C): Existing vegetation coverage of the area, (D): Proposed vegetation coverage for the area

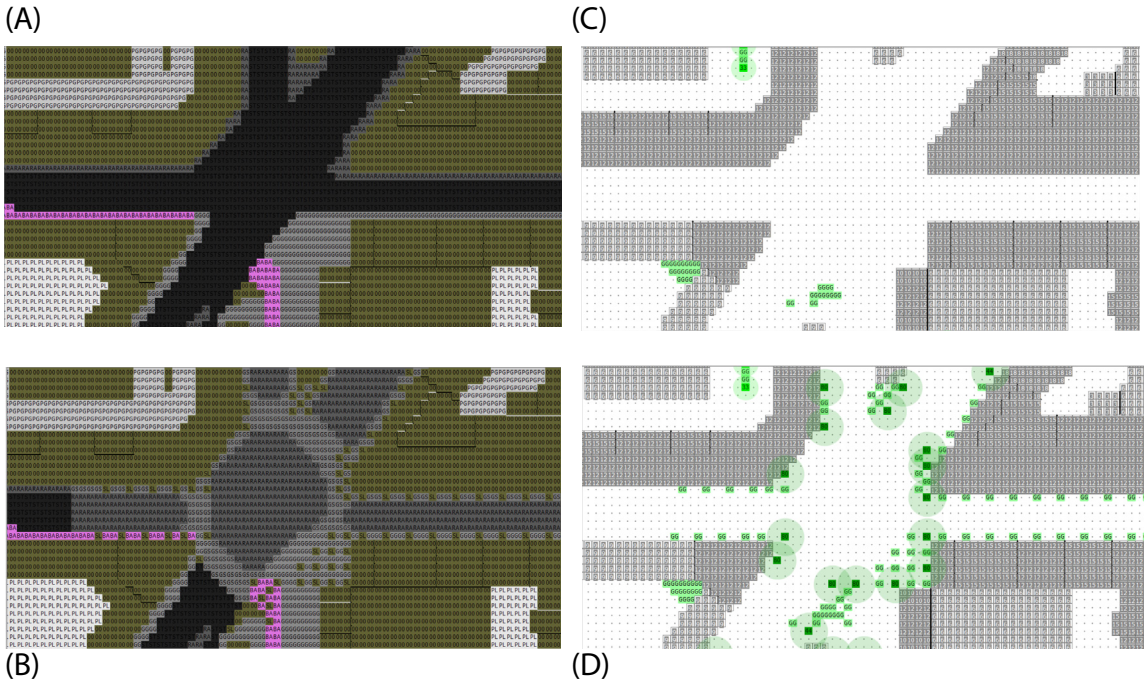

Fig. 113 ENVI-met model at point 4 shown in figures 109-110, the intersection of Corso Palermo, Via Foggia and Via Pisa (A): showing the area with the existing surfaces, (B): showing the area with proposed Pavement material replacements, (C): Existing vegetation coverage of the area, (D): Proposed vegetation coverage for the area

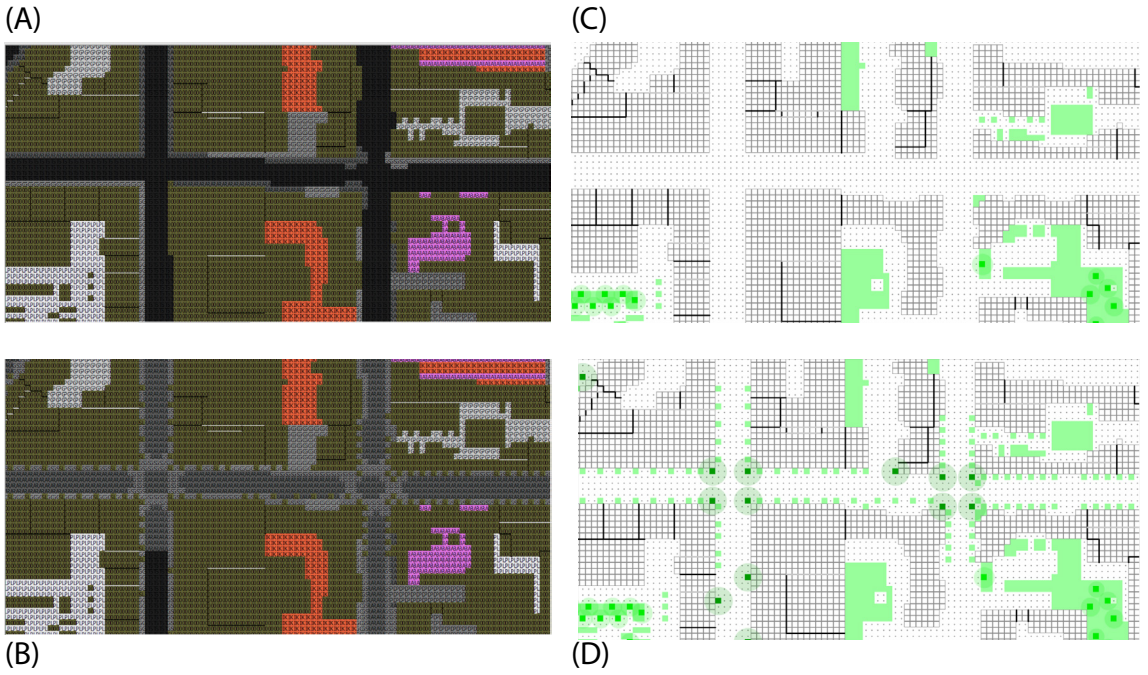

Fig. 114 ENVI-met model at point 5 in figures 109-110 in Via Foggia (A): showing the area with the existing surfaces, (B): showing the area with proposed Pavement material replacements, (C): Existing vegetation coverage of the area, (D): Proposed vegetation coverage for the area

3.4.2 Integrating Canopies

Vegetation in the area of study brings in the influence that trees do have a contribution to thermal comfort regarding shading and evapotranspiration, though their efficiency remains low compared to the solid shading elements (Pejović, 2022).
For this reason, in large open public spaces with extended asphalt surfaces-such as open-air parking areas-I recommend the use of canopies and other devices that provide additional shade, thus enhancing microclimate performance. Integrating timber-based shading structure solutions into the design of my case study area provides an opportunity to introduce lightweight, sustainable elements capable of supporting vegetation while contributing significantly to heat mitigation. The shading systems in timber-whether pergolas or modular covered parking-can help reduce heat absorption, increase shaded zones, and create surfaces suitable for climbing or hanging vegetation. This module can be developed to include adaptable structural components corresponding to a variety of spatial conditions within the district while maintaining coherence with the overall mitigation strategy.

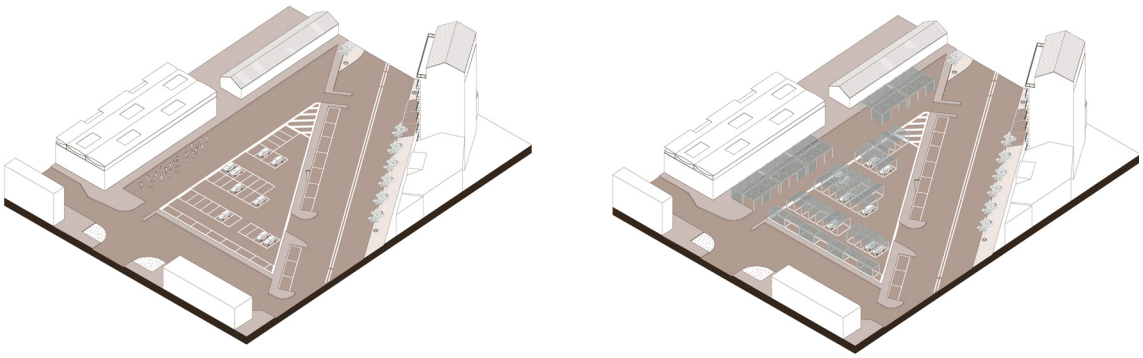

Fig. 115 Isometric View of Integrating canopies Strategy

3.4.3 Strategies Results on ENVI-met

The following figures 116-118 show Potential Air Temprature maps of the area with Strategies at 09:00, 12,00, 15,00 h. Date: 27.06.2019, x//y cut at K=4 (1.8 meters)

Fig. 116 Existing Potential Air Temprature map at 09:00 h

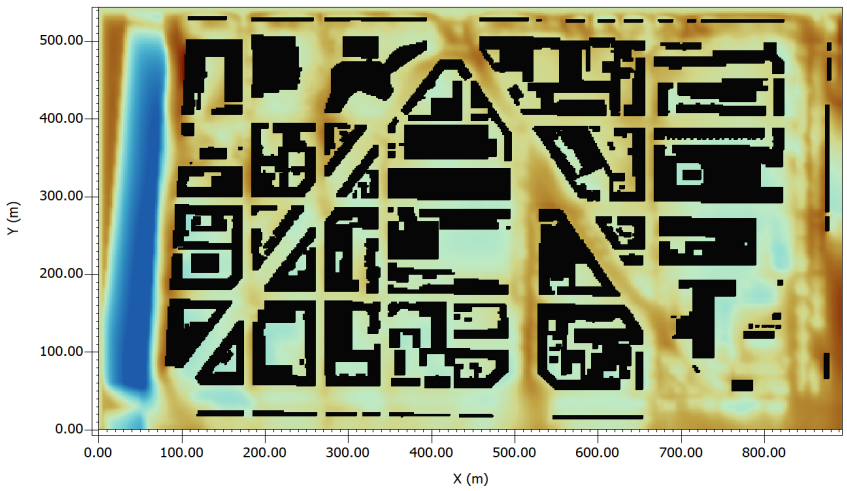

Fig. 117 Existing Potential Air Temprature map at 12:00 h

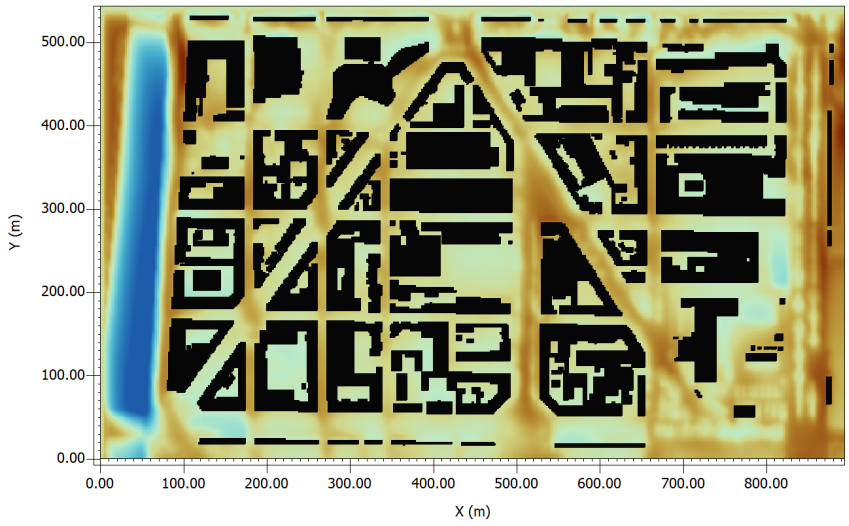

Fig. 118 Existing Potential Air Temprature map at 15:00 h

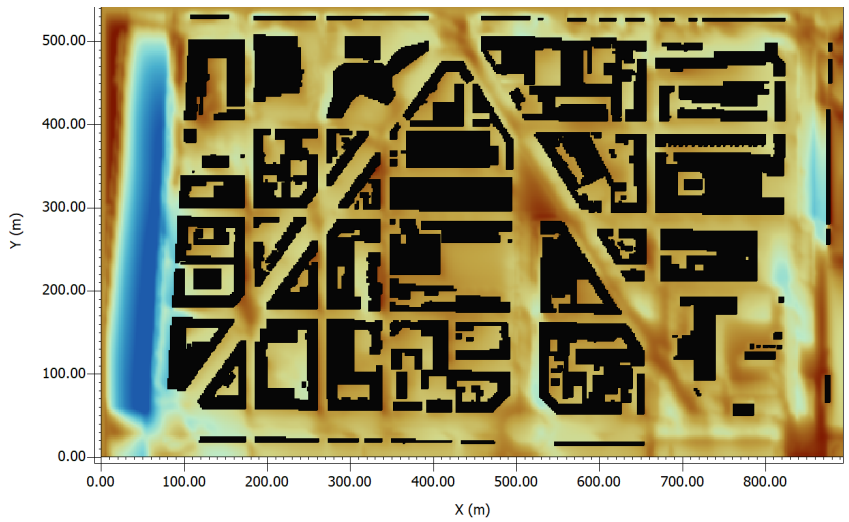

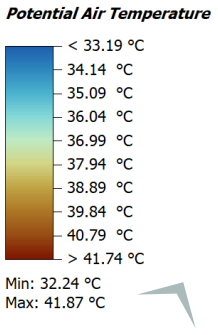

The following figures 119-121 show PET maps of the area with Strategies at 09:00, 12,00, 15,00 h.

Date: 27.06.2019, x//y cut at K=4 (1.8 meters)

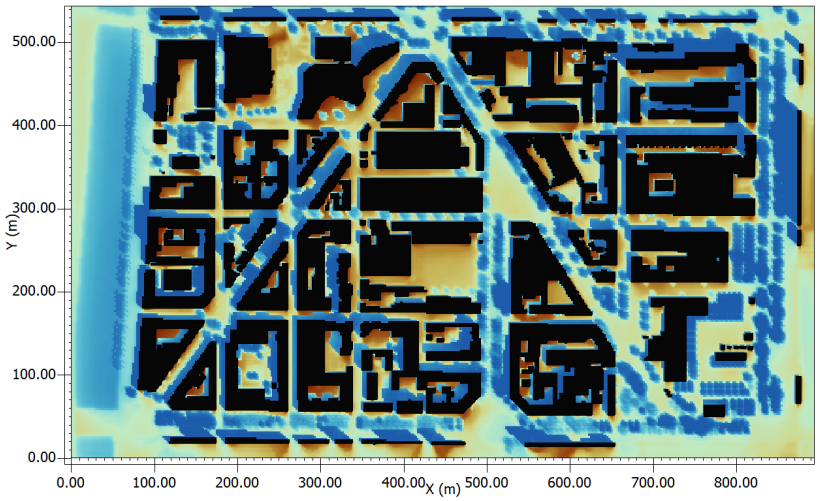

Fig. 119 Existing Potential Air Temprature map at 09:00 h

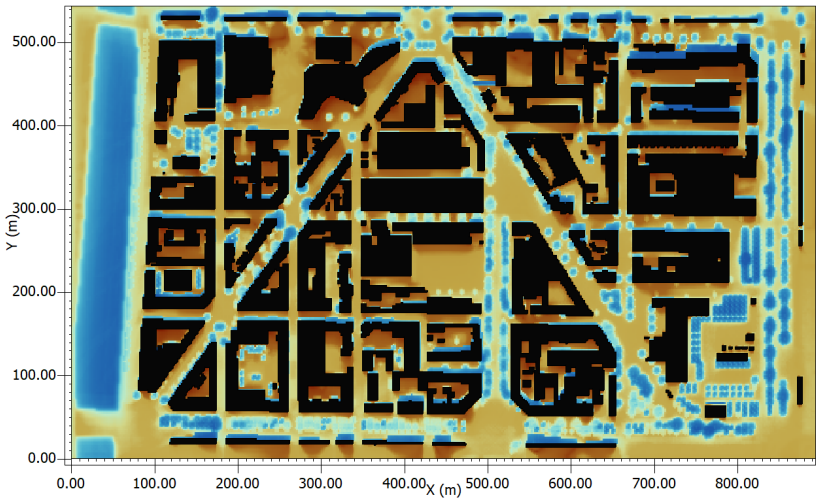

Fig. 120 Existing Potential Air Temprature map at 12:00 h

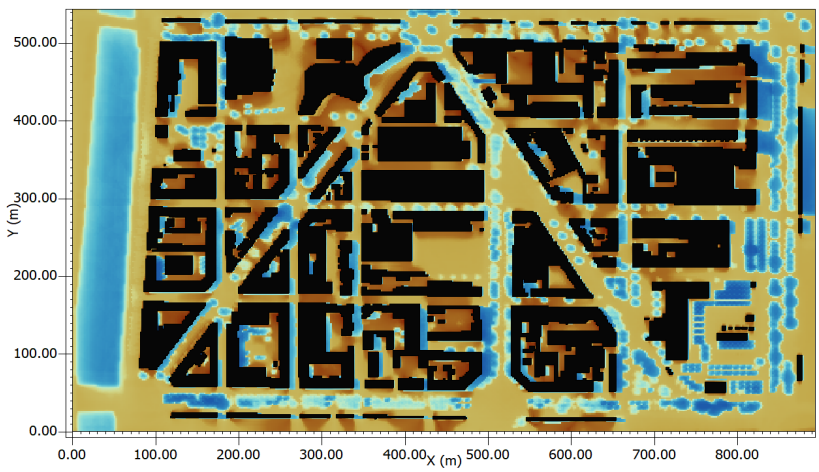

Fig. 121 Existing Potential Air Temprature map at 15:00 h

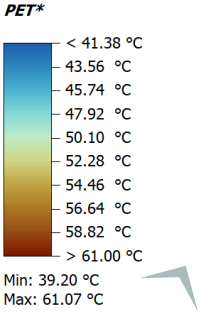

The following figures 122-124 show Surface Temprature maps of the area with Strategies at 09:00, 12,00, 15,00 h.

Date: 27.06.2019, x//y cut at K=4 (1.8 meters)

Fig. 122 Existing Surface Temprature map at 09:00 h

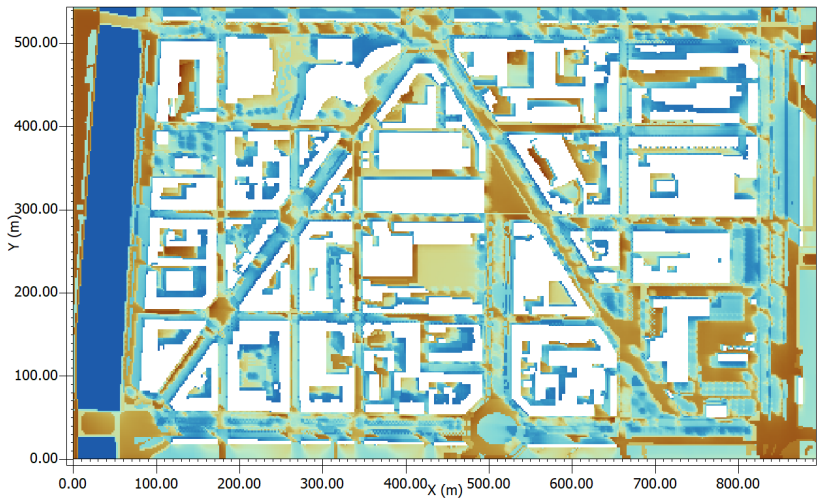

Fig. 123 Existing Surface Temprature map at 12:00 h

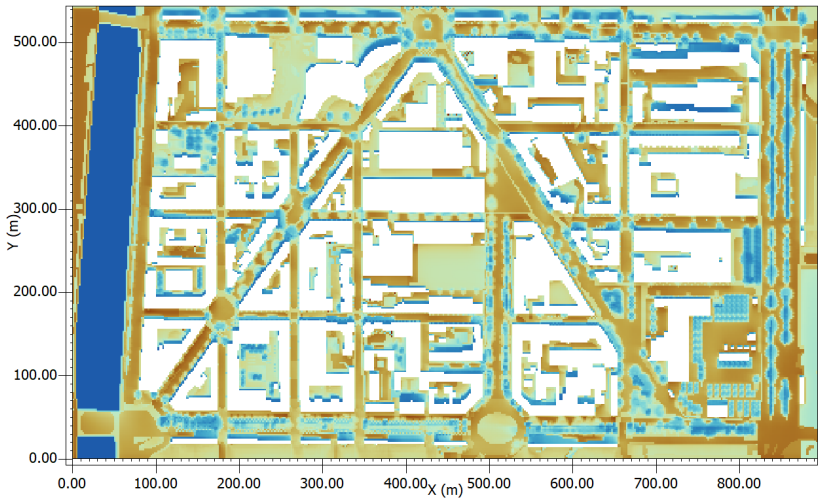

Fig. 124 Existing Surface Temprature map at 15:00 h

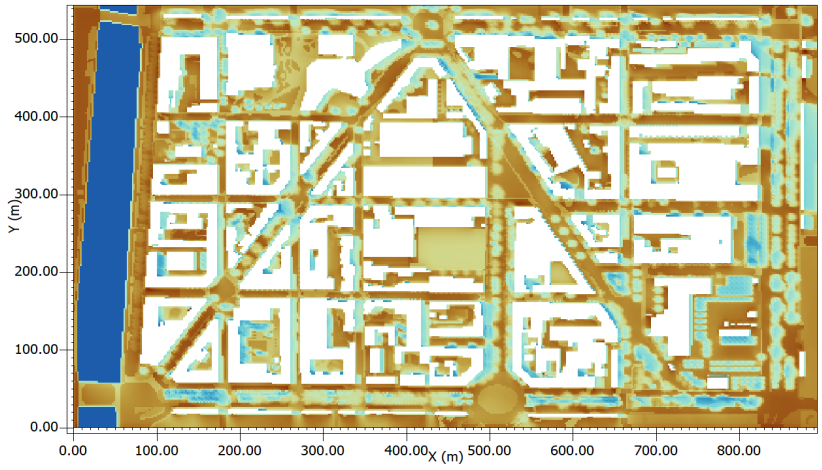

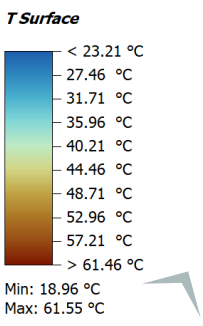

The following figures 125-127 show Wind Flow in the area with Strategies at 09:00, 12,00, 15,00 h.

Date: 27.06.2019, x//y cut at K=4 (1.8 meters)

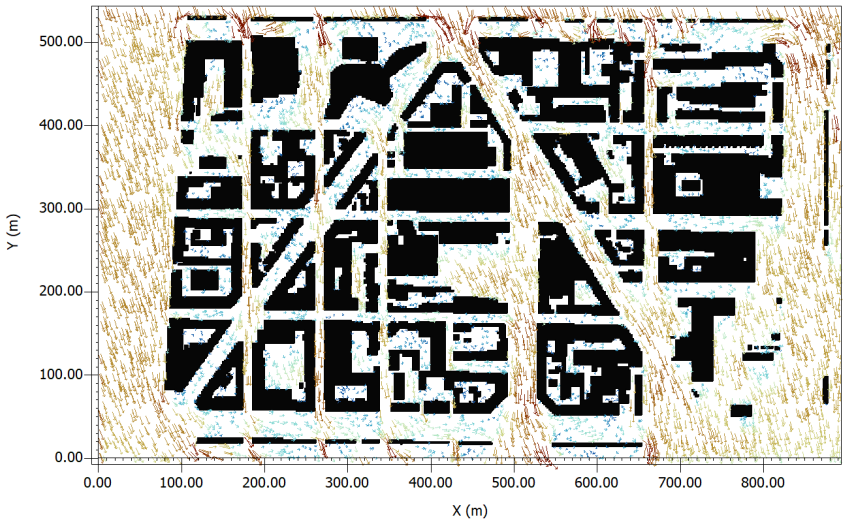

Fig. 125 Wind Flow map with strategies at 09:00 h

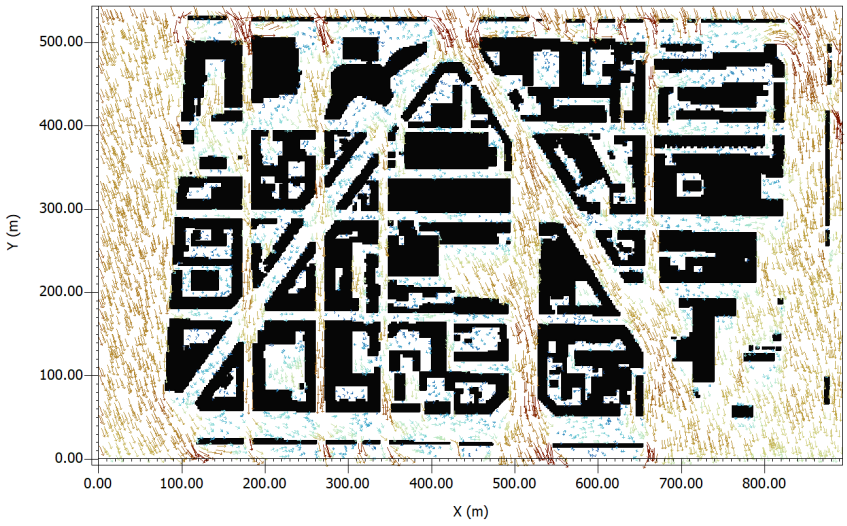

Fig. 126 Wind Flow with strategies at 12:00 h

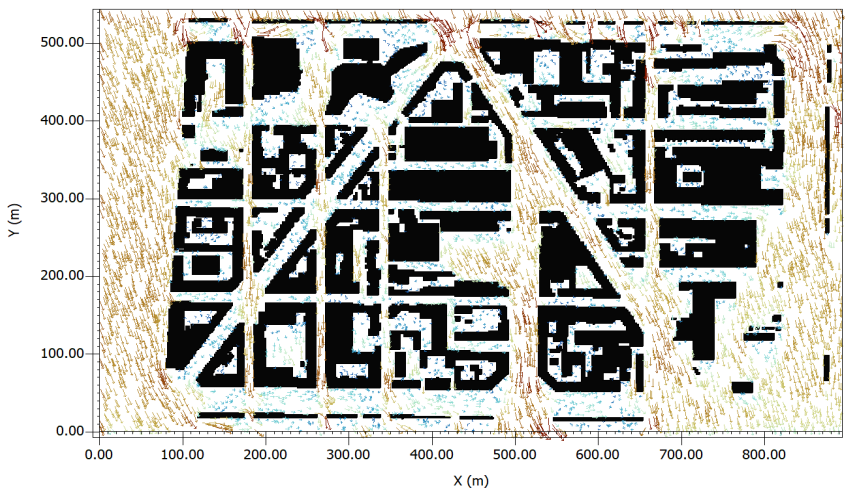

Fig. 127 Wind Flow map with strategies at 15:00 h

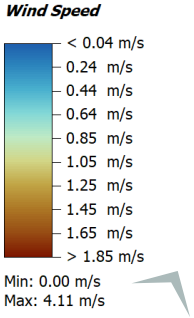

3.4.4 Comparing the Existing Results with the Strategies

Fig. 128- Comparison maps of Air Temprature at 15:00 h (A): Showing air temprature map with the existing condition of the area (B): The area at the same time after interventions (C): Comparison of the two maps (A and B)

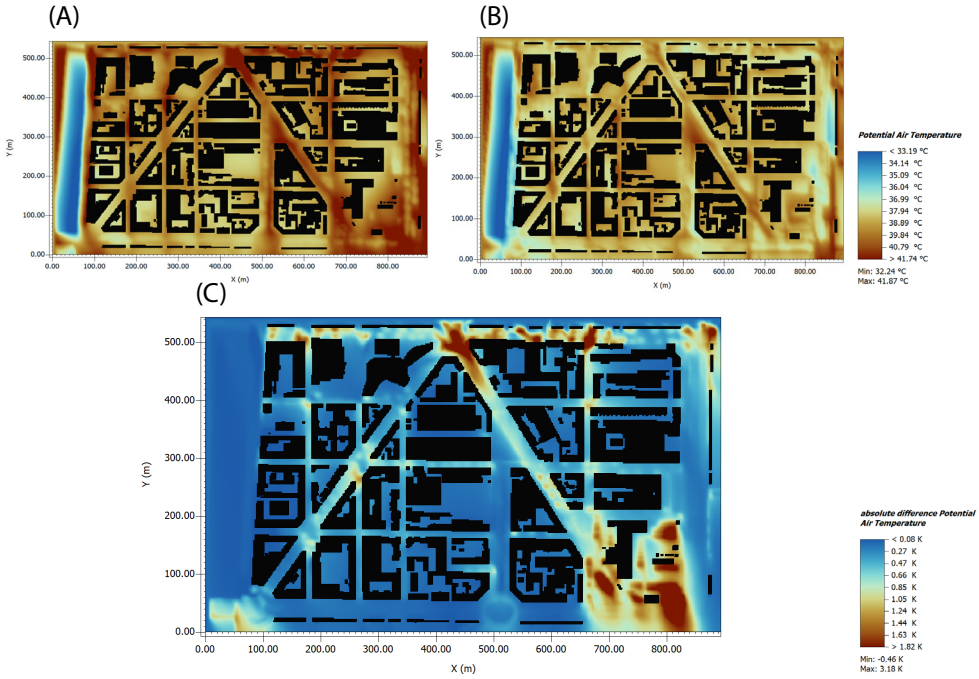

Fig. 129 Comparison maps of PET at 15:00 h (A): Showing PET map with the existing condition of the area (B): The area at the same time after interventions (C): Comparison of the two maps (A and B)

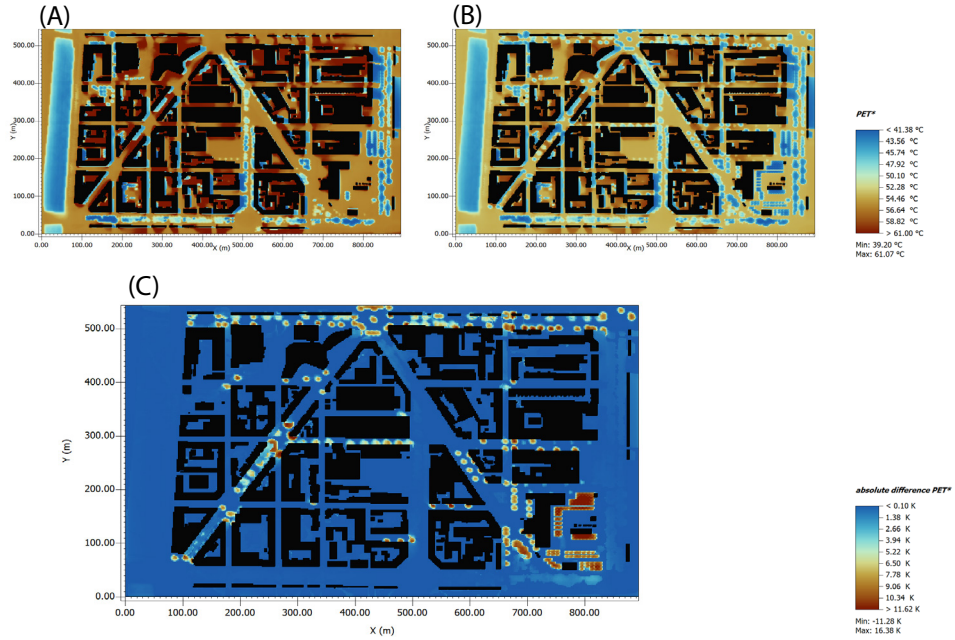

Fig. 130 Comparison maps of Surface Temprature at 15:00 h (A): Showing surface temprature map with the existing condition of the area (B): The area at the same time after interventions (C): Comparison of the two maps (A and B)

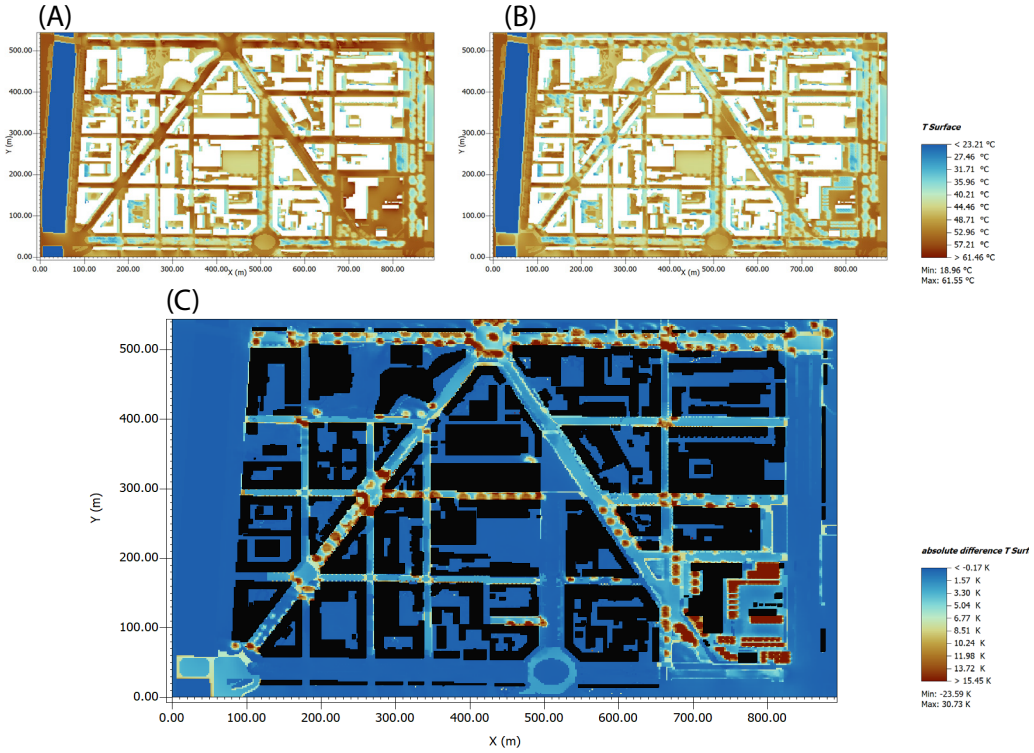

Fig. 131 Comparison maps of Wind Flow at 15:00 h (A): Showing wind flow in the area with the existing condition (B): wind flow in the area at the same time after interventions (C): Comparison of the two maps (A and B)

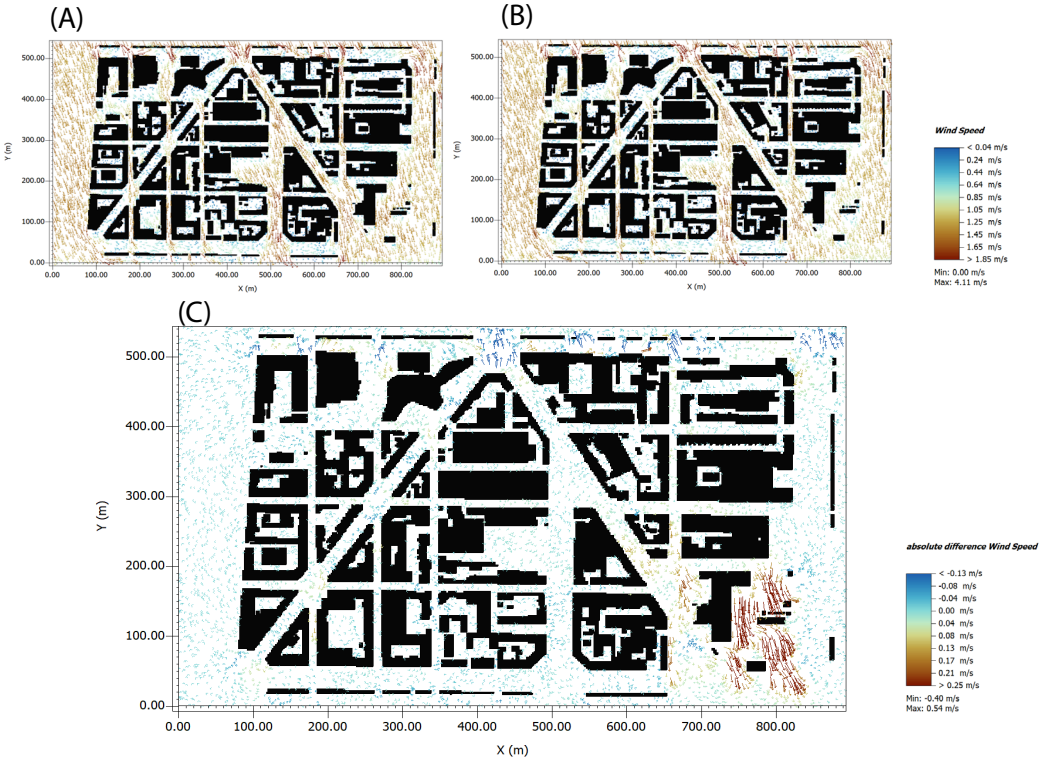

3.3.5 Discussion on the Results of Strategies

The results from the ENVI-met outputs, including the strategies, show that the proposed solutions have worked well and have reduced the Surface temperature and PET values, especially in more critical zones.

In the northeast-southwest-oriented streets, where surface temperature was higher compared to the other streets, the strategies, which were cool pavements + vegetation, have a positive result in terms of thermal comfort, and the comparison maps of the surface temperature show a 3.30K-5.04K difference for the same areas in the existing model and the one including strategies.

In the streets such as Corso Palermo and Via Bologna where the pavement of large asphalt areas and side walks are replaced with materials with higher albedo and better thermal settings, including permeable surfaces applied along the sidewalks, a significant temprature difference can be seen in the comparison maps that proves the magnitude of the heat stress is strongly regulated by the arrangement and composition of urban surfaces particularly canyon aspect ratio and impervious surface coverage (Oke, 1988; Emmanuel et al., 2007)

It is also seen in the comparison maps of PET, Surface temperature, and potential air temperature that the most improvements in terms of thermal comfort were in the areas where the strategy of cool pavement + vegetation was applied. While integrating canopies has not resulted in a visible difference in terms of thermal conditions in none of the maps.

The comparative maps show that the most effective strategy was the implementation of trees and vegetation. This is highlighted in red in the comparison maps which represents the strongest temperature differences, and it appears effective across all the areas where it was applied.

The maps of air temprature and surface temprature show that the cool pavement strategy has worked better in Corso Palermo, Corso Brescia and the Northeast-Southwest oriented streets compared to the Northwest-Southeast oriented streets and result a 5.04 K difference in the surface temprature.

In the areas where shaders were integrated the least heat stress difference can be seen in the comparison maps which is 1.57 K difference in terms of surface temprature, less than 0.10 K in the PET map and, 0.47 K absolute fifference in potential air temprature map.

Moreover, it can be seen from the maps related to wind flow, that the Wind speed has increased in areas where trees have been planted up to 0.25 m/s.

Chapter 04

Conclusion

4 Conclusion

The present thesis has advanced the understanding of microclimate conditions in the case study area located in the Aurora district of Turin. Based on an ENVI-met simulation analysis supported by morphological research and climatic backgrounding, the study explored how urban form influences the UHI and thermal performance.

Based on studying Turin's climate conditions, evaluating comparable case studies under similar climate conditions, and finally, research and analyses on the study area, the thesis aimed to propose microclimate mitigation strategies in alignment with climate-responsive design principles and the Sustainable Development Goals.

The results in all sections of the thesis, including research, previous practices, and analysis of the zone, demonstrate that urban morphology plays a crucial role in shaping microclimatic conditions.

These analyses of the zone were done considering the existing condition of the area, revealed that the microclimate of the area is significantly influenced by surface materials, streets orientation, and the geometry of the streets, which includes building heights, dimensions, and the urban canyon ratio of a street.

Regarding Orientation, streets oriented northwest–southeast present better thermal comfort and lower air temperatures compared to those oriented northeast–southwest. Corso Palermo, with its north–south orientation, is the least optimal thermal conditions among all streets in the area. In terms of Urban canyon, the streets with a deeper ratio show better results in surface temperature and PET maps, while the wind flow maps show that in specific zones of these streets. The surface temperature maps show a significant difference between the streets paved with high albedo materials and permeable pavements, and the streets that are paved with a great amount of asphalt. ENVI-met simulations showed substantial surface temperature variations ranging from 18.96°C to 62.35°C in the existing model.

All the resulting maps of the existing condition show that the streets and areas covered with vegetation or shaded with trees have better thermal performance conditions compared to the zones that lack vegetation and trees.

By understanding the most effective solutions, and considering the simulation outcomes, the most effective mitigation strategies for the area include:
Replacing high-temperature pavements with cool pavement, Introducing vegetation where space allows and, Integrating shading structures such as lightweight canopies especially in large open asphalted areas like open public parkings.
Depending on the morphological and movement characteristics of each street, the combination of these strategies can further enhance thermal comfort and the quality of public space.

In the final strage, the proposed strategies were modeled into an ENVI-met simulation model to assess their effectiveness. The results show significant improvements: at some points during the hottest day of the year and hottest time of the day, PET values improved by up to 16.38 K, surface temperatures decreased by 15.45 K, and potential air temperature dropped by 3.18 K in some locations within the area. The comparison maps indicate that using a combination of plants and cool pavements to replace the surfaces is the most successful method in this zone.

The results show that the microclimatic conditions of the Aurora district can be markedly improved by a climate-responsive layout that includes cool materials, vegetation, and shading. This would provide a much more resilient, comfortable, and sustainable urban setting.

Bibliography and Sitography

Bibliography

A

Akbari, H., Pomerantz, M., & Taha, H. (2001). Cool surfaces and shade trees to reduce energy use and improve air quality in urban areas. Solar Energy, 70(3), 295–310.

Alcoforado, M. J., et al. (2009). The application of climatic knowledge in urban planning, exemplified by the city of Lisbon. In: K. A. L. Salih, N. K. Ghaffar, & H. B. Shakar (Eds.), Proceedings of the 4th International Scientific Conference of Salahaddin University (pp. 53–65).

Alonso, C., Oteiza, I., García-Navarro, J., & Martín-Consuegra, F. (2016). Energy consumption to cool and heat experimental modules for the energy refurbishment of faades. Three case studies in Madrid. Energy and Buildings, 126, 252–262.

Antoniou, N., Montazeri, H., Neophytou, M., & Blocken, B. (2019). CFD simulation of urban microclimate: Validation using high-resolution field measurements. Science of The Total Environment, 695, 133743. https://doi.org/10.1016/j.scitotenv.2019.133743.

B

Bande, L., Afshari, A., Al Masri, D., Jha, M., Norford, L., Tsoupos, A., Marpu, P., Pasha, Y., & Armstrong, P. (2019). Validation of UWG and Envi-Met Models in an Abu Dhabi District, Based on Site Measurements. Sustainability, 11.

Basagaña, X., Smargiassi, A., Tobias, A., Iniguez, C., Smargiassi, A., Gariépy, Y., Gascon, M., & Forns, J. (2011). Ambient heat and sudden infant death: A case-crossover study spanning 30 years in Montreal, Canada. Environmental Health Perspectives, 119(9), 1329–1333. https://doi.org/10.1289/ehp.1003264

Battista, G., de Lieto Vollaro, E., Ocłoń, P., & de Lieto Vollaro, R. (2023). Effects of urban heat island mitigation strategies in an urban square: A numerical modelling and experimental investigation. Energy and Buildings, 282, 112809.

Biesbroek, G. R., Swart, R. J., & van der Knaap, W. G. M. (2009). The mitigation-adaptation dichotomy and the role of spatial planning. Habitat International,33(3),230–237. https://doi.org/10.1016/j.habitatint.2008.10.001

Binte Ali, S. (2018). Thermal comfort in urban open spaces: Objective assessment and subjective perception study in tropical city of Bhopal, India. Urban Climate, 23, 114–129. https://doi.org/10.1016/j.uclim.2017.07.004

Bishara, A., Kramberger, K. H., & Ptatschek, V. (2017). Influence of different pigments on the facade surface temperatures. Energy Procedia, 132, 447–453.

Bowler, D. E., Buyung-Ali, L., Knight, T. M., & Pullin, A. S. (2010). Urban greening to cool towns and cities: A systematic review. Landscape and Urban Planning, 97(3), 147–155.

Bruse, M., & Fleer, H. (1998). Simulating Surface–Plant–Air Interactions inside Urban Environments with a Three-Dimensional Numerical Model. Environmental Modeling & Software, 13(4), 373–384.

C

Cecil Konijnendijk. (2021). The 3-30-300 Rule for Urban Forestry and Greener Cities. Medium. Retrieved November 17, 2025,

Chen, L., & Ng, E. (2011). Outdoor thermal comfort and outdoor activities: A review of research in the past decade. Cities, 29(4), 118–125.

Chao Hong, Wang, Y., Gu, Z., & Yu, C. W. (2022). Cool facades to mitigate urban heat island effects. International Journal of Thermophysics, 43(11). https://doi.org/10.1177/1420326X221115369

Cintolesi, C., et al. (2021). Use large-eddy simulations to analyze thermal effects in urban canyons, including vortex behavior and airflow. Building and Environment, 203, 108031. https://doi.org/10.1016/j.buildenv.2021.108031

Coseo, P., & Larsen, L. (2015). Microclimate modeling and analysis of mitigation strategies for the urban heat island in Chicago. Urban Climate, 14, 94–113. https://doi.org/10.1016/j.uclim.2015.05.004

Costanzo, V., Evola, G., & Marletta, L. (2016). Cooling potential of green roofs in different climate zones of Europe. Energy and Buildings, 127, 1041–1053. https://doi.org/10.1016/j.enbuild.2016.06.066

Crank, P. J., et al. (2023). Assessing microclimate impacts of neighborhood redesign in a desert urban climate using ENVI-Met and MaRTy. Sustainable Cities and Society, 95, 104634. https://doi.org/10.1016/j.scs.2023.104634

Cui, P. Y., Li, Z., & Tao, W. Q. (2016). Wind-tunnel measurements for thermal effects on the air flow and pollutant dispersion through different scale urban areas. Building and Environment, 97, 137–151. https://doi.org/10.1016/j.buildenv.2015.12.015

D

Deilami, K., Kamruzzaman, M., & Liu, Y. (2018). Urban heat island effect: A systematic review of spatio-temporal factors, data, methods, and mitigation measures. International Journal of Applied Earth Observation and Geoinformation, 73, 467–483. https://doi.org/10.1016/j.jag.2017.12.009

Dihkan, M., et al. (2015). Urban morphology and its effect on microclimate: a review. [Requires full citation]

E
Dihkan, M., et al. (2015). Urban morphology and its effect on microclimate: a review. Energy and Buildings, 97, 96–107. https://doi.org/10.1016/j.enbuild.2015.03.047cis. (Book)

Emmanuel, R. (2021). Urban microclimate in temperate climates: a summary for practitioners. Buildings and Cities, 2(1), 402–410. https://doi.org/10.5334/bc.109

Emmanuel, R., & Fernando, H. J. S. (2007). Urban heat islands in tropical and subtropical cities. Geography Compass, 1(4), 856–871.

Erell, E. (2008). The Application of Urban Climate. Research in the Design of Cities. In: M. K. B. B. L. B. M. L. W. (Ed.), Advances in Building Energy Research: Volume 2 (pp. 41–64). Earthscan.

Erell, E., Pearlmutter, D., & Williamson, T. (2011). Urban microclimate: Designing the spaces between buildings. Earthscan, UK. (Book)

G
Gagge, A. P., Fobelets, A. P., & Berglund, L. G. (1986). A Standard Predictive Index of Human Response to the Thermal Environment. ASHRAE Transactions 1986, 92(2), 709–731.

Golden, J. S., & Kaloush, K. E. (2006). Simulation of thermal and energy performance of parking lot pavements. Journal of Solar Energy Engineering, 128(1), 98–105. https://doi.org/10.1115/1.2168346

Gorsevski, P. V., Taha, H., Quattrochi, D. A., & Luvall, J. C. (1998). Air pollution prevention through urban heat island mitigation: An update on the Urban Heat Island Pilot Project. Atmospheric Environment, 32(18), 3051–3061. https://doi.org/10.1016/S1352-2310(98)00028-0

Grimmond, C. S. B. (2007). Urbanization and global environmental change: Local climate perspectives. In S. T. A. Pickett & M. L. Cadenasso (Eds.), The Oxford Handbook of Urban Environmental Planning. Oxford University Press.

H
Hadavi, M., & Pasdarshahri, H. (2021). Impacts of urban buildings on microclimate and cooling systems efficiency: Coupled CFD and BES simulations. Sustainable Cities and Society, 74, 102740. https://doi.org/10.1016/j.scs.2021.102740.

He, S., Zhang, Y. W., Gu, Z. L., & Su, J. W. (2019). Local climate zone classification with different source data in Xi'an, China. Indoor and Built Environment, 28(9), 1190–1199.

Hoag, H. (2015). Cities Cool Down With Green Roofs and Cool Roofs. Nature News. https://www.nature.com/news/cities-cool-down-with-green-roofs-and-cool-roofs-1.18316

Höppe, P. (1999). The physiological equivalent temperature – a universal index for the biometeorological assessment of the thermal environment. International Journal of Biometeorology, 43(1), 71–75.

Hu, Z., & Jia, G. (2010). Urban Land-use/Land-cover Change and the Urban Heat Island Effect. Proceedings of the International Conference on Computer and Information Application (ICCIA), 401–404. https://doi.org/10.1109/ICCIA.2010.6141386

Huang, M., et al. (2025). Numerical Simulation Study on Air Flow and Pollutant Dispersion in Urban Street Canyons.

I

International Organization for Standardization (ISO). (1998). ISO 7726: Ergonomics of the thermal environment - Instrument for measuring physical quantities.

J

Jendritzky, G., de Dear, R., & Havenith, G. (2012). UTCI—Why another thermal index? International Journal of Biometeorology, 56(3), 421–430. https://doi.org/10.1007/s00484-011-0513-7

Jiyao Zhao, Chen, G., Yu, L., Ren, C., Xie, J., Chung, L., Ni, H., & Gong, P. (2023). Mapping urban morphology changes in the last two decades based on local climate zone scheme: A case study of three major urban agglomerations in China. Urban Climate, 47, 101391. https://doi.org/10.1016/j.uclim.2022.101391

Jong Soo Lee, Kim, J. T., & Lee, M. G. (2013). Mitigation of urban heat island effect and greenroofs. International Journal of Thermophysics, 34(1), 162–176. https://doi.org/10.1177/1420326X12474483

K

Kabisch, N., et al. (2016). Nature-based solutions to climate change mitigation and adaptation in urban areas: Perspectives on indicators, knowledge gaps, barriers and opportunities for action. Ecology and Society, 21(2), 39.

Klein, R. J. T., Eriksen, S. E. H., Naess, L. O., Hammill, A., Tanner, T. M., Robledo, C., & O'Brien, K. L. (2007). Portfolio screening to support the mainstreaming of adaptation to climate change into development assistance. Climatic Change, 84(1), 23–44.

Kotharkar, R., et al. (2024). Investigating outdoor thermal comfort variations across local climate zones in Nagpur, India, using ENVI-met. Building and Environment. [Requires full citation]

Kouklis, K. (2021). [Requires full citation for 2021 paper]

Kume, E. V. (2020). Urban micro-climate implications of Barcelona's superblocks strategy: a computational assessment [Diploma Thesis, Technische Universität Wien]. reposiTUm. https://doi.org/10.34726/hss.2021.66497

Kwok, Y. T., & Ng, E. Y. Y. (2021). Trends, topics, and lessons learnt from real case studies using mesoscale atmospheric models for urban climate applications in 2000–2019. Urban Climate, 38, 100868.

L

Lai, D., Liu, W., Gan, T., Liu, K., & Chen, Q. (2019). A review of mitigating strategies to improve the thermal environment and thermal comfort in urban outdoor spaces. Science of The Total Environment, 661, 141–157.

Lauzet, N., Rodler, A., Musy, M., Azam, M. H., Guernouti, S., Mauree, D., & Colinart, T. (2019). How Building Energy Models Take the Local Climate into Account in an Urban Context A Review. Renewable and Sustainable Energy Reviews, 107, 438–454.

Lee, H., & Mayer, H. (2016). Validation of the Mean Radiant Temperature Simulated by the RayMan Software in Urban Environments. International Journal of Biometeorology, 60(5), 697–711.

Lee, T., Yang, H., & Blok, A. (2020). Does mitigation shape adaptation? The urban climate mitigation–adaptation nexus. Climate Policy, 20(3), 341–353. https://doi.org/10.1080/14693062.2020.1730152

Lin, T. P. (2009). Thermal perception, adaptation and attendance in a public square in hot and humid regions. Building and Environment, 44(10), 2017–2026.

Lopez-Cabeza, V. P., & Diz-Mellado, E. (2022). Albedo influence on the microclimate and thermal comfort of courtyards under Mediterranean hot summer climate condition. Energy and Buildings, 266, 112097.

M

Mahgoub, A. O., Gowid, S., & Ghani, S. (2020). Global Evaluation of WBGT and Set Indices for Outdoor Environments Using Thermal Imaging and Artificial Neural Networks. Sustainable Cities and Society, 60, 102182. https://doi.org/10.1016/j.scs.2020.102182.

Marando, F., Heris, M. P., Zulian, G., Udías, A., Mentaschi, L., Chrysoulakis, N., Parastatidis, D., & Maes, J. (2022). Urban heat island mitigation by green infrastructure in European Functional Urban Areas. Sustainable Cities and Society, 76, 103564. https://doi.org/10.1016/j.scs.2021.103564

McEvoy, D., Lindley, S., & Handley, J. (2006). Adaptation and mitigation in urban areas: synergies and conflicts. Municipal Engineer, 159(4), 184–191. https://doi.org/10.1680/muen.2006.159.4.185

Mills, G. (2014). An update to the urban heat island research agenda. Urban Climate, 7, 56–75.

Mirzaei, P. A. (2015). Recent Challenges in Modeling of Urban Heat Island. Sustainable Cities and Society, 19, 268–275.

Mohajerani, A., Bakaric, J., & Jeffrey-Bailey, T. (2017). The urban heat island effect, its causes, and mitigation, with reference to the thermal properties of asphalt concrete. Journal of Environmental Management, 197, 522–538. https://doi.org/10.1016/j.jenvman.2017.03.095

Mohamed Irfeey Abdul Munaf, Chau, H. W., Mohamed Mahusoon Fathima Sumaiya, Wai, C. Y., Muttil, N., & Jamei, E. (2023). Sustainable Mitigation Strategies for Urban Heat Island Effects in Urban Areas. Sustainability, 15(3), 2608.

Monaco, Michela, and Giorgio Baldinelli. "On the Role of the Building Envelope on the Urban Heat Island Intensity: A Case Study in a Mediterranean City." Urban Science, vol. 12, no. 8, 2024, p. 113. MDPI, https://doi.org/10.3390/urbansci12080113

Morakinyo, T. E., et al. (2018). Performance of Hong Kong's common trees species for outdoor temperature regulation, thermal comfort and energy saving. Building and Environment, 137, 223–236.

Mullaney, J., Lucke, T., & Trueman, S. J. (2015). A review of benefits and challenges in growing street trees in paved urban environments. Landscape and Urban Planning, 134, 157–166.

N

Nazarian, N., Dumas, C., & Santamouris, M. (2019). Effect of high-albedo materials on pedestrian heat stress in urban street canyons. Urban Climate, 27, 100451. https://doi.org/10.1016/j.uclim.2018.100451.

Nikolopoulou, M., Baker, N., & Steemers, K. (2001). Thermal comfort in outdoor urban spaces: understanding the human parameter. Solar Energy, 70(3), 227–235.

O

Oke, T. R. (1978). Boundary-Layer Climates. Routledge. (Book)

Oke, T. R. (1982). The energetic basis of the urban heat island. Quarterly Journal of the Royal Meteorological Society, 108(455), 1–24.

Oke, T. R. (1984). Towards a more rational approach to the planning of the urban environment. Energy and Buildings, 7(4), 307–313.

Oke, T. R. (1988). Street design and urban climate—Review and suggestions. Energy and Buildings, 11(1–3), 103–113.

Orlanski, I. (1975). A rational subdivision of scales for atmospheric processes. Bulletin of the American Meteorological Society, 56(5), 527–538.

Ozalp, M. (2022a). Effects of tree groupings on urban thermal comfort in open spaces. Sustainable Cities and Society, 86, 104157.

Ozalp, M. (2022). Microclimatic response to urban morphology -The case of Turin [Master's Thesis, Politecnico di Torino]. http://webthesis.biblio.polito.it/23925/

P

Pejović, A. (2022). Microclimate mitigation, analysis and design tools: Case study of controviali in Turin [Master's Thesis, Politecnico di Torino]. http://webthesis.biblio.polito.it/23297/

Peng, M., et al. (2022). Synergistic Effect of Urban Canyon Geometries and Planting in Mitigating Urban Heat Island in Subtropical Coastal City. Frontiers in Earth Science, 10. https://doi.org/10.3389/feart.2022.951804

Petralli, M., et al. (2014). The influence of urban parameters on the urban heat island effect: a study in Florence, Italy. Advances in Science and Research, 11(1), 1–6.

Pollo, R., Biolchini, E., Squillacioti, G., & Bono, R. (2020). Designing the healthy city: an interdisciplinary approach. SMC Magazine, 12, 150–155.

Pollo, R., & Trane, M. (2021). Adaptation, Mitigation, and Smart Urban Metabolism towards the Ecological Transition. In C. Sposito (Ed.), Possible and preferable scenarios of a Sustainable Future. Towards 2030 and beyond (pp. 74–89). Palermo University Press.

Prataviera, E., Romano, P., Carnieletto, L., Pirotti, F., Vivian, J., & Zarrella, A. (2021). EU-ReCA: An open-source urban building energy modelling tool for the efficient evaluation of cities energy demand. Renewable Energy, 175, 786–801.

Q

Qin, Y. (2015a). A review on the development of cool pavements to mitigate urban heat island effect. Renewable and Sustainable Energy Reviews, 52, 268–277. https://doi.org/10.1016/j.rser.2015.07.177

Qin, Y. (2015b). Influence of urban canyon geometry on pedestrian-level radiation and temperature in urban environments. Energy and Buildings, 89, 22–33. https://doi.org/10.1016/j.enbuild.2014.12.010

R

Rajagopalan, P., Lim, K. C., & Jamei, E. (2014). Urban heat island and wind flow characteristics of a tropical city. Solar Energy, 107, 308–321. https://doi.org/10.1016/j.solener.2014.05.042

Razzaghmanesh, M., Beecham, S., & Salemi, H. (2016). The impact of cool roofs on urban heat island mitigation and energy saving in buildings. Sustainability, 8(4), 329. https://doi.org/10.3390/su8040329

Rossi, F., Pisello, A. L., Nicolini, A., Filipponi, M., & Palombo, M. (2014). Analysis of retro-reflective surfaces for urban heat island mitigation: A new analytical model. Applied Energy, 114(C), 621–631. https://doi.org/10.1016/j.apenergy.2013.10.038

Ruiz-Villanueva, V. (2015). PERCEPCIÓN POST-CRECIDA DE LOS RESTOS DE VEGETACIÓN EN CAUCES DE MONTAÑA DE LA PENÍNSULA IBÉRICA. Cuadernos de Investigación Geográfica / Investigaciones Geográficas, 41(2), 527–549. https://doi.org/10.18172/cig.2801

S

Sanjuan, M. A., Morales, A., & Zaragoza, A. (2022). Precast Concrete Pavements of High Albedo to Achieve the Net "Zero-Emissions" Commitments. Applied Sciences, 12(4), 1955. https://doi.org/10.3390/app12041955

Santamouris, M. (2014a). Cooling the Cities—A Review of Reflective and Green Roof Mitigation Technologies to Fight Heat Island and Improve Comfort in Urban Environments. Solar Energy, 103, 682–703.

Santamouris, M. (2014b). On the energy impact of urban heat island and global warming on buildings. Energy and Buildings, 82, 100–113.

Santamouris, M. (2015). Analyzing the heat island magnitude and characteristics in one hundred Asian and Australian cities and regions. Science of The Total Environment, 512-513, 582–598. https://doi.org/10.1016/j.scitotenv.2015.01.060

Santamouris, M., Papanikolaou, N., Livada, I., Koronakis, I., Georgakis, C., Argiriou, A., & Assimakopoulos, D. N. (2001). On the impact of urban climate on the energy consumption of building. Solar Energy, 70(3), 201–216. https://doi.org/10.1016/S0038-092X(00)00095-5.

Santamouris, M., Synnefa, A., & Karlessi, T. (2011). Using advanced cool materials in the urban built environment to mitigate heat islands and improve thermal comfort conditions. Solar Energy, 85(12), 3085–3102.

Sharmin, T., Steemers, K., & Matzarakis, A. (2017). Microclimatic Modelling in Assessing the Impact of Urban Geometry on Urban Thermal Environment. Sustainable Cities and Society, 34, 293–308.

Shashua-Bar, L., & Hoffman, M. E. (2000). Vegetation as a climate modifier in urban areas and heat-island mitigation. Energy and Buildings, 31(3), 221–235.

Sheng, L., et al. (2017). Effects of urban morphology on the urban heat island in a high-rise high-density city. Landscape and Urban Planning, 173, 114–126.

Smargiassi, A., et al. (2009). Ambient Heat and Sudden Infant Death: A Case-Crossover Study Spanning 30 Years in Montreal, Canada. Environmental Health Perspectives, 117(10), 1545–1549. https://doi.org/10.1289/ehp.0800318

Sola-Caraballo, J., Lopez-Cabeza, V. P., Roa-Fernández, J., Rivera-Gómez, C., & Galan-Marin, C. (2024). Assessing and upgrading urban thermal resilience of a Spanish MoMo neighbourhood over the span of 1960–2080. Building and Environment, 256, 111485. https://doi.org/10.1016/j.buildenv.2024.111485

Stewart, I. D., & Oke, T. R. (2012). Local Climate Zones for Urban Temperature Studies. Bulletin of the American Meteorological Society, 93(12), 1879–1900.

Stone, B., Hess, J. J., & Frumkin, H. (2010). Urban form and extreme heat events: are sprawling cities more vulnerable to climate change than compact cities? Environmental Health Perspectives, 118(10), 1425–1428. https://doi.org/10.1289/ehp.0901879

Synnefa, A., Karlessi, T., Gaitani, N., Santamouris, M., Assimakopoulos, D. N., & Papakatsikas, C. (2011). Experimental testing of cool colored thin layer asphalt and estimation of its potential to improve the urban microclimate. Building and Environment, 46(1), 126–134. https://doi.org/10.1016/j.buildenv.2010.06.014

T

Tablada, A.; De Troyer, F.; Blocken, B.; Carmeliet, J.; Verschure, H. (2009). On natural ventilation and thermal comfort in compact urban environments—The Old Havana case. Build. Environ. 2009, 44*(2), 437–446.

Takebayashi, H., & Moriyama, M. (2012). Surface heat budget on pavement and grass: effects of water evaporation and surface temperature on air temperature. International Journal of Biometeorology, 56(5), 911–920. https://doi.org/10.1007/s00484-011-0462-3

Taleghani, M., Swan, W., Johansson, E., & Ji, Y. (2021). Urban cooling: which façade orientation has the most impact on a microclimate? Sustainable Cities and Society, 64, 102547.

Tan, J., Wong, N. H., Tan, C. L., Jusuf, S. K., & Chiam, Z. (2015). Thermal performance of extensive green roofs in Singapore. Building and Environment, 92, 307–317. https://doi.org/10.1016/j.buildenv.2015.04.010

Tan, Z., Lau, S. S. Y., & Ng, E. (2016). Urban tree design approaches for mitigating daytime urban heat island effects in a tropical city. Landscape and Urban Planning, 148, 45–56. https://doi.org/10.1016/j.landurbplan.2015.12.011

Tarkhan, N., Klimenta, M., Fang, K., Durate, F., Ratti, C., & Reihnhart, C. F. (2025). Mapping facade materials utilizing zero-shot segmentation for applications in urban microclimate research. [Requires full citation]

Toparlar, Y., Blocken, B., Maiheu, B., & van Heijst, G. J. F. (2017). A Review on the CFD Analysis of Urban Microclimate. Renewable and Sustainable Energy Reviews, 76, 161–180.

Trane, M., Giovanardi, M., Pejović, A., & Pollo, R. (2021a). Urban climate and microclimate models and their role to achieve the Sustainable Development Goals. An overview. In: C. Sposito (Ed.), Architecture and design for Industry (pp. 53–70). Springer.

Trane, M., Giovanardi, M., Pollo, R., & Martoccia, C. (2021b). Microclimate design for micro-urban design. A case study in Granada, Spain. Sustainable Mediterranean Construction, 14, 149–155.

Trane, M., Ricciardi, G., Scalas, M., & Ellena, M. (2023). From CFD to GIS: a methodology to implement urban microclimate georeferenced databases. TECHNE, 25.

Tumini, I., Higueras, E., & Baereswly, S. (2016). Urban microclimate and thermal comfort modelling: strategies for urban renovation. Journal of Asian Architecture and Building Engineering, 15(1), 161–168. https://doi.org/10.1080/209376 1X.2016.1152204

W

Watson, D. (n.d.). Bioclimatic Design Principles and Practices.

Williams, T. B. (1991). Microclimatic temperature relationships over different surfaces. Journal of Geography, 90(6), 253–257. https://doi.org/10.1080/00221349108979321.

Woolley, H. (2003). Urban Open Spaces. Spon Press. https://doi. org/10.4324/9780203402146

X

Xu, C., Ma, X., & Yu, C. W. (2019). Photovoltaic double-skin facade: a combination of active and passive utilizations of solar energy. Indoor and Built Environment, 28(9), 1013–1017.

Xu, Y., et al. (2017). Urban climate change and planning: A review. Renewable and Sustainable Energy Reviews, 74, 1445–1455. https://doi.org/10.1016/j.rser.2016.11.233

Z

Zhang, Y., et al. (2022). An improved algorithm of thermal index models based on ENVI-met. Urban Climate, 44, 101190.

Sitography

A
Arpa Piemonte. Homepage Arpa Piemonte. https://www.arpa.piemonte.it/

C
Città di Torino. (Data di pubblicazione o ultima modifica non specificata). Torino Facile: Sito Istituzionale e Servizi Digitali. https://servizi.torinofacile.it/

Città di Torino. (Data di pubblicazione o ultima modifica non specificata). Geoportale - Città di Torino. http://geoportale.comune.torino.it/

I
ICLEI – Local Governments for Sustainability. (2020). ICLEI's Climate Neutrality Framework. https://e-lib.iclei.org/publications/ICLEIs_Climate_Neutrality_Framework

IPCC. (2018). Global Warming of 1.5°C: An IPCC Special Report.https://www.thesunprogram.com

IPCC. (2022). AR6 WGI Regional Fact Sheet Urban Areas. IPCC. https://www.thesunprogram.com

IUCN. (2016). Nature-based Solutions are defined as actions to protect, sustainably manage, and restore natural or modified ecosystems... IUCN Official Definition. Retrieved November 17, 2025

P
PWC Global. (2017). The long view: How will the global economic order change by 2050? PwC Report.

U
UN-HABITAT. (2023). The Critical Role of Nature-Based Solutions for Enhancing Climate Resilience. https://unhabitat.org/sites/default/files/2023/10/unh._2023._the_critical_role_of_nature-based_solutions_for_enhancing_climate_resilience_in_informal_areas.pdf

UN-HABITAT. (2024). World Cities Report 2024. https://unhabitat.org/wcr/

United Nations. (2024). UN regulations and programmes for healthier, sustainable cities.

United Nations Secretary-General António Guterres. (2023, June 16). General Assembly on Climate, Equity and Justice. https://news.un.org/en/story/2023/06/1137342

UN Sustainable Development. (n.d.). Communications Material. https://www.un.org/sustainabledevelopment/news/communications-material/

W

Webb, B. (2016). The Use of Urban Climatology in Local Climate Change Strategies: A Comparative Perspective. International Planning Studies, 21(1), 1–19.

WHO. (n.d.). Urban green spaces and health report. https://iris.who.int/handle/10665/345751